

Final Report

**Impact of Uncertainty on Modeling and Testing
PRC 95-001**

10 January 1994 to 30 April 1995

**National Aeronautics and Space Administration
Marshall Space Flight Center
Contract Number NAS8-38609
Delivery Order #106**

by

**Hugh W. Coleman (Principal Investigator)
Kendall K. Brown (Graduate Research Assistant)
Propulsion Research Center
Department of Mechanical and Aerospace Engineering
University of Alabama in Huntsville**

(NASA-CR-196637) IMPACT OF
UNCERTAINTY ON MODELING AND TESTING
Final Report, 10 Jan. 1994 - 30
Apr. 1995 (Alabama Univ.) 118 p

N95-30013

Unclas

G3/61 0054606

Final Report

10 January 1994 to 30 April 1995

Impact of Uncertainty on Modeling and Testing

National Aeronautics and Space Administration

Marshall Space Flight Center

Contract Number NAS8-38609

Delivery Order #106

by

Hugh W. Coleman (Principal Investigator)

Kendall K. Brown (Graduate Research Assistant)

Propulsion Research Center

Department of Mechanical and Aerospace Engineering

University of Alabama in Huntsville

Table of Contents

<u>Section</u>	<u>Topic</u>
1.0	Introduction
2.0	Uncertainty Analysis
3.0	Results of Application of Uncertainty Analysis to TTB Testing
4.0	Results of Application of Uncertainty Analysis in SSME Modeling
5.0	Summary
6.0	Bibliography
I	Appendix I - Venturi Flowmeter Data Reduction
II	Appendix II - Mass Flow Rate Uncertainty Determination
III	Appendix III - ASME Technical Paper
IV	Appendix IV - AIAA Paper
V	Appendix V - Elemental Bias Limits Used in Venturi Uncertainty Determination
VI	Appendix VI - Engine Configuration and Averaged Test Data
VII	Appendix VII - Calculated Venturi Mass Flowrate Data and Test-to-Test Standard Deviations
VIII	Appendix VIII - Venturi Mass Flowrate Data and Calculated Bias Limits
IX	Appendix IX - Plots of Venturi Mass Flowrates
X	Appendix X- Output from Venturi Uncertainty Program
XI	Appendix XI - Venturi Uncertainty Analysis Computer Program

ab = ① ②

1.0 Introduction

1.1 Statement of Work

A thorough understanding of the uncertainties associated with the modeling and testing of the Space Shuttle Main Engine (SSME) Engine will greatly aid decisions concerning hardware performance and future development efforts. The goals of this research effort are delineated in the the Statement of Work, reproduced below:

The goal of this effort is to enhance the rocket engine steady-state performance computer models through the incorporation of uncertainty analysis concepts. Analytical tools and analysis techniques are being investigated to better support performance analysis requirements. These requirements include assessing vehicle/engine feed system interface flow characteristics, engine hardware design changes, evaluating engine hardware performance, predicting engine hardware operation, and supporting failure investigations.

A major shortcoming within the current SSME power balance modeling scheme is that experimental data and the fundamental physical relationship are treated as absolutes. Both experimental data and the property requirements contain various sources or errors. The primary sources of error within the instrumentation system are calibration errors, signal processing and localized effects. The primary sources or errors within the fundamental relationships are uncertainties in physical approximations and fluid property computational predictions are forces to agree with the data at instrumented locations, often at the expense of physical consistency. This situation degrades the capability of the analytical tools and thus, reduces the amount of confidence in the results generated.

A test data integration strategy was developed based upon evaluating test data with respect to basic fluid conservation principles (mass, energy, and momentum relationships). This strategy systematically transforms uncertain experimental data into a physically self consistent set of data. This is accomplished by forcing the minimum adjustment required in engine pressures, temperatures, and flowrates necessary to satisfy prescribed uncertainty constraints.

This strategy incorporate uncertainty requirements explicitly. The overall success of the test data integration strategy is a function of determining these required uncertainty estimates.

Another major shortcoming within the current modeling scheme is that the current performance models do not present uncertainty estimates with predictions. A general framework for modular uncertainty estimates with predictions. A general framework for modular rocket engine performance models do not present uncertainty estimates with predictions. A general framework for modular rocket engine performance prediction program is currently being developed that will integrate physical principles, rigorous mathematical formalism, component and system level test data, and theory-observation reconciliation. This development effort will allow for simple implementation of uncertainty estimates associated with physical relationships. Incorporation of these estimates within the rocket engine performance model will support two crucial functions. First, These uncertainty estimates will represent a confidence band associated with each prediction. Secondly, these estimates will provide a measure of the success of the performance model.

The research required to implement these uncertainty analysis concepts will be conducted within the SSME engine 3001 test program which is currently being conducted on the technology test bed (TTB) test facility. Engine 3001 provides a significantly larger number of propellant property measurements as compared to standard SSME modeling strategies, and ultimately, improve the use of test data in generating performance predictions. Phase 1 involves applying uncertainty analysis techniques to obtain estimates for both the bias and the precision uncertainties of engine measurements. Phase 2 involves incorporating uncertainty analysis techniques to estimate uncertainties associated with model computation. A detail description of the specific tasks to support these phase are described below:

Phase 1 - Perform uncertainty analysis for engine 3001 test measurements.

1. Examine TTB instrumentation systems
2. Evaluate data from previous TTB testing
3. Identify all significant sources of errors
4. Estimate both precision and bias uncertainties for the TTB test measurements
5. Evaluate the use of these measurement uncertainty estimates by the PRM for supporting TTB test analysis

Phase 2 - Perform uncertainty analysis on the physical relationships within the Performance Reconciliation Model (PRM)

1. Identify assumptions and physical analysis on the physical approximations made by representing a real physical process as a mathematical model.
2. Determine methods for quantifying the influence of such assumptions and physical approximations.
3. Estimate the modeling uncertainties.
4. Evaluate the use of these uncertainty estimates within the PRM computations for supporting TTB test analysis.

1.2 Report Overview

This report will describe the determination of uncertainties in the modeling and testing of the Space Shuttle Main Engine test program at the Technology Test Bed facility at Marshall Space Flight Center. Section 2 will present a summary of the uncertainty analysis methodology used and discuss the specific applications to the TTB SSME test program. Section 3 will discuss the application of the uncertainty analysis to the test program and the results obtained. Section 4 presents the results of the analysis of the SSME modeling effort from an uncertainty analysis point of view. The appendices at the end of the report contain a significant amount of information relative to the analysis, including discussions of venturi flowmeter data reduction and uncertainty propagation, bias uncertainty documentation, technical papers published, the computer code generated to determine the venturi uncertainties, and the venturi data and results used in the analysis.

2.0 Uncertainty Analysis

The use and application of uncertainty analysis in engineering has evolved considerably since Kline and McClintock's classic paper¹ in 1953. Developments in the field have been especially rapid and significant over the past decade, with the methods formulated by Abernethy and co-workers² that were incorporated into ANSI/ASME Standards in 1984³ and 1986⁴ being superseded by a more rigorous approach⁵. Publication in late 1993 by the International Organization for Standardization (ISO) of the *Guide to the Expression of Uncertainty in Measurement*⁵ in the name of ISO and six other international organizations has, in everything but name only, established a new international experimental uncertainty standard.

The approach in the ISO Guide deals with "Type A" and "Type B" categories of uncertainties, not the more traditional engineering categories of bias and precision uncertainties, and is of sufficient complexity that its application in normal engineering practice is unlikely. This issue has been addressed by AGARD Working Group 15 on Quality Assessment for Wind Tunnel Testing and by the Standards Subcommittee of the AIAA Ground Test Technical Committee. The documents^{6,7} produced by these groups present and discuss the additional assumptions necessary to achieve a less complex "large sample" methodology that is consistent with the ISO Guide, that is applicable to the vast majority of engineering testing (including most single-sample tests), and that retains the use of the traditional engineering concepts of bias and precision uncertainties. (The chapters on uncertainty methodology in the AGARD⁶ and AIAA⁷ documents were authored by the Principal Investigator of this research program.)

2.1 Overview

The word *accuracy* is generally used to indicate the relative closeness of agreement between an experimentally-determined value of a quantity and its true value. *Error* (δ) is the difference between the experimentally-determined value and the truth, thus as error decreases accuracy is said to increase. Only in rare instances is the true value of a quantity known. Thus, one is forced to

¹ Kline, S. J., and McClintock, F. A., "Describing Uncertainties in Single-Sample Experiments," *Mechanical Engineering*, Vol. 75, 1953.

² Abernethy, R. B., Benedict, R. P., and Dowdell, R. B., "ASME Measurement Uncertainty," *J. Fluids Engineering*, Vol. 107, 1985.

³ American National Standards Institute/American Society of Mechanical Engineers, *Measurement Uncertainty for Fluid Flow in Closed Conduits*, MFC-2M-1983, ASME, 1984

⁴ American National Standards Institute/American Society of Mechanical Engineers, *Measurement Uncertainty*, PTC 19.1-1985 Part 1, ASME, 1986.

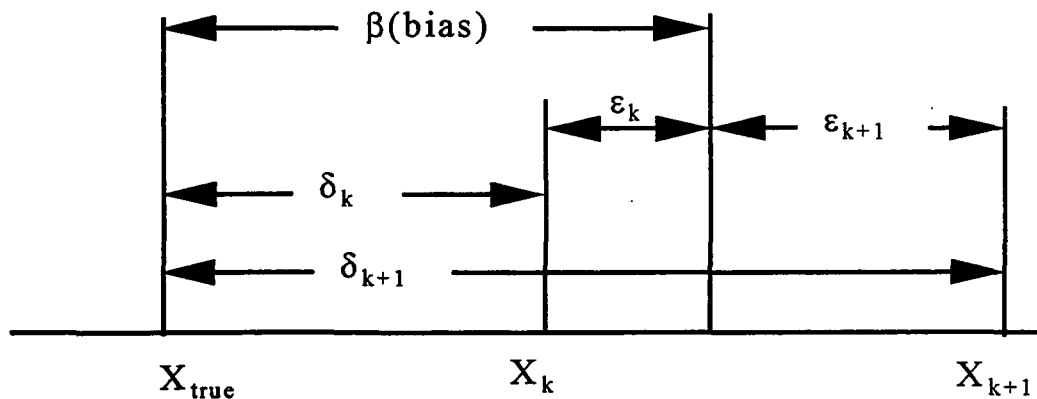
⁵ International Organization for Standardization, *Guide to the Expression of Uncertainty in Measurement*, ISO, ISBN 92-67-10188-9, 1993

⁶ *Quality Assessment for Wind Tunnel Testing*, AGARD-AR-304, 1994.

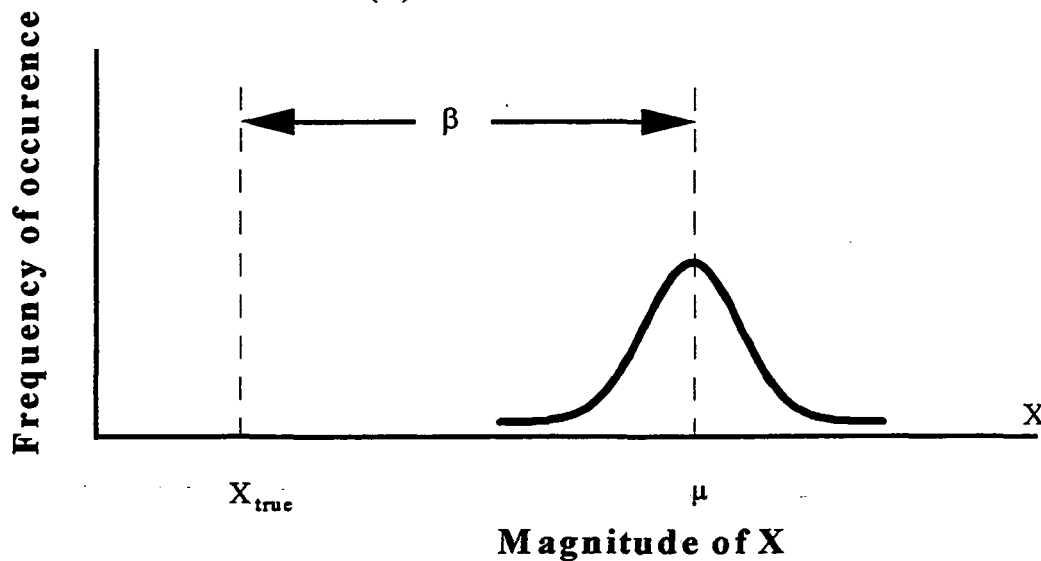
⁷ American Institute of Aeronautics and Astronautics, *Assessment of Wind Tunnel Data Uncertainty*, AIAA Standard S-071, 1995.

estimate error, and that estimate is called an uncertainty, U . Uncertainty estimates are made at some confidence level -- a 95% confidence estimate, for example, means that the true value of the quantity is expected to be within the $\pm U$ interval about the experimentally-determined value 95 times out of 100.

As shown in Figure 1(a), total error δ can be considered to be composed of two components: a *precision* (random) component ϵ and a *bias* (systematic) component β . An error is classified as precision if it contributes to the scatter of the data; otherwise, it is a bias error. It is assumed that corrections have been made for all systematic errors whose values are known. The remaining bias errors are thus equally as likely to be positive as negative.



(a)



(b)

Figure 2.1 Errors in the Measurement of a Variable X :(a) two readings; (b) infinite number of readings.

Suppose that we are making a number of measurements of the value of a variable X that is absolutely steady. The k and $k+1$ measurements are shown in Figure 1(a). Since the bias is a fixed error, it is the same for each measurement. However, the precision error will have a different value for each measurement. It then follows that the total error in each measurement will be different, since the total error is the sum of the bias error and precision error in a measurement.

If we continued to take measurements as previously described until we had a sample of N readings, more than likely as N approached infinity the data would behave as shown in Figure 1(b). The bias error would be given by the difference between the mean (average) value μ of the N readings and the true value of X , whereas the precision errors would cause the frequency of occurrence of the readings to be distributed about the mean value.

As an estimator of β , a bias limit B is defined⁸. A 95% confidence estimate is interpreted as the experimenter being 95% confident that the true value of the bias error, if known, would fall within $\pm B$. A useful approach to estimating the magnitude of a bias error is to assume that the bias error for a given case is a single realization drawn from some statistical parent distribution of possible bias errors. For example, suppose a thermistor manufacturer specifies that 95% of samples of a given model are within ± 1.0 C of a reference resistance-temperature (R-T) calibration curve supplied with the thermistors. One might assume that the bias errors (the differences between the actual, but unknown, R-T curves of the various thermistors and the reference curve) belong to a Gaussian parent distribution with a standard deviation $b=0.5$ C. Then the interval defined by $\pm B = \pm 2b = \pm 1.0$ C would include about 95% of the possible bias errors that could be realized from the parent distribution. (The bias limit is sometimes called the "systematic uncertainty".)

As an estimator of the magnitude of the precision errors (the width of the distribution of readings in Figure 1(b)), a precision limit P is defined⁸. A 95% confidence estimate of P is interpreted to mean that the $\pm P$ interval about a single reading of X_i should cover μ 95 times out of 100. (The precision limit is sometimes called the "precision uncertainty".)

In nearly all experiments, the measured values of different variables are combined using a data reduction equation (DRE) to form some desired result. A good example is the experimental determination of mass flow rate using a venturi meter as discussed in Appendix II of this report. Functionally, the mass flow rate is given as

⁸ Coleman, H. W., and Steele, W. G., *Experimentation and Uncertainty Analysis for Engineers*, Wiley, New York, 1989.

$$W_e = W_e(P, T, \Delta P, d, D, \alpha, C_D) \quad (1)$$

One can envision that errors in the values of the variables on the right hand side of Eq. (1) will cause errors in the experimental result W_e .

A more general representation of a data reduction equation is

$$r = r(X_1, X_2, \dots, X_J) \quad (2)$$

where r is the experimental result determined from J measured variables X_i . Each of the measured variables contains bias errors and precision errors. These errors in the measured values then propagate through the data reduction equation, thereby generating the bias and precision errors in the experimental result, r .

If the "large sample assumption" is made^{6,7} then the 95% confidence expression for U_r becomes

$$U_r^2 = \sum_{i=1}^J \theta_i^2 B_i^2 + 2 \sum_{i=1}^{J-1} \sum_{k=i+1}^J \theta_i \theta_k B_{ik} + \sum_{i=1}^J \theta_i^2 P_i^2 + 2 \sum_{i=1}^{J-1} \sum_{k=i+1}^J \theta_i \theta_k P_{ik} \quad (3)$$

where

$$\theta_i = \frac{\partial r}{\partial X_i} \quad (4)$$

and where the 95% confidence precision limit for a variable X_i is estimated as

$$P_i = 2 S_i \quad N \geq 10 \quad (5)$$

and the sample standard deviation is calculated using

$$S_i = \left[\frac{1}{N-1} \sum_{k=1}^N [(X_i)_k - \bar{X}_i]^2 \right]^{1/2} \quad (6)$$

where the mean value is defined as

$$\bar{X}_i = \frac{1}{N} \left[\sum_{k=1}^N (X_i)_k \right] \quad (7)$$

and P_{ik} is the 95% confidence estimator of the covariance of the precision errors in X_i and X_k , and B_{ik} is the 95% confidence estimator of the covariance of the bias errors in X_i and X_k .

If we define the bias limit (systematic uncertainty) of the result as

$$B_r^2 = \sum_{i=1}^J \theta_i^2 B_i^2 + 2 \sum_{i=1}^{J-1} \sum_{k=i+1}^J \theta_i \theta_k B_{ik} \quad (8)$$

and the precision limit (precision uncertainty) of the result as

$$P_r^2 = \sum_{i=1}^J \theta_i^2 P_i^2 + 2 \sum_{i=1}^{J-1} \sum_{k=i+1}^J \theta_i \theta_k P_{ik} \quad (9)$$

then Eq. (3) can be written as

$$U_r^2 = B_r^2 + P_r^2 \quad (10)$$

and Eqs. (8) and (9) can be viewed as propagation equations for the bias limits and precision limits, respectively.

2.2 Determining Precision Limits

Single Test. When the result is determined from a single test -- that is, at a given test condition the result is determined once using Eq. (2)

$$r = r(X_1, X_2, \dots, X_J) \quad (2)$$

and when the X_i 's are considered single measurements, then Eq. (9) is used to find the precision limit of the result. This situation is often encountered in large scale engineering tests in which measurements of the variables are made at a given set point over a period that is small compared to the periods of the factors causing variability in the experiment. A proper precision limit (one indicative of the dispersion of the variable over several cycles of the factors causing its variation) cannot be calculated from readings taken over such a small time interval. For such data, the measurement(s) of a variable X_i should be considered a single reading -- whether the value of X_i is the average of 10, 10^3 or 10^6 readings taken during the short measurement time. In such a test, the value for the precision limit to be associated with a single reading would have to be based on previous information about that measurement obtained over the appropriate time interval⁹. If previous readings of a variable over an appropriate interval are not available, then the experimenter must estimate a value for P_i using the best information available at that time^{6,7}.

For single tests in which some of the variables (X_2 and X_3 , for instance) can be determined as averages from multiple readings over an appropriate time period but the other variables cannot be, then

$$r = r(X_1, \bar{X}_2, \bar{X}_3, \dots, X_J) \quad (11)$$

⁹ Steele, W. G., Taylor, R.P., Burrell, R. E., and Coleman, H. W., "The Use of Data from Previous Experience to Estimate the Precision Uncertainty of Small Sample Experiments," *ALAA Journal*, Vol. 31, No. 10, 1993.

and Eq. (9) is used to find the precision limit of the result as follows. For the variables that are single readings, the P_1 's are the precision limits determined from previous information or estimated from the best available information. For the averaged variables when N_2 and N_3 are equal to or greater than 10, P_2 and P_3 should be taken as precision limits of means, $(2S_2)/(N_2)^{1/2}$ and $(2S_3)/(N_3)^{1/2}$, with the S 's calculated using Eq. (6). When N_2 and N_3 are less than 10, it is the authors' recommendation that the precision limits used in Eq. (9) for the averaged variables be taken as $(P_2)/(N_2)^{1/2}$ and $(P_3)/(N_3)^{1/2}$, where P_2 and P_3 are determined from previous information, as is done for the single reading variables.

For tests in which multiple readings of *all* of the variables can be obtained over an appropriate period, the following method is recommended.

Multiple Tests. If a test is performed so that M multiple sets of measurements $(X_1, X_2, \dots, X_j)_k$ at the same test condition are obtained, then M results can be determined using Eq. (2) and an average result \bar{r} can be determined using

$$\bar{r} = \frac{1}{M} \sum_{k=1}^M r_k \quad (12)$$

If the M sets of measurements were obtained over an appropriate time period, the precision limit that should be associated with a single result would be

$$P_r = t S_r \quad (13)$$

where t is determined with $M-1$ degrees of freedom and is taken as 2 for $M \geq 10$ and S_r is the standard deviation of the sample of M results

$$S_r = \left[\frac{1}{M-1} \sum_{k=1}^M (r_k - \bar{r})^2 \right]^{1/2} \quad (14)$$

The precision limit that should be associated with the average result is given by

$$P_{\bar{r}} = \frac{P_r}{\sqrt{M}} \quad (15)$$

with P_r given by Eq. (13). Using the large sample assumption, the uncertainty that should be associated with a single result would be

$$U_r^2 = B_r^2 + (2S_r)^2 \quad (16)$$

and with an average result \bar{r}

$$U_{\bar{r}}^2 = B_{\bar{r}}^2 + \left(2S_r / \sqrt{M} \right)^2 \quad (17)$$

with $B_{\bar{r}}$ given by Eq. (8).

Correlated Precision Uncertainties. The P_{ik} terms in Eq. (3) take into account the possibility of precision errors in different variables being correlated. These terms have traditionally been neglected^{1,3,4,5,7}, although precision errors in different variables caused by the same uncontrolled factor(s) are certainly possible and can have a substantial impact on the value of the precision limit¹⁰. In such cases, one would need to acquire sufficient data to allow a valid statistical estimate of the precision covariance terms to be made if using Eq. (3). Note, however, that the multiple tests approach using Eq. (14) implicitly includes the correlated error effect -- a definite advantage when multiple sets of measurements over an appropriate time period are available.

2.3 Estimating Bias Limits

Bias Limits of Individual Variables. When attempting to estimate the bias limits B_i of the individual variables in Eq. (8), one might separate the bias errors which influence the measurement of a variable into different categories: calibration errors, data acquisition errors, data reduction errors, test technique errors, etc. Within each category, there may be several elemental sources of bias. For instance, if for the J th variable, X_J , there are M elemental bias errors identified as significant and whose bias limits are estimated as $(B_J)_1, (B_J)_2, \dots, (B_J)_M$, then the bias limit for the measurement of X_J is calculated as the root-sum-square (RSS) combination of the elemental limits

$$B_J = \left[\sum_{k=1}^M (B_J)_k^2 \right]^{1/2} \quad (18)$$

The elemental bias limits, $(B_i)_k$, must be estimated for each variable X_i using the best information one has available at the time. In the design phase of an experimental program, manufacturer's specifications, analytical estimates and previous experience will typically provide the basis for most of the estimates. As the experimental program progresses, equipment is assembled, and calibrations are conducted, these estimates can be updated using the additional information gained about the accuracy of the calibration standards, errors associated with the calibration process and curvefit procedures, and perhaps analytical estimates of installation errors.

As Moffat¹¹ suggests, there can be additional conceptual bias errors resulting from not measuring the variable whose symbol appears in the data reduction equation. An example would be a point temperature measurement interpreted to be indicative of a cross-section averaged temperature, but there may be a cross-sectional variation of temperature, which may or may not have a

¹⁰ Hudson, S. T., Bordelon, W., and Coleman, H. W., "Effect of Correlated Precision Errors on the Uncertainty of a Subsonic Venturi Calibration," AIAA-95-0797, 1995.

¹¹ Moffat, R. J., "Describing the Uncertainties in Experimental Results," *Experimental Thermal and Fluid Science*, Vol. 1, 1988.

predictable profile, causing the "average" value to be different than the point value. Hence, the inclusion of an elemental bias term for the conceptual error would be appropriate.

Correlated Bias Limits. Correlated bias limits are those that are not independent of each other, typically a result of different measured variables sharing some identical elemental error sources. It is not unusual for the uncertainties in the results of experimental programs to be influenced by the effects of correlated bias errors in the measurements of several of the variables. A typical example occurs when different variables are measured using the same transducer, such as multiple pressures sequentially ported to and measured with the same transducer or temperatures at different positions in a flow measured with a single probe that is traversed across the flow field. Obviously, the bias errors in the variables measured with the same transducer are not independent of one another. Another common example occurs when different variables are measured using different transducers all of which have been calibrated against the same standard, a situation typical of the electronically scanned pressure (ESP) measurement systems in wide use in aerospace test facilities. In such a case, at least a part of the bias error arising from the calibration procedure will be the same for each transducer, and thus some of the elemental bias error contributions in the measurements of the variables will be correlated.

The B_{ik} terms in Eq. (8) must be approximated -- there is in general no way to obtain the data with which to make a statistical estimate of the covariance of the bias errors in X_i and the bias errors in X_j . The approximation of such terms was considered in detail in Ref. 12, where it was shown that the approach that consistently gives the most satisfactory approximation for the correlated bias limits was

$$B_{ik} = \sum_{\alpha=1}^L (B_i)_{\alpha} (B_k)_{\alpha} \quad (19)$$

where L is the number of elemental systematic error sources that are common for measurements of variables X_i and X_k .

If, for example,

$$r = r(X_1, X_2) \quad (20)$$

and it is possible for portions of the bias limits B_1 and B_2 to arise from the same source(s), then Eq. (8) gives

¹² Brown, K. K., Coleman, H. W., Steele, W. G., and Taylor, R. P., "Evaluation of Correlated Bias Approximations in Experimental Uncertainty Analysis," AIAA 94-0772, 1994.

$$B_r^2 = \theta_1^2 B_1^2 + \theta_2^2 B_2^2 + 2 \theta_1 \theta_2 B_{12} \quad (21)$$

For a case in which the measurements of X_1 and X_2 are each influenced by 4 elemental error sources and sources 2 and 3 are the same for both X_1 and X_2 , Eq. (18) gives

$$B_1^2 = (B_1)_1^2 + (B_1)_2^2 + (B_1)_3^2 + (B_1)_4^2 \quad (22)$$

and

$$B_2^2 = (B_2)_1^2 + (B_2)_2^2 + (B_2)_3^2 + (B_2)_4^2 \quad (23)$$

while Eq. (19) gives

$$B_{12} = (B_1)_2(B_2)_2 + (B_1)_3(B_2)_3 \quad (24)$$

2.4 Application of Uncertainty Analysis to TTB Testing

The focus in this effort is to identify the uncertainty that should be associated with a measured variable such as temperature or pressure or with a determined result such as flowrate that is calculated using a number of measured variables. The uncertainty given by Eq. (16) -- that associated with a single result -- is the appropriate uncertainty to use when data from a single TTB test are compared with the output of a predictive model.

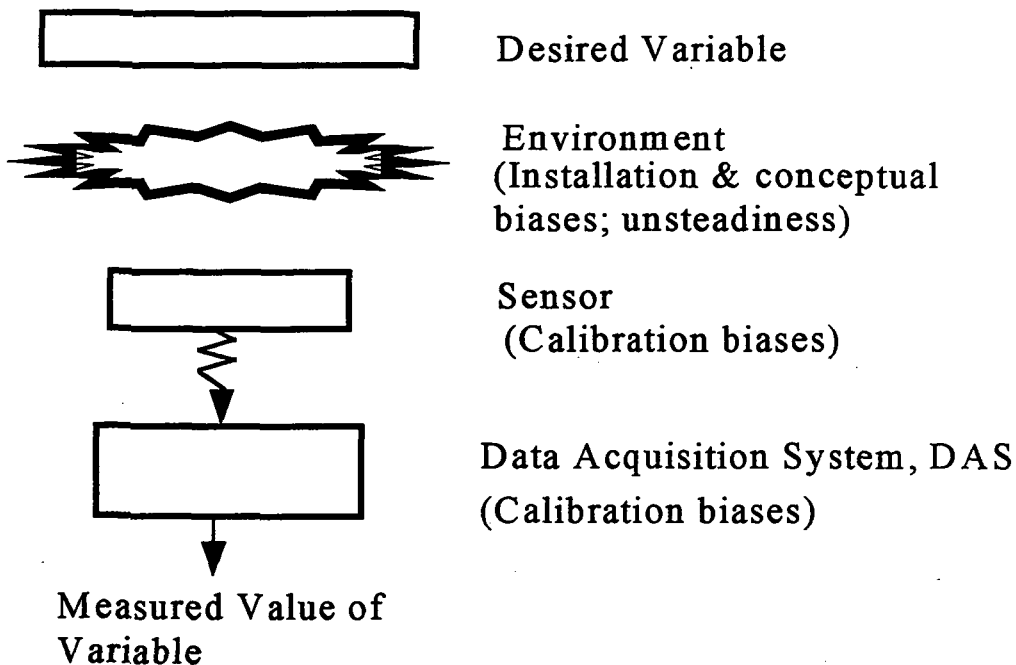


Figure 2.2 Schematic of TTB Measurement Process from an Error Sources Viewpoint

Figure 2.2 shows a schematic of the viewpoint used in identifying error sources that contribute to the overall uncertainty. The desired variable is taken to be the one with which a model output will be compared -- a cross-section averaged temperature, for example, that would usually be referred to as "the temperature" of the flow at a particular location in the engine. If the sensor responds to temperature at a point, then an installation or conceptual bias exists due to the sensor not actually responding to the desired variable (the average temperature). This is an elemental source that must be included in Eq. (18), and it is potentially one of the dominant elemental sources in temperature and pressure data in TTB testing. The estimation of these sources is a task in the follow-on effort to the work documented in this report. The traditional "measurement uncertainty" sources are shown as biases in the sensor calibration and biases in the calibration of the data acquisition system (DAS). Additionally, the effect of unsteadiness in, and due to, the operating environment must be considered since the sensor calibrations and DAS pre-test calibration checks are not done with the engine operating, and the unsteadiness certainly can have an effect on the final system output - the measured value of the variable.

Choice of the appropriate precision limit to use with TTB data needs to be carefully done. A precision limit determined using a standard deviation from a time slice during one test gives information about the steadiness of the "steady state" at that operating condition during that particular test, but includes no effects of the test-to-test variation of the variable at that operating condition. As discussed in Section 3, the authors believe that computing a standard deviation of a variable or result from multiple tests, all of which were at the same operating condition, gives the appropriate precision estimate for use in discussing the uncertainty in a measured TTB variable. It is also the appropriate precision limit to consider when comparing the results from one test to results from another test in an effort to determine if a change in component, for instance, had any discernible effect on the value of the result.

Detailed discussion of the uncertainty estimates associated with TTB flowrate measurements is given in Section 3 of this report.

2.5 Application of Uncertainty Analysis in SSME Modeling

When comparing output of a model with experimental data, the uncertainties that should be associated with the model predictions must be considered for proper conclusions to be drawn. In the past, most of the work reported in this area has simply considered the sensitivity of the model output to uncertainties in the input data. This obviously does not include any uncertainties in the model itself and thus is not a satisfactory approach. In this research effort, we have divided the sources that cause uncertainty in the model output into three categories: (1) uncertainties due to assumptions and approximations in the model, (2) uncertainties due to the incorporation of previous experimental data into the model, and (3) uncertainties due to the

numerical solution algorithm. Consideration of the third category is not within the scope of this program.

The first category, uncertainties due to assumptions and approximations in the model, does not include the installation and/or conceptual bias source shown in Figure 2.2 and discussed above since that uncertainty is associated with the measured value. Consider the temperature at a particular position in the flow. The uncertainty associated with the measured value of the temperature includes the effect of making a point measurement but desiring a cross-sectional averaged value. The inability of the model to calculate a correct average temperature at a particular location because the one-dimensional flow approximation has been made results in an uncertainty in the predicted temperature. (Stated another way, if the model predicts the correct average temperature at a particular location, then the one-dimensional flow approximation has caused no uncertainty in the model output.)

The uncertainties due to the incorporation of previous experimental data in the model arise when material property data is used, when valve resistance characteristics are used, when pump maps are used, etc. These are all instances in which previous experimental data has been used by replacing the data with curvefits. The original data contained uncertainties, but the curvefit equations used in the predictive models have been treated as the "truth" in most previous considerations of uncertainty in model outputs. Adding further complication, there is no accepted way of estimating the influence of systematic uncertainties on the uncertainty that should be associated with a regression. This aspect has been investigated in this program and is discussed in Section 4. An AIAA paper reporting the progress of this effort is included as Appendix IV.

3.0 Results of Application of Uncertainty Analysis to TTB Testing

An investigation to determine the experimental uncertainties associated with the test measurements from the SSME Engine 3001 installed in the Technology Test Bed facility was conducted. This investigation consisted of reviewing existing documents, discussions with NASA personnel, review of other technical literature, and new analyses. Since the thermodynamic performance analysis of the SSME was the motivation behind this contractual effort, the pressure, differential pressure, temperature, and mass flow rate measurements were the focus of the investigation. Initial discussions concluded to initially focus on the determination of uncertainty in the flowrate measurements, with particular emphasis on the venturi flowmeter determinations. This section will discuss the information obtained upon which the assessment of individual uncertainty source estimates were made.

3.1 Measurement System

The Technology Test Bed test measurement system is described here as all components between the phenomena being measured and the final computer data file in engineering units, including the sensors, transducers, data acquisition systems, and data reduction routines. A previous study by Sverdrup Technology¹³ studied the MFSC test facilities to assess the uncertainty in the measurement systems and to assess if any significant discrepancies existed between test areas. That report identified and quantified the uncertainties between the sensor and the final data file. However, several important points about this study need to be made. First, this study did not assess the uncertainty in a given measurement during the engine test, therefore any additional uncertainty due to the operating environment was not assessed. Secondly, no installation or conceptual uncertainties were considered. Finally, the study was performed in 1992 and prior to the adoption of new standards for the assessment of uncertainties⁵, and some of the specific procedures used to combine uncertainty sources were not in accordance with the current standard.

The specific aspects of the TTB measurement system were reviewed with the TTB data acquisition personnel. This review showed the procedures and techniques being used are self-consistent, with a pre-test procedure conducted which recalibrates the data acquisition system prior to each test. This ensures that measurement system drift and gross errors do not go undetected.

3.2 Analysis of Previous TTB Test Data

¹³ Fish, James E., NASA/MSFC Test Area Measurement System Uncertainty Study, Sverdrup Technology, Inc., MSFC Group, Report No. 335-002-92, October 1992.

The review of previous test data was cumbersome due to the format of the data being incompatible with commercially available software and the initial difficulties in utilizing MSFC resources for data analysis. To achieve a set of data to review which could be defined as the "same" hardware, tests TTB039 through TTB 051 were chosen. These tests were conducted with Engine 3001 with the large throat combustion chamber and a consistent set of other hardware. Another difficulty in the data analysis to assess uncertainties was the lack of repetition in the test profiles, with each test being conducted for the analysis of specific performance aspects. The data was reviewed in the full sample-rate format (25 or 50 samples/sec) and at the reduced sample-rate format (1 sample/sec). Because of inconsistencies in the way test data is stored in the computer systems, all of the measurements for these tests are not readily accessible. For example, most of the venturi mass flowrate calculations are not available from the computer systems being used. This created problems in assessing the precision uncertainties for the venturi flowrate measurements, particularly trying to assess test-to-test precision uncertainty behavior. To alleviate this situation a new computer program was developed by the COTR to access the test data directly and compute the mass flowrates. This program was then modified by the researchers to calculate the uncertainties associated with the given test data. A discussion of this new software tool is given in Section 3.5.

3.3 Determination Of Mass Flow Rate Uncertainties

The mass flow rate uncertainties for the venturi flowmeters were determined using the methodology previously discussed in Section 2. The data reduction equation is the equation for mass flow rate presented in Appendix III and the expression for the uncertainty in the mass flow rate and the necessary partial derivatives are presented in Appendix IV. This expression shows the density of the fluid within the square root, however the density of the fluid cannot be explicitly measured and must be determined within the data reduction by using the measured pressure and temperature and some equation of state.

The bias limits used in the uncertainty propagation equations were estimated based upon the information gathered from the available documentation, discussions with TTB personnel, and engineering experience. The values used in the calculation of the flowrate uncertainties are shown in Appendix V.

Potentially significant bias uncertainties to be addressed in the TTB measurements are the conceptual bias uncertainties discussed in Section 2. The conceptual bias uncertainties in the temperature and pressure measurements are particularly important in this effort because of the interest in comparing the experimental results with the analytical predictions. In many of the SSME measurements the flowfield is highly

complex due to the sharp turns and bends, valves, pump and turbine inlets and discharges, and other complicating factors. These factors accentuate the difference between the physical quantity at the sensor and the quantity for which the measurement is desired, typically an average value at a cross-section. Assessment of these bias uncertainties has not been accomplished. These assessments will require extensive review of the measurement, the sensor and its installation, the thermodynamic and fluid dynamic flowfield, and their interaction. This detailed analysis of the measurements will take place during the next contract period and based upon a prioritized list developed with the COTR.

The precision limits for the mass flowrate uncertainties are dependent upon the question being asked, or rather, what is purpose for the information. Precision limits can be calculated in many different ways, but the interpretation of the precision limit and the use of it depends upon data used to calculate it. The variables which must be considered for the precision limit calculation include:

- engine number
- specific engine component configuration
- engine test(s)
- power level
- test profile
- specific engine adjustments
- time slice within the test
- data sample rate (data points used for standard deviation calculation)

The precision limits for the flowrate uncertainties were based upon review of the flowrate data for the chosen time slice. Precision limits were estimated in two primary ways. First, one was based upon the full sample-rate data within each test. The second precision limit was estimated based upon averaging the full sample-rate data over a given time slice, for a given test, at a chosen power level to provide a single data point for that test condition and using similar points from other tests to estimate a precision limit.

The uncertainty in the thermophysical property data must be included in the uncertainty analysis since there was some experimental uncertainty in the original experiments upon which the property tables were developed. If the property data is represented by a curve-fit of the experimental data an uncertainty associated with the data and with the curve-fit must be included. The venturi flowrate data reduction utilizes the thermophysical property routine GASP¹⁴. The GASP documentation shows the uncertainty in density

¹⁴ Hendricks, Robert C., Baron Anne K., and Peller, Ildiko C., "GASP - A Computer Code for Calculating the Thermodynamic and Transport Properties for Ten Fluids: Parahydrogen, Helium, Neon,

for liquid hydrogen and liquid oxygen to be within 0.25%. The GASP program is based upon National Bureau of Standards data for the thermodynamic properties of hydrogen and oxygen.

3.4 Calibration of Mass Flowmeters, Determination of Discharge Coefficient, C_D

The accurate determination of the mass flow rate for cryogenic rocket propellants is difficult because of the special problems presented. These problems arise because of the extremely cold temperatures, the property data uncertainty, the difference in density and viscosity with respect to the calibration fluid, and limitations on the calibration procedures because of safety considerations. Each of these can introduce an uncertainty in the mass flow rate determination.

The accurate determination of a mass flow rate depends upon the ability to trace the output from a given device back to a standard certified by the National Institute of Standards and Technology (NIST) or some other respected standard. The basic problem with cryogen flowmeters is that there are very limited facilities which can produce an accurate standard using the actual cryogenic fluid. The facilities which do exist are limited to the calibration of liquid nitrogen flows, or have limited capacity. A few facilities exist which can perform calibration with the appropriate cryogen, but the reference standard in these systems use a meter which was calibrated with water and then adjusted for the particular cryogenic fluid. This procedure relies on the concept of dynamic similarity, matching the Reynolds number of the test fluid with the Reynolds number of the calibration fluid, and making corrections for the dimensional changes due to thermal contraction and other miscellaneous effects. A literature survey indicates that very little work has taken place to assess the accuracy of this procedure, primarily due to the cost and complexity involved with developing the necessary experiments with liquid oxygen and liquid hydrogen. Most of the documented work describes the calibration and use of turbine-type flowmeters. Since the facility flowmeters are turbine meters this is an important aspect to study. One of these studies conducted with liquid oxygen which used liquid nitrogen as the calibration fluid indicated that there is a difference on about the same order of magnitude as the uncertainty in the physical property data, about 0.25%¹⁵. This study also used liquid argon and the researcher concluded that turbine flowmeters have a dependence on the fluid properties. However, that study was too limited to make a firm conclusion. Since a property dependence was

Methane, Nitrogen, Carbon Monoxide, Oxygen, Fluorine, Argon, and Carbon Dioxide," NASA TN D-7808, February 1975.

¹⁵ Brennan, J.A. LaBrecque, J.F., and Kneebone, C.H., "Progress Report on Cryogenic Flowmetering at the National Bureau of Standards," *Instrumentation in the Cryogenic Industry, Volume 1*, Proceedings of the first Biennial Symposium on Cryogenic Instrumentation, October 11-14, 1976, Held in Conjunction with the 31st Annual ISA Conference and Exhibit.

noted between the cryogenic argon and nitrogen in comparison with the cryogenic oxygen, one would expect a difference between water at room temperature and cryogenic oxygen. Another study¹⁶ investigated the use of calibrating the liquid hydrogen turbine flowmeters with high-pressure nitrogen because: "Comparisons have been made between water and liquid hydrogen calibrations. Results of these comparisons indicated that for inaccuracies less than 1 percent at full-scale flow, water calibrations are inadequate in predicting the meter constant for liquid-hydrogen flow in turbine-type flowmeters."

Very little literature is available which discusses attempts to assess the uncertainty due to differences in the calibration fluids for differential pressure producer mass flowmeters, such as venturis and orifices, particularly for the operating Reynolds numbers of the SSME venturis. However, it seems obvious from a review of the fluid and thermodynamic processes going on in the venturi that a non-negligible difference exists. The description of the venturi flowmeter data reduction equation shown in Appendix III and the Rocketdyne venturi calibration report¹⁷ show that significant assumptions and approximations are made to achieve the data reduction equations. Two of the fundamental assumptions are that the flow through the venturi is adiabatic and one-dimensional, which is not true during engine operation. Another significant factor is that none of the venturis are installed with the recommended length of upstream straight duct. Rocketdyne attempted to account for this problem by calibrating the venturis with the "as-installed" ducts connected, however they could not reproduce the other flow characteristics, such as flow swirl, turbulence, oscillations, etc.

The Rocketdyne venturi calibration report develops a polynomial curve-fit to obtain the value of the discharge coefficients where the curve-fit is based upon the Reynolds number of the flow through the venturi. They recommended using an iterative method to determine the discharge coefficient to use to determine flowrate through the venturi. For all of the venturi flowmeters calibrated with water in Rocketdyne's facility dynamic similarity could not be obtained, that is, the flowmeters could not be calibrated at the Reynolds number expected during an engine test. In fact, most of the calibrations were performed at a fraction of the operating Reynolds number, from 1.7% to 10%, and the curve-fits were extrapolated out to the operating condition.

¹⁶ Szanislo, Andrew J., and Krause, Lloyd N., "Simulation of Liquid-Hydrogen Turbine-Type Flowmeter Calibrations using High-Pressure Gas," NASA TN D_3773.

¹⁷ Lepore, Frank A., Rocketdyne Division, Space Shuttle Main Engine No. 3001, Technology Test Bed, Differential Flowmeters Calibration Final Report, Contract No. NAS8-27980, March 1980.

The extrapolation of the calibration curve-fits and the use of a different fluid for the calibration introduce an uncertainty which must be associated with the determination of the mass flowrate. In the absence of performing detailed experiments to assess these uncertainties, an estimate must be made based upon the existing information. The information upon which to base these estimates are the calibration data figures in the Rocketdyne report and the literature review previously discussed. A review of the calibration data figures shows that a curve was fit through the data, but for which a different curve would produce a substantially different result at the operating conditions. Figure 3.1 can be used as an example. The curve generated by Rocketdyne is used in the data reduction, however it can be observed that a significantly different calibration curve would have been obtained if a higher order curvefit was used, or if the last few data points were more heavily weighted.

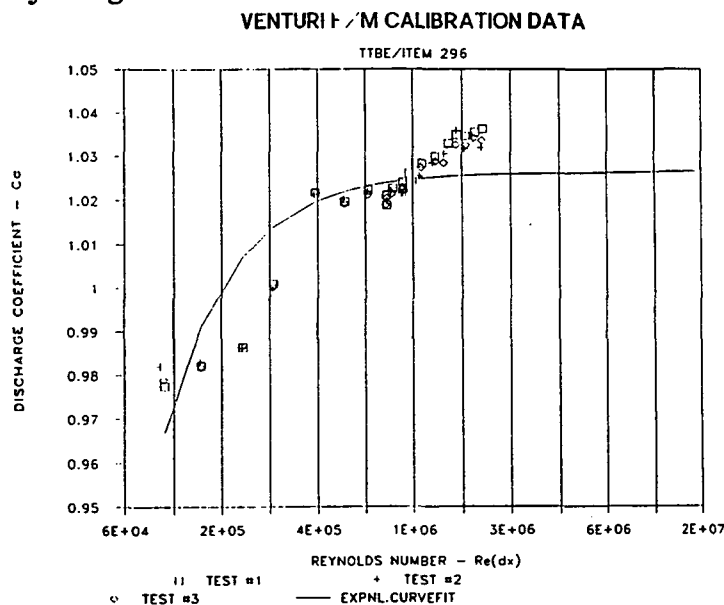


Figure 3.1 Venturi #296 Calibration Curve

3.5 Venturi Flowmeter Uncertainty Computer Program

A computer program was developed to calculate the uncertainty in the mass flowrate determinations. This program was based upon a program initially developed by the COTR to calculate the flowrates for the venturi flowmeters and expanded to perform the uncertainty calculations. This program resides within the EADS10 (Engineering Acquisition and Data System) computer system and assesses the raw, full sample-rate data for all of the engine measurements. The program uses the measured pressure, differential pressure, and temperature for each venturi, combined with the specific dimensional data and other constants (such as discharge coefficient), averages the data for the chosen time slice and calculates the mass flowrate. The bias limits and precision limits for the uncertainty sources for each

venturi are stored in the program as constants and propagated through data reduction equation using the uncertainty propagation equation presented in Appendix IV. The only correlated bias uncertainty included in the uncertainty propagation equation is the uncertainty in the venturi dimensions. All other possible bias correlations were considered negligible, particularly with respect to the magnitude of the discharge coefficient bias uncertainty. The partial derivatives are determined numerically using a finite difference technique, often referred to as a jitter routine. The data used for the bias limits and precision limits and a short description of how the estimates were obtained is shown in Appendix V.

The TTB venturi data reduction utilizes the methodology recommended by Rocketdyne which includes an iterative technique to determine the value of the discharge coefficient. The purpose behind the iterative technique is to provide a value for the discharge coefficient from the polynomial curvefit generated during the calibration. However, the value of the discharge coefficient does not change much within the operating range, so that using a constant value of C_D is more appropriate. The iterative technique tends to encourage a higher level of confidence than is warranted, based upon the previously discussed uncertainties in the discharge coefficients. The program developed to determine the uncertainty in the mass flowrates does not use this iterative technique and provides essentially the same values for the calculated flowrate.

This program will allow the uncertainties in the venturi flowrates to be determined from any TTB test and allows the recalculation of the uncertainties when the bias and precision limits for the individual venturis are updated.

3.6 Flowrate Uncertainty Results

Tests TTB039 through TTB050 were chosen as the basic data to conduct the uncertainty analysis upon. These tests were conducted with the large-throat combustion chamber and represented engine configurations upon which comparisons to the analytical model were desired. A time slice at each of three power levels (100% RPL, 104% RPL, and 109% RPL) was chosen, and the full-sample rate (50 samples/sec) data was averaged over the time slice to obtain a single data point for each PID at each power level. The time slices used at each power level are shown in Table 3.1.

The averaged data was used in the venturi mass flowrate and mass flowrate uncertainty program to obtain the venturi flowrate and the bias limit for each power level for each test. It was observed that the bias limit, as a percent of the flowrate, was constant for all tests and all power levels. The venturi mass flowrate, the bias limit, and the percent bias uncertainty calculated for each of the tests considered at each power level and for each

Test #	100% RPL	104% RPL	109% RPL
TTB039	80-85 sec	95-100 sec	195-200 sec
TTB040	60-65 sec	80-85 sec	120-125 sec
TTB041	80-85 sec	95-100 sec	195-200 sec
TTB042	80-85 sec	95-100 sec	195-200 sec
TTB043	50-55 sec	75-80 sec	34-39 sec
TTB044	45-50 sec	100-105 sec	34-39 sec
TTB045	100-105 sec	150-155 sec	185-190 sec
TTB047	10-15 sec	35-40 sec	50-55 sec
TTB048	115-120 sec	85-90 sec	50-55 sec
TTB049	145-150 sec	50-55 sec	25-30 sec
TTB050	16-21 sec	25-30 sec	34-38 sec

Table 3.1 Time Slices used for Precision Limit Determinations

* TTB046 not included because test profile did not include a steady-state time slice at chosen power levels.

venturi are shown in the tables in Appendix VII. The bias limits, standard deviations, and uncertainties for the venturis are shown in Table 3.2, for 100% rated power level. Appendix VII contains the mass flowrate data for the tests from which the standard deviations were calculated as well as the calculated bias limits for each test. It is observed that the bias limit is primarily a function of the bias uncertainty in the discharge coefficient.

The preferred method of determining the precision limit for a result is to calculate the standard deviation of the results (mass flowrates in this case) instead of propagating the precision limits of the individual variables. This allows for any correlated precision error sources to be inherently accounted for. Thus a set of tests which represents the nominal engine configuration is desired. The series of tests between TTB039 and TTB050 was chosen because the engine configuration was based upon the large-throat combustion chamber and design changes. However, during this series of tests a Taguchi test matrix was conducted and engine components were varied simultaneously. The changes between the standard Rocketdyne designed high pressure oxidizer turbopump (HPOTP) and the Pratt and Whitney HPOTP, and changes in the high pressure fuel turbopump create problems with data analysis. Since these engine components have different performance the grouping is not appropriate. If the components changed had all been "line-replacement" units, where each unit is expected to provide the same performance as the replaced unit the grouping would be meaningful. The specific engine component configuration for each test is shown in Figure A-VI.1 in Appendix VI. Review of this table showed that four tests were conducted with Rocketdyne HPOTP's, with the other major components being the same or being line replacement units, thus this series of four was grouped. Other specific engine test variable changes are potentially responsible for some of the precision uncertainty, but the lack of test profile repetition in the TTB program makes specific distinctions difficult.

A standard deviation for the flowrates for the ten tests, as well as the four-test group, designated as RD HPOTP, was obtained, as shown Appendix VII. When these standard deviations are combined with the calculated bias limits using the "large-sample" approximation the results for 100% RPL are shown in Table 3.2, below.

PID	Venturi ID	W (lb/sec)	B _w (%)	S _w (%) 10 Tests	S _w (%) RD HPOTP	U _w (%) 10 Tests	U _w (%) RD HPOTP
8801	LPFT Inlet	28.0	2.1	2.3	1.9	5.1	4.3
8818	CCV Inlet	73.8	3.0	3.4	0.6	7.4	3.2
8815	Nozzle Clint #1	13.8	2.1	5.5	4.1	11.2	8.5
8816	Nozzle Clint #2	13.5	2.1	4.7	1.2	9.6	3.2
8817	Nozzle Clint #3	13.6	2.1	18.5	7.5	37.1	15.1
8802	LPOT Inlet	188.	2.1	2.4	1.8	5.2	4.2
8819	HPOP Discharge	947.	2.1	1.2	0.8	3.2	2.6
8804	OPB LOX	26.1	2.1	8.7	1.6	17.5	3.8
8805	OPB LH ₂	35.7	2.0	3.6	1.5	7.5	2.5
8810	FPB LOX	61.3	2.1	4.6	3.9	9.4	8.1

Table 3.2 - Venturi Mass Flowrates and Flowrate Uncertainties @100% RPL

PID #8817, Nozzle Coolant #3 is shown to have a very large precision uncertainty at all three power levels. Further review of the test data shows that the large standard deviation is caused by exceptionally low measurements during tests TTB043 and TTB045. This could be an actual result due to a specific hardware characteristic, a random phenomena, or due to an instrumentation malfunction. From the information available a specific cause cannot be identified and thus the data point cannot be eliminated.

It is interesting to note from Tables A-VII.1 - A-VII.6 in Appendix VII that the standard deviation of the total of the 10 venturi flowmeters is much lower than the standard deviation of any of the individual flowmeters, 0.8% at 100% RPL, for the 10 tests and 0.5% for the four tests. Since the primary engine control point is the main combustion chamber pressure, and since the chamber pressure is directly proportional to the total flowrate (for a set mixture ratio), this result is not surprising. It also indicates the overall performance variation from test-to-test is small, however the variation within the engine changes from test-to-test as the engine re-balances due to specific hardware changes.

The input data for the venturi flowrate calculations are shown in Table A-VI.2 and show that the pressure and temperature measurements have a small standard deviation and the differential pressure measurements have a large test-to-test variation. This verifies the opinion of the TTB

instrumentation engineers that the differential pressure measurements were not as accurate as the other measurements.

4.0 Application of Uncertainty Analysis in SSME Modeling

Assessing the uncertainties in the output of the SSME model is important to making decisions based upon those results. Uncertainties in the model output can be separated into three general categories, uncertainties due to modeling assumptions and approximations, uncertainties due to the numerical solution, and uncertainties due to using previous experimental information.

The primary methodology identified in the literature for assessing uncertainties in analytical models is a perturbation technique, perturbing the model inputs and checking the resultant output. This technique cannot adequately account for all of the identified modeling uncertainties and another methodology is needed.

The model of the SSME being used in this effort is a model based upon the rocket engine modeling platform developed by Pratt and Whitney, ROCETS (Rocket Engine Transient Simulations). This model provides a more structured format wherein the individual engine components are modeled in individual modules and the modules are solved simultaneously to provide the performance prediction.

4.1 Modeling Assumptions and Approximations

When a mathematical or engineering model of a physical system is developed certain assumptions and approximations about the system are made to simplify the system to one for which mathematical expressions can describe. By making these simplifications an error is introduced and the model cannot exactly describe the physical system.

Some of the primary assumptions and approximations made within the SSME model include:

- 1-dimensional
- fully developed
- steady-state
- adiabatic
- ideal gas

The primary problem with attempting to assess uncertainties with respect to these assumptions and approximations is that if the uncertainty to associate with a particular assumption or approximation can be estimated, then the model could be improved to include this estimate instead of trying to estimate the uncertainty. For example, it was determined by a researcher working on a complementary effort that a turbine exit temperature was being predicted using an ideal gas, constant specific heat approximation, which for the specific temperature range of interest was a poor approximation. Instead

of trying to estimate an uncertainty to associate with that approximation the model is being altered to include a better thermodynamic description of the process. Hence, extensive effort within this research program was not warranted in this area.

4.2 Numerical Solution Uncertainties

When the system of equations is solved numerically the exact solution will not be obtained. The error in the numerical solution is a combination of the round-off error specific to the computer system and the truncation error in the numerical solution scheme. The magnitude of the numerical solution uncertainties are assumed to be negligible with respect to the other uncertainties. Hence, extensive effort was not warranted in this area under this contract.

4.3 Uncertainties from using previous experimental information

In all of the component modules, information from previous testing is used. For example, the model of the liquid oxygen flow through a given duct or through a given valve is based upon its component testing, which provides an equation for the resistance through the duct as function of the flowrate. This test information is often reduced to the form of a line or curve.

The value of the discharge coefficient used in the test data reduction or the polynomial constants in the thermodynamic property routines are examples of using previously obtained uncertain test information in a model.

4.4 Linear Regression Uncertainty

The methodology to assess the uncertainty in the coefficients of a linear regression were developed as part of this effort. The uncertainty analysis methodology discussed in Section 2 was applied to the expressions for the regression coefficients to develop the technique. The details of this methodology were presented at a recent conference¹⁸. This technical paper is attached in Appendix IV. The work presented in this paper demonstrates that this technique provides a method to determine the uncertainty in linear regression coefficients, and includes the effect of some correlated bias uncertainties. This technique is the first methodology which considers bias uncertainties and correlated bias uncertainties in determining regression coefficient uncertainties.

The methodology is fully developed at this time for linear regressions, but extension to the more general regression forms used in most models requires additional effort.

¹⁸ Brown, Kendall K., Coleman, Hugh W., and Steele, Glenn W., "Estimating Uncertainty Intervals for Linear Regression," AIAA Paper 95-0796, 33rd Aerospace Sciences Meeting and Exhibit, January 9-12, 1995, Reno, NV.

5.0 Summary

An uncertainty analysis of the SSME test program at the Technology Test Bed facility has shown that non-negligible uncertainties exist in the determination of the mass flowrates, ranging from 2% to up to 10%, and even larger in some cases. The bias uncertainty is dominated by the bias limit in the experimentally determined venturi discharge coefficient. The bias limits for the venturis can be refined as more, and more specific, information about the instrumentation and the installation bias uncertainties is obtained.

The uncertainty intervals provided in this report can be used for comparison to performance prediction models; however the engine configuration being modeled must be representative of the engine configuration for which the precision uncertainty was determined.

A primary source of uncertainty in the analytical modeling of the SSME is from the use of previous experimental information. This information is usually utilized in the form of regressions or curvefits. Initial research efforts to determine a methodology to properly account for the uncertainty in the regression coefficients has shown to be promising, and work is continuing to develop the methodology.

6.0 Bibliography

- 1 Kline, S. J., and McClintock, F. A., "Describing Uncertainties in Single-Sample Experiments," *Mechanical Engineering*, Vol. 75, 1953.
- 2 Abernethy, R. B., Benedict, R. P., and Dowdell, R. B., "ASME Measurement Uncertainty," *J. Fluids Engineering*, Vol. 107, 1985.
- 3 American National Standards Institute/American Society of Mechanical Engineers, *Measurement Uncertainty for Fluid Flow in Closed Conduits*, MFC-2M-1983, ASME, 1984.
- 4 American National Standards Institute/American Society of Mechanical Engineers, *Measurement Uncertainty*, PTC 19.1-1985 Part 1, ASME, 1986.
- 5 *Guide to the Expression of Uncertainty in Measurement*, International Organization for Standardization, Geneva, Switzerland, 1993.
- 6 *Quality Assessment for Wind Tunnel Testing*, AGARD-AR-304, 1994.
- 7 American Institute of Aeronautics and Astronautics, *Assessment of Wind Tunnel Data Uncertainty*, AIAA Standard S-071-1995, 1995.
- 8 Coleman, H. W., and Steele, W. G., *Experimentation and Uncertainty Analysis for Engineers*, Wiley, New York, 1989.
- 9 Steele, W. G., Taylor, R. P., Burrell, R. E., and Coleman, H. W., "The Use of Data from Previous Experience to Estimate the Precision Uncertainty of Small Sample Experiments," *AIAA Journal*, Vol. 31, No. 10, 1993.
- 10 Hudson, S. T., Bordelon, W., and Coleman, H. W., "Effect of Correlated Precision Errors on the Uncertainty of a Subsonic Venturi Calibration," AIAA-95-0797, 1995.
- 11 Moffat, R. J., "Describing the Uncertainties in Experimental Results," *Experimental Thermal and Fluid Science*, Vol. 1, 1988.
- 12 Brown, K. K., Coleman, H. W., Steele, W. G., and Taylor, R. P., "Evaluation of Correlated Bias Approximations in Experimental Uncertainty Analysis," AIAA 94-0772, 1994.
- 13 Fish, James E., NASA/MSFC Test Area Measurement System Uncertainty Study, Sverdrup Technology, Inc., MSFC Group, Report No. 335-002-92, October 1992.
- 14 Hendricks, Robert C., Baron Anne K., and Peller, Ildiko C., "GASP - A Computer Code for Calculating the Thermodynamic and Transport Properties for Ten Fluids: Parahydrogen, Helium, Neon, Methane, Nitrogen, Carbon Monoxide, Oxygen, Fluorine, Argon, and Carbon Dioxide," NASA TN D-7808, February 1975.
- 15 Brennan, J.A. LaBrecque, J.F., and Kneebone, C.H., "Progress Report on Cryogenic Flowmetering at the National Bureau of Standards," *Instrumentation in the Cryogenic Industry, Volume 1*, Proceedings of the first Biennial Symposium on Cryogenic Instrumentation, October 11-14, 1976, Held in Conjunction with the 31st Annual ISA Conference and Exhibit.

16. Szaniszló, Andrew J., and Krause, Lloyd N., "Simulation of Liquid-Hydrogen Turbine-Type Flowmeter Calibrations using High-Pressure Gas," NASA TN D_3773.
17. Lepore, Frank A., Rocketdyne Division, Space Shuttle Main Engine No. 3001, Technology Test Bed, Differential Flowmeters Calibration Final Report, Contract No. NAS8-27980, March 1980.
18. Brown, Kendall K., Coleman, Hugh W., and Steele, Glenn W., "Estimating Uncertainty Intervals for Linear Regression," AIAA Paper 95-0796, 33rd Aerospace Sciences Meeting and Exhibit, January 9-12, 1995, Reno, NV.
19. Fluid Meters: Their Theory and Application, 6th Ed., The American Society of Mechanical Engineers, New York, NY, 1971.
20. Hildebrand, F. B., *Advanced Calculus for Applications*, Prentice-Hall, Englewood Cliffs, NJ, 1962.
21. Coleman, H. W., and Steele, W. G., "Some Considerations in the Propagation of Bias and Precision Errors into an Experimental Result," *Experimental Uncertainty in Fluid Measurements*, ASME FED Vol. 58, 1987.
22. Taylor, B. N., and Kuyatt, C. E., "Guidelines for Evaluating and Expressing the Uncertainty of NIST Measurement Results," NIST Technical Note 1297, September 1994.
23. Coleman, H. W., Hosni, M. H., Taylor, R. P., and Brown, G. B., "Using Uncertainty Analysis in the Debugging and Qualification of a Turbulent Heat Transfer Test Facility," *Experimental Thermal and Fluid Science*, Vol 4, No. 6, 1991.
24. Technology Test Bed Program Data Requirements Document, TTB-045.

Appendix I Venturi Flowmeter Data Reduction

The data reduction methodology for the determination of mass flow rate from differential pressure venturi flowmeters is reproduced from Fluid Meters: Their Theory and Application by ASME¹⁹ and the Rocketdyne Final Report [ref 17].

The mass flow rate through a differential pressure venturi mass flow meter is designated as W_e , with units of [lbm/sec] and the data reduction equation is:

$$W_e = KY_a F_a C_w \sqrt{\rho \Delta P}$$

where K is a unit conversion factor

$$K = \frac{\pi}{4} \sqrt{\frac{2g_c}{12^2}} = 0.5250204$$

Y_a is an expansion factor

$$Y_a = \sqrt{x^{\frac{2}{k}} \left(\frac{k}{k-1} \right) \left(\frac{1-x^{\left(\frac{k-1}{k}\right)}}{1-x} \right) \left(\frac{1-\beta^4}{1-\beta^4 x^{\frac{2}{k}}} \right)}$$

where k is ratio of specific heats, C_p/C_v and x is the pressure ratio, defined as

$$x = 1 - \frac{\Delta P}{P}$$

F_a is a thermal expansion factor, defined as

$$F_a = 1 + 2\alpha(T - 528)$$

C_w is the calibration coefficient for the particular venturi, defined as

$$C_w = \frac{d^2 C_D}{\sqrt{1-\beta^4}}$$

where β is the ratio of throat diameter to the inlet diameter, $\beta=d/D$, and C_D is the discharge coefficient. The discharge coefficient must be determined experimentally, Rocketdyne developed curvefit equations for C_D as a function of inlet Reynolds number. For all the venturis except No. 247 the curvefit equation is

¹⁹ Fluid Meters: Their Theory and Application, 6th Ed., The American Society of Mechanical Engineers, New York, NY, 1971.

$$C_D = A_0 - \left[B_0 \left(\frac{(\text{Re}_d)_t}{\text{Re}_d} \right)^a \right]$$

where the Reynolds number is determined from

$$\text{Re}_d = \frac{4W_e}{\pi\mu d}$$

$(\text{Re}_d)_t$ is the transition Reynolds number and the curvefit for venturi item No. 247 is

$$C_D = A + B(\text{Re}_d) + C(\text{Re}_d)^2 + D(\text{Re}_d)^3 + E(\text{Re}_d)^4$$

Further information and details on the venturi calibration is found in the Rocketdyne Flowmeter Final Report, reference [17].

Appendix II
Mass Flow Rate Uncertainty Determination

When the equations in Appendix I are combined for incompressible fluids ($Y_a = 1$) the equation for the mass flow rate can be written as

$$W_e = (0.525)(1 + 2\alpha(T - 528)) \frac{d^2 C_d}{\sqrt{1 - \left(\frac{d}{D}\right)^4}} \sqrt{\rho \Delta P}$$

and performing a general uncertainty analysis the equation for the uncertainty in the mass flow rate can be written as

$$U_{W_e}^2 = \theta_\alpha^2 U_\alpha^2 + \theta_T^2 U_T^2 + \theta_d^2 U_d^2 + \theta_D^2 U_D^2 + \theta_{C_d}^2 U_{C_d}^2 + \theta_\rho^2 U_\rho^2 + \theta_{\Delta P}^2 U_{\Delta P}^2$$

and the partial derivatives are written as

$$\theta_\alpha = (0.525)2(T - 528) \frac{d^2 C_d}{\sqrt{1 - \left(\frac{d}{D}\right)^4}} \sqrt{\rho \Delta P}$$

$$\theta_T = (0.525)2\alpha \frac{d^2 C_d}{\sqrt{1 - \left(\frac{d}{D}\right)^4}} \sqrt{\rho \Delta P}$$

$$\theta_d = (0.525)(1 + 2\alpha(T - 528)) \frac{d^2 C_d}{\sqrt{1 - \left(\frac{d}{D}\right)^4}} \sqrt{\rho \Delta P}$$

$$\theta_d^2 = (0.525)(1 + 2\alpha(T - 528)) \left\{ \frac{C_d \sqrt{\rho \Delta P}}{\sqrt{1 - \left(\frac{d}{D}\right)^4}} d + \frac{2d^5}{D^4 \left(1 - \left(\frac{d}{D}\right)^4\right)^{3/2}} \right\}$$

$$\theta_D^2 = (0.525)(1 + 2\alpha(T - 528)) \left\{ \frac{-2C_D \sqrt{\rho \Delta P} d^6}{D^5 \left(1 - \left(\frac{d}{D}\right)^4\right)^{3/2}} \right\}$$

$$\theta_\rho^2 = (0.525)(1 + 2\alpha(T - 528)) \frac{d^2 C_D}{\sqrt{1 - \left(\frac{d}{D}\right)^4}} \frac{1}{2} \sqrt{\frac{\Delta P}{\rho}}$$

$$\theta_{\Delta P}^2 = (0.525)(1 + 2\alpha(T - 528)) \frac{d^2 C_D}{\sqrt{1 - \left(\frac{d}{D}\right)^4}} \frac{1}{2} \sqrt{\frac{\rho}{\Delta P}}$$

Since the density of the fluid is not a measured variable, but must be determined as a function of the measured pressure and temperature, it is replaced in the data reduction equation with its functional relationship.

$$W_e = (0.525)(1 + 2\alpha(T - 528)) \frac{d^2 C_d}{\sqrt{1 - \left(\frac{d}{D}\right)^4}} \sqrt{\rho(P, T) \Delta P}$$

Using this data reduction equation and applying the uncertainty propagation equation in a slightly different form we obtain the expression for the uncertainty as

$$U_{W_e}^2 = \left\{ \begin{aligned} & \left(\frac{\partial W_e}{\partial C_D} \right)^2 B_{C_D}^2 + \left(\frac{\partial W_e}{\partial \Delta P} \right)^2 B_{\Delta P}^2 + \left(\frac{\partial W_e}{\partial P} \right)^2 B_P^2 \\ & + \left(\frac{\partial W_e}{\partial T} \right)^2 B_T^2 + \left(\frac{\partial W_e}{\partial D} \right)^2 B_D^2 + \left(\frac{\partial W_e}{\partial d} \right)^2 B_d^2 \\ & + \left(\frac{\partial W_e}{\partial \alpha} \right)^2 B_\alpha^2 + 2 \left(\frac{\partial W_e}{\partial D} \right) \left(\frac{\partial W_e}{\partial d} \right) B_{dD} \end{aligned} \right\} + P_{W_e}^2$$

where it is assumed that the uncertainty in the determination of the density from the property subroutine is absorbed within the bias limits estimated for the temperature and pressure. From review of the thermophysical property subroutine used in the data reduction, the uncertainty in the density given by the routine is approximately 0.25% at 95% confidence. Note that the precision limit of the flowrate is combined directly and not propagated with the partial derivatives, as are the bias limits. This method provides a

better estimate of the precision limit and automatically accounts for any correlated precision error behavior within the measured variables.

If the bracketed term is multiplied and divided by W_e^2 , terms such as

$$\frac{1}{W_e^2} \left(\frac{\partial W_e}{\partial C_D} \right)^2 = \left(\frac{1}{C_D} \right)^2 \approx 1$$

are obtained. This term for C_D is important since it indicates that the square of the bias limit for the discharge coefficient is linear with respect to the square of the uncertainty in the flowrate. This indicates that the uncertainty in the discharge coefficient is an important parameter. Similarly the other terms of this nature can be obtained, (except for the pressure and temperature used in the density function) but are more complicated and are not as easily interpreted.

Appendix III
ASME International Mechanical Engineering Congress and Exposition
Technical Paper

Impact of Uncertainty on Modeling and Testing of the Space Shuttle Main Engine

by
Kendall K. Brown
Hugh W. Coleman
John P. Butas

IMPACT OF UNCERTAINTY ON MODELING AND TESTING OF THE SPACE SHUTTLE MAIN ENGINE

Kendall K. Brown

Hugh W. Coleman

Propulsion Research Center

Department of Mechanical and Aerospace Engineering

University of Alabama in Huntsville

Huntsville, Alabama

John P. Butas

Liquid Propulsion Branch

NASA/Marshall Space Flight Center

Marshall Space Flight Center, Alabama

ABSTRACT

The Space Shuttle Main Engine (SSME) tests conducted at Marshall Space Flight Center's (MSFC) Technology Test Bed (TTB) facility are being used to assess the performance of new SSME hardware components. The experimental data from the engine tests is analyzed and compared with predictions from the engine's performance prediction model. A research effort is in progress to quantify experimental uncertainties and analytical uncertainties within the SSME performance prediction model. This paper will discuss some of the unique problems encountered in quantifying these uncertainties.

INTRODUCTION

The Space Shuttle Main Engine (SSME) tests conducted at Marshall Space Flight Center's (MSFC) Technology Test Bed (TTB) facility are being used to assess the performance of new SSME hardware components. These new components are being tested in the SSME Engine 3001 program because it provides a significantly higher number of instrumentation points than a normal flight engine. The data is being used to guide the development of new hardware for SSME flight engines as well as future advanced liquid hydrogen/liquid oxygen engines. The test data is also used with the SSME Power Balance Model (PBM), the engine's steady-state performance prediction model, to assess the predictions the model provides and in some cases to make alterations to the model based upon the test data. The fact that the test data contains uncertainties has not been taken into account, and no assessment has been made of the uncertainty in the model's predictions due to the

assumptions, approximations, and uncertain data used in the development and solution of the model. The goal of the current effort is to enhance rocket engine steady-state performance models and rocket engine performance analysis through the incorporation of uncertainty analysis techniques. This paper discusses this on-going effort and some of the unique problems being investigated.

TECHNOLOGY TEST BED FACILITY

The Technology Test Bed (TTB) facility "was established to validate new propulsion technology hardware advances for large liquid oxygen and liquid hydrogen rocket engines." (NASA, 1991) The need for a facility in which detailed knowledge of the internal environment of large rocket engines could be obtained was recognized as being necessary for the technology development required for advanced hydrogen/oxygen engines. Planning for the TTB began in 1982 to use a highly instrumented Space Shuttle Main Engine and the test stand at MSFC which was originally constructed for the testing of the first stage of the Saturn V, a five engine cluster of F-1 RP-1/LO₂ rocket engines. The facility modifications were completed in 1984 and the first tests were conducted in 1989 with a SSME with standard flight instrumentation (NASA, 1991). Testing of the highly instrumented SSME, identified as Engine 3001, began in December of 1990 and has continued since then. The technology development items which have been tested in the TTB include the following (NASA, 1991):

- * Large throat combustion chamber
- * Combustion stability studies
- * Engine start transient modifications

- * Engine shutdown evaluation
- * Test turnaround time reduction
- * Continuous fuel system purge
- * LH₂ umbilical leak tests
- * Advanced fuel turbopump
- * Advanced oxidizer turbopump

Engine 3001 provides "over 750 special measurements, including flowrates, pressures, temperatures, and strains" (McConnaughey, et al., 1992).

SSME PERFORMANCE ANALYSIS

The major requirements of the SSME performance analysis include assessing vehicle/engine feed system interface flow characteristics, engine hardware design changes, evaluating engine hardware performance, predicting engine hardware operation, and supporting failure investigations. In much of this analysis the test data is compared to the predictions provided by the SSME performance prediction model, commonly referred to as the Power Balance Model (PBM). The PBM was originally formulated during the initial development of the SSME and has been continuously modified and updated.

In its current form, the PBM utilizes information from previous tests and property data for the propellants to develop a model prediction. A problem with this approach is that both the experimental data and the physical relationships in the model are treated as absolutes. The data from previous tests and the property data contain uncertainties. The physical relationships in the model are only approximations (1-D, etc) of reality and therefore have their own uncertainties. Previously, experimental data has been treated as absolute and computational predictions were forced to agree with the data at instrumented locations, often at the expense of physical consistency (conservation of energy, for example).

The highly empirical nature of the Power Balance Model provides significant areas for uncertainties to be introduced; however, there is no mechanism in the model to propagate those uncertainties and provide an uncertainty associated with the model's prediction. Also, because of its empirical nature the model's capability to provide meaningful predictions for engines which contain significant new hardware is in question.

In an effort prior to the one discussed in this paper, a test data/model reconciliation strategy was developed based upon evaluating test data with respect to basic fluid conservation principles (mass, energy, and momentum relationships). This strategy systematically transformed uncertain experimental data into a physically self consistent set of data. This was accomplished by forcing the minimum adjustment required in engine pressures, temperatures, and flowrates necessary to satisfy prescribed uncertainty constraints. This strategy

explicitly incorporated uncertainty estimates for experimental data as well as the physical properties, but did not account for model uncertainties.

In a research effort parallel to the one discussed in this paper, a new performance model is being developed. This model is based upon a general rocket engine performance analysis computational tool developed by Pratt & Whitney known as ROCETS (ROCKET Engine Transient Simulation). While the model was developed with the capability of performing transient analyses, starts, throttling, and shutdowns, it is also useful as a steady state prediction model. ROCETS is a modular platform in which modules are put together, along with the specific hardware and thermodynamic cycle characteristics, to generate a computational model for most types of rocket engines. This is advantageous for the SSME Engine 3001 program since the specific hardware characteristics for a particular new component can be easily changed within the ROCETS model. These types of changes would be extremely difficult to accomplish within the PBM. The development of the reconciliation strategy for incorporation with the ROCETS based model (similar to that discussed in the preceding paragraph) is a concurrent research effort (Santi, 1994).

CONSIDERING UNCERTAINTY IN TESTING AND MODELING

Since both experimental results and "predictions" from a model contain uncertainties, one needs to consider how these uncertainties should be taken into account when evaluating a comparison of test results and model output. The general case is shown schematically in Figure 1. A physical system is studied both experimentally and analytically. In most situations, the analytical model is "calibrated" using experimental data from the physical system being studied or from a similar system -- friction factor vs. Reynolds number correlations, for example. The model also uses property data, which originally was found experimentally and contains uncertainties.

The methodology for estimating the experimental uncertainties has received considerable attention, and the most current approaches are presented and discussed in Coleman and Steele (1989), ISO (1993) and AGARD (1994). To the authors' knowledge, no equivalent methodology exists for estimating the uncertainty that should be associated with the "predictions" of a model.

In the analytical modeling approach the physical system is studied from the aspect of what physical laws can be applied and which laws of physics will help answer the posed questions. In a fluid system the conservation laws (continuity, momentum, energy) are important; however, these laws are generally not applied in an exact sense in a model. To obtain a solution which will answer the

posed question assumptions and approximations to the physical laws are typically made--for example, making a one-dimensional approximation for a three-dimensional physical process or assuming a structural material behaves linearly with a constant modulus of elasticity.

There are many other assumptions and approximations which are commonly used to reduce general equations to solvable forms, including assumptions such as homogeneous, isotropic, steady, incompressible, isothermal, adiabatic, isentropic, constant acceleration, rigid body, constant rotation, etc. It should be realized that these assumptions and approximations introduce an uncertainty into the output of the model. As mentioned above, often in the analytical approach results from an experiment or physical property data must be introduced along with the assumptions and approximations, thus introducing more elements of uncertainty. With the assumptions and approximations reducing the general physical laws to a solvable form and the necessary other data included, the model is complete and a mathematical solution can be found, that is, a prediction obtained from the model. This solution contains some uncertainty, but there is not any recognized methodology to quantify the uncertainty. In computational approaches, such as computational fluid dynamics, there are methods to estimate the error involved in the numerical solution of the differential equations. But little attention has been paid to how the other assumptions and approximations affect the degree of goodness of the final solution.

This can be taken further by asking how should the two answers, the experimental solution and the analytical solution, be compared. It is extremely unlikely that the two answers will be the same and since each has an uncertainty interval associated with it what can be said about how the two uncertainty intervals interact? Do the intervals overlap? If so, what does it mean and what conclusions can or should be drawn? If the uncertainty intervals do not overlap and a significant difference exists between the analytical solution and the experimental solution, is there justification for adjusting the analytical solution with a "fudge-factor"?

UNCERTAINTY IN SSME TESTING

The aspect of the Engine 3001 test program that is of primary interest in this effort is the engine's thermodynamic performance. As such, the variables of primary interest are the mass flowrates, pressures, and temperatures in various points of the engine. When Engine 3001 was developed 9 flowmeters, 15 temperature transducers, and 12 pressure transducers were added. Both differential pressure venturi flowmeters and orifice plate flowmeters are used for the flowrate determinations, depending on the location and type of flow to be

measured. The temperature probes used are mainly thermocouples with a few RTD's in special locations, and the pressure transducers include absolute transducers, differential pressure transducers, and some high frequency pressure transducers.

The operating environment in a Space Shuttle Main Engine is very harsh, much harsher than that in most systems in which an uncertainty analysis has been applied. The combustion chamber operates at greater than 3000 psia, the high pressure fuel turbopump pressurizes the hydrogen fuel to over 5500 psia, and the oxygen is pressurized to over 3800 psia. At these pressures both of the propellants are in the supercritical region while at cryogenic temperatures. The size constraints necessary for the SSME's to fit in the Space Shuttle dictate that the ducting be very compact. The extreme nature of the SSME environment creates some unique problems in instrumentation and measurement and in the interpretation of those measurements.

One of the major tasks in this research effort is to assess the major contributors to the uncertainty in the measurements taken in the TTB Engine 3001 program. Some of the more significant uncertainty sources that have been identified and are being investigated are discussed below. These include the venturi discharge coefficient uncertainty and conceptual uncertainties.

In the analysis of the SSME performance the system flowrates are key parameters. The determination of the uncertainty in the discharge coefficient for the differential pressure venturi flowmeters appears to be a major contributor to the flowrate uncertainty. The SSME's are manufactured by Rocketdyne Corporation, and Engine 3001 was a specially built engine with modifications to the piping and ducting to install the venturi nozzles, orifice plates, and pressure and temperature probe taps. Because one of purposes of the Engine 3001 program was to characterize the internal flow environment in the SSME, Engine 3001 needed to be as similar to flight engines as possible, but with the added instrumentation. This created a number of problems for the design and installation of the venturi flowmeters, the most critical of these being encroachment on the required length of straight duct upstream of the nozzle entrances. The venturis were also designed with consideration of minimizing the pressure drop to help ensure that the cryogenic fluids would not be prone to cavitation and to minimize the added flow resistance.

In an attempt to account for some of these issues, Rocketdyne designed the calibration system to calibrate the venturis with the associated connecting ducting. They then performed calibrations on the venturis in their facility with ambient temperature water as the calibration fluid since a cryogenic calibration facility

capable of handling similar flowrates was not, and is not, available. The dynamic similarity between the calibration fluid and the operating fluid conditions was relied upon to provide appropriate values for the discharge coefficients for the test venturis. In most of the engine venturis the maximum Reynolds number tested during the calibration process was less than the Reynolds numbers expected during engine testing, in some cases by over an order of magnitude. The orifice plates were calibrated by Colorado Engineering Experiment Station, Inc. and were calibrated with the associated ducting from the engine, but were calibrated with ambient air as the calibration fluid and good Reynolds number correlations were able to be obtained.

The potential difference between calibrating the venturis and orifices with water or air and testing with supercritical cryogenic fluids is an effect we believe might be a significant source of uncertainty. From the lack of published literature and from comments from individuals working in the field, at this time it appears this effect has not been fully addressed.

Another important area of uncertainty to be investigated is the conceptual uncertainty associated with the meaning of a particular measurement. Moffat (1988) introduced the concept of conceptual bias error as the error due to the difference in what the instrument or probe was reading and the use of that measurement in the data reduction routine. For example, if the flowrate of a fluid in a duct is desired, and the velocity of that fluid is measured at a single point in the flow field, there will be a conceptual bias error due to the probe measuring the velocity at a single point instead of measuring the average velocity of the bulk flow. The complicated and complex nature of the flows in the piping and ducting of the engine, due to sharp bends, valves, pump exits, and the like, assure that the readings of the pressure tap or thermocouple located at the inner surface of the pipe are not representative of the bulk flow in the duct.

Difficulties arise in quantifying the value of the conceptual bias errors. If one is able to determine an estimate for the conceptual error, that estimate could be used to adjust the measured value and an uncertainty due to the correction included. The error can be estimated by either analytical methods or by additional experimentation. In the Engine 3001 program additional experimentation for the purpose of assessing conceptual bias errors is prohibitive, with respect to the overall testing goals and the competition for resources. Thus the process of making analytical estimates for the conceptual bias errors is being undertaken. In some cases, CFD modeling of the flows in particular ducts has been previously completed for other purposes and that information will be used in formulating estimates.

The uncertainty introduced with the use of equations of state to represent the physical properties of the propellants also needs to be addressed, particularly since much of the system operates much above the critical point. Experimental physical property data for hydrogen and oxygen at these conditions is limited and that available has a non-negligible uncertainty, about 0.5% for liquid hydrogen.

UNCERTAINTY IN SSME MODELING

As previously mentioned, the ROCETS SSME model is based upon each hardware component having its own module in the program which contains the mathematical model for that component. Each of the modules is a one-dimensional thermodynamic and fluid dynamic model for the particular piece of hardware. The ROCETS program contains the equations for the hardware components typically found in rocket engines and inputs for the specific hardware characteristics for the engine being modeled adjust the general equations to complete the model. The modules then form a set of equations which have to be solved. The ROCETS platform is a more structured platform which is more conducive to the development of the modeling uncertainties.

In order to understand why the modelling of the SSME is such a difficult task, a description of the engine is presented. The Space Shuttle Main Engine operates in a staged combustion cycle. The staged combustion cycle is the highest performance rocket engine cycle available and accordingly the most complicated. The maximum amount of available energy is extracted from the propellants by using the propellants to provide the power to operate the turbopumps and then ensuring that all of the propellants enter the main combustion chamber. The combustion processes occurring in the oxidizer preburner and the fuel preburner occur at approximately 5500 psia, and the main combustion chamber operates at 3160 psia, at 100% rated power.

In trying to assess the uncertainties which are introduced in the modelling process a comparison between the real operation of the engine and the operation of the engine as it is being modelled is necessary. For example, consider the flow of liquid oxygen through the main oxidizer valve. In the real engine the flow is three-dimensional, non-uniform, highly turbulent, and heat transfer is occurring. In the modeling process it is assumed that the axial velocity is the only important velocity and the flow is completely uniform, the effect of the turbulence can be characterized by the Reynolds number or the velocity in conjunction with the valve characteristics, the flow is adiabatic and the process is isenthalpic. A method to estimate the uncertainty propagated through the model due to each of these

assumptions and approximations must be formulated.

The modeling of the combustion processes is another uncertainty contributor. It models the combustion processes with an adiabatic flame temperature calculation using pressure corrected ideal gas assumptions. It does not account for real thermodynamic effects such as dissociation and non-equilibrium, which are potentially significant effects at the high chamber pressures involved. What is the uncertainty propagated through the model due to these assumptions and approximations? Again, a method to quantify these uncertainties must be developed and their influence on the overall result assessed.

After the conditions for which the model is to be solved and reasonable initial guesses are input, the ROCETS model uses a combination of a Newtonian and a Broyden numerical solution scheme to obtain a solution for the conditions throughout the engine. This solution scheme is relatively robust - it converges to a solution quickly and reliably. However, the solution scheme only provides a result within some preassigned tolerance, thus introducing an uncertainty due to the mathematical solution process and necessitating a methodology to assess this uncertainty.

SUMMARY

The ultimate goal of this research effort is to improve the development of rocket propulsion systems by providing information about the uncertainty of the experimental data and analytical predictions upon which decisions are based. Assessment of the experimental uncertainties in the SSME test program is presenting some interesting challenges due to the severe environment of the engine. Assessment of the uncertainties in the analytical predictions is even more challenging because there is not an accepted methodology to follow.

As of August 1994, several tasks are being pursued in support of the two research efforts described above. The progress in support of quantifying experimental uncertainties include the gathering of necessary information about the SSME and test program, a review of the instrumentation systems, identification of some significant uncertainty sources, and assessment of the uncertainties in the venturi flow measurements. Determination of the final values for flow rate, pressure, and temperature uncertainties will be completed by the end of CY 94. The progress in support of quantifying analytical uncertainties within the SSME performance prediction model includes identification of the key questions to be investigated. Further work on the modeling uncertainties will be pursued upon completion of the ROCETS SSME test data reductions model (Santi, 1994).

REFERENCES

- Coleman, H. W., and Steele, W. G., *Experimentation and Uncertainty Analysis for Engineers*, Wiley, New York, 1989.
- Technology Test Bed: The Future for Rocket Engine Design*, Office of Space Flight, NASA, September 1991.
- McConnaughey, H. V., Leopard, J. L., Lightfoot, R. M., "Test Results of the Highly Instrumented Space Shuttle Main Engine", AIAA paper #92-3452, Presented at the 28th Joint Propulsion Conference and Exhibit, Nashville, TN, July 1992.
- Guide to the Expression of Uncertainty in Measurement*, International Organization for Standardization, Geneva, Switzerland, 1993.
- "Assessment of Wind Tunnel Data Uncertainty," AGARD-AR-304, 1994(in press).
- Moffat, R. J., Describing the Uncertainties in Experimental results," *Experimental Thermal and Fluid Science*, Vol 1., 1988.
- Santi, L. Michael, personal communication, June 1994.

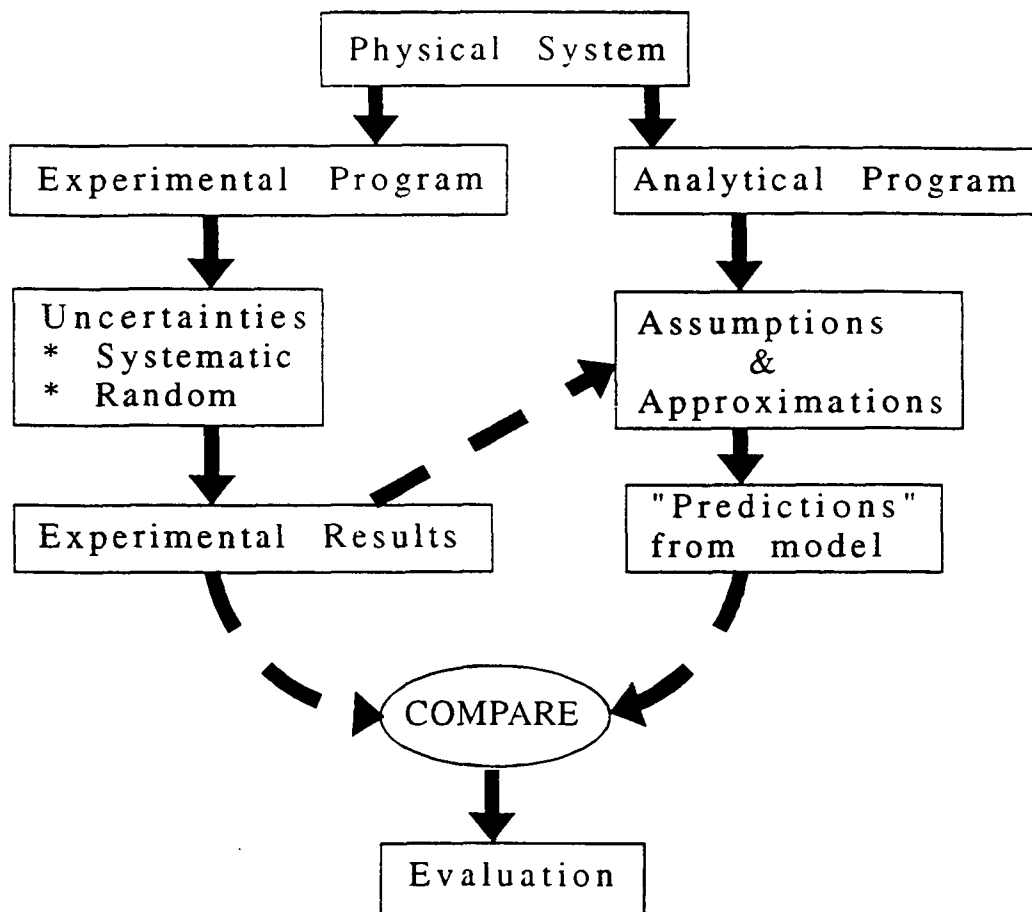


FIGURE 1. EXPERIMENTAL AND ANALYTICAL ANALYSIS FLOWCHART

Appendix IV
1995 AIAA Aerospace Sciences Meeting and Exhibit
Technical Paper

Estimating Uncertainty Intervals for Linear Regression

by
Kendall K. Brown
Hugh W. Coleman
W. Glenn Steele



AIAA 95-0796

**Estimating Uncertainty Intervals for
Linear Regression**

Kendall K. Brown and Hugh W. Coleman
Propulsion Research Center
Department of Mechanical and Aerospace Engineering
University of Alabama in Huntsville
Huntsville, AL 35899

W. Glenn Steele
Department of Mechanical Engineering
Mississippi State University
Mississippi State, MS 39762

**33rd Aerospace Sciences
Meeting and Exhibit
January 9-12, 1995 / Reno, NV**

ESTIMATING UNCERTAINTY INTERVALS FOR LINEAR REGRESSION

Kendall K. Brown* and Hugh W. Coleman†
University of Alabama in Huntsville, Huntsville, AL

W. Glenn Steele‡
Mississippi State University, Mississippi State, MS

Abstract

The best straight line through a set of experimental data is often obtained through the application of linear regression analysis, which provides the values of the slope and intercept for this line. The uncertainty intervals that should be associated with the values of the slope and intercept are also important and needed information. Standard statistical techniques to estimate the uncertainties in the slope and intercept are of limited use, primarily due to their assumptions which preclude their use with bias uncertainties. The approach to determining the uncertainty in the values of slope and intercept presented in this paper is based upon applying the uncertainty propagation equations to the regression analysis equations for the slope and intercept. This approach provides for the inclusion of precision uncertainties, bias uncertainties, and correlated bias uncertainties. Using a Monte Carlo type simulation technique, it is shown that this approach provides appropriate estimates of the uncertainty intervals in cases with bias uncertainties and precision uncertainties in both the X and Y measurements.

Nomenclature

B_b =bias limit
 B_{ik} =covariance estimator
 c = Y -intercept
 m =slope of line
 M =number of dependent variable measurements per independent variable
 N =number of data points
 P_i =precision limit
 r =experimental result

S_i =standard deviation
 X =independent variable
 X_i =measured variables
 Y =dependent variable
 U_i =uncertainty interval
 β =actual bias error
 θ_i =sensitivity, Eq.8
 ρ_{ik} =correlation coefficient

Introduction

In many experimental programs, the quantity of interest is not the data itself, it is the relationship within the data. For example, a tensile test is often conducted to determine the modulus of elasticity for a specimen, where the modulus of elasticity is the slope of the stress-strain relationship that is assumed linear in the elastic region. This relationship can be expressed in the general form

$$Y = mX + c \quad (1)$$

where m is the slope of the line and c is the intercept on the Y -axis.

What are the uncertainties in the calculated values of m and c and why are they needed? A use which partially motivated this work is an on going effort to determine the uncertainty from a Space Shuttle Main Engine prediction model which uses regression coefficients from experimental data. This requires knowledge of the uncertainty in the regression coefficients.

The uncertainties in the slope, m , and the Y -intercept, c , are functions of the uncertainties in the determinations of the X and Y variables. The values of m and c are obtained by minimizing the sum of the squares of the deviations between the line and the data points, commonly known as the method of least squares. The development of the equations to calculate m and c can be found in statistics books^{1,2,3} and only the equations will be presented here. For N (X_i, Y_i) data pairs, the slope of the line, m , is determined from

* Graduate Research Assistant, Propulsion Research Center, Mechanical and Aerospace Engineering Department. Student Member AIAA.

† Eminent Scholar in Propulsion and Professor, Propulsion Research Center, Department of Mechanical and Aerospace Engineering, Senior Member, AIAA

‡ Professor and Head, Department of Mechanical Engineering, Senior Member AIAA.

$$m = \frac{N \sum_{i=1}^N X_i Y_i - \sum_{i=1}^N X_i \sum_{i=1}^N Y_i}{N \sum_{i=1}^N (X_i^2) - \left(\sum_{i=1}^N X_i \right)^2} \quad (2)$$

and the intercept, c , is determined from

$$c = \frac{\sum_{i=1}^N (X_i^2) \sum_{i=1}^N Y_i - \sum_{i=1}^N X_i \sum_{i=1}^N (X_i Y_i)}{N \sum_{i=1}^N (X_i^2) - \left(\sum_{i=1}^N X_i \right)^2} \quad (3)$$

In this paper we present a methodology to determine the uncertainties in linear regression coefficients. The effectiveness of this methodology was analyzed using a Monte Carlo-type simulation assuming the true relationship between the X and Y variables is in fact linear.

Experimental Uncertainty Analysis

The background of the methodology to obtain uncertainty estimates and how they propagate through a given data reduction equation is not presented in this paper -- only a brief overview is given. The reader is referred to references [4], [5], and [6] for a more thorough discussion.

The word accuracy is generally used to indicate the relative closeness of agreement between an experimentally-determined value of a quantity and its true value. Error is the difference between the experimentally-determined value and the truth, thus as error decreases accuracy is said to increase. Only in rare instances is the true value of a quantity known. Thus, it is necessary to estimate error, and that estimate is called an uncertainty, U . Uncertainty estimates are made at some confidence level -- a 95% confidence estimate, for example, means that the true value of the quantity is expected to be within the $\pm U$ interval about the experimentally-determined value 95 times out of 100.

Total error can be considered to be composed of two components: a precision (random) component ϵ and a bias (systematic) component β . An error is classified as precision if it contributes to the scatter of the data; otherwise, it is a bias error. As an estimator of β , a systematic uncertainty or bias limit, B , is defined. A 95% confidence estimate is interpreted as the experimenter being 95% confident that the true value of the bias error, if known, would fall within $\pm B$. A useful approach to estimating the

bias limit is to assume that the bias error for a given case is a single realization drawn from some statistical parent distribution of possible bias errors. For example, suppose a thermistor manufacturer specifies that 95% of samples of a given model are within ± 1.0 C of a reference resistance-temperature (R-T) calibration curve supplied with the thermistors. One might assume that the bias errors (the differences between the actual, but unknown, R-T curves of the various thermistors and the reference curve) belong to a Gaussian parent distribution with a standard deviation $b=0.5$ C. Then the interval defined by $\pm B = \pm 2b = \pm 1.0$ C would include about 95% of the possible bias errors that could be realized from the parent distribution.

As an estimator of the magnitude of the precision errors, a precision uncertainty or precision limit P is defined. A 95% confidence estimate of P is interpreted to mean that the $\pm P$ interval about a single reading of X_i should cover the (biased) parent population mean 95 times out of 100.

In nearly all experiments, the measured values of different variables are combined using a data reduction equation (DRE) to form some desired result. A general representation of a data reduction equation is

$$r = r(X_1, X_2, \dots, X_J) \quad (4)$$

where r is the experimental result determined from J measured variables X_i . Each of the measured variables contains bias errors and precision errors. These errors in the measured values then propagate through the data reduction equation, thereby generating the bias and precision errors in the experimental result, r .

If the "large sample assumption" is made⁶, then the 95% confidence expression for U_r becomes

$$U_r^2 = B_r^2 + P_r^2 \quad (5)$$

where we define the bias limit (systematic uncertainty) of the result as

$$B_r^2 = \sum_{i=1}^J \theta_i^2 B_i^2 + 2 \sum_{i=1}^{J-1} \sum_{k=i+1}^J \theta_i \theta_k B_{ik} \quad (6)$$

and the precision limit (precision uncertainty) of the result as

$$P_r^2 = \sum_{i=1}^J \theta_i^2 P_i^2 + 2 \sum_{i=1}^{J-1} \sum_{k=i+1}^J \theta_i \theta_k P_{ik} \quad (7)$$

and where B_{ik} is the 95% confidence estimate of the covariance appropriate for the bias errors in X_i and X_k and P_{ik} is the 95% confidence estimate of the covariance appropriate for the precision errors in X_i and X_k , and

$$\theta_i = \frac{\partial r}{\partial X_i} \quad (8)$$

The 95% confidence precision limit for a variable X_i can be estimated as

$$P_{X_i} = 2S_{X_i} \quad (9)$$

where the sample standard deviation for X_i is

$$S_{X_i} = \left[\frac{1}{N-1} \sum_{k=1}^N [(X_i)_k - \bar{X}_i]^2 \right]^{1/2} \quad (10)$$

and the mean value for X_i is defined as

$$\bar{X}_i = \frac{1}{N} \left[\sum_{k=1}^N (X_i)_k \right] \quad (11)$$

Typically, correlated precision uncertainties have been neglected so that the P_{ik} 's in Eq. (7) are taken as zero, and that is assumed in the work reported here. For a thorough discussion of the estimation of the B_{ik} 's in Eq. (6), the reader is referred to Reference [7]. For the assumptions used in the work reported in this paper,

$$B_{ik} = B_i B_k \quad (12)$$

Regression Uncertainty

The standard statistical techniques for the determination of uncertainties in regression coefficients have been mainly restricted to random uncertainties. Recently it has been accepted that bias uncertainties and particularly correlated bias uncertainties play an important role in engineering measurements and must be properly accounted for.⁶ As such, a methodology which properly accounts for the propagation of both precision and bias uncertainties through linear least squares regression equations has been the subject of recent work.

Price⁸ presents a suggested methodology which provides an uncertainty interval associated with a given predicted value of Y . Price's method uses the traditional statistical techniques for the random uncertainties (standard error of the estimate equations) and a new technique to propagate bias uncertainties from elemental error sources in X and Y into the predicted Y value. The ability of the

methodology to handle correlated bias uncertainties is not explicitly discussed, nor is it shown that the methodology implicitly accounts for correlated bias uncertainty sources.

Clark⁹ again utilizes the traditional statistical techniques to calculate the standard deviations of the slope and intercept due to the precision uncertainties. He then uses a separate technique to propagate the elemental bias uncertainties into a bias limit for the slope and intercept, but the technique does not account for correlated bias uncertainties.

Montgomery¹ is a standard statistical linear regression analysis text and discusses the Ridge Regression method as an appropriate technique to use with biased data and is generally used with higher order regressions. The Ridge technique is still mainly interested in providing the "best fit" of the data and does not allow for the inclusion of bias limits estimated by non-statistical methods.

The approach presented in this paper is an application of the uncertainty analysis methodology presented above to the regression equations for slope and intercept.

Considering Eq.s (2) and (3) to be data reduction equations of the form

$$m = m(X_1, X_2, \dots, X_N, Y_1, Y_2, \dots, Y_N) \quad (13)$$

and

$$c = c(X_1, X_2, \dots, X_N, Y_1, Y_2, \dots, Y_N) \quad (14)$$

and applying the uncertainty analysis equations, Eq.s (5)-(12), the most general form of the expression for the uncertainty in the slope of the line, m , is

$$\begin{aligned} U_m^2 = & \sum_{i=1}^J \left(\frac{\partial m}{\partial Y_i} \right)^2 B_{Y_i}^2 + 2 \sum_{i=1}^{J-1} \sum_{k=i+1}^J \left(\frac{\partial m}{\partial Y_i} \right) \left(\frac{\partial m}{\partial Y_k} \right) B_{Y_i Y_k} \\ & + \sum_{i=1}^J \left(\frac{\partial m}{\partial Y_i} \right)^2 P_{Y_i}^2 + \sum_{i=1}^J \left(\frac{\partial m}{\partial X_i} \right)^2 B_{X_i}^2 \\ & + 2 \sum_{i=1}^{J-1} \sum_{k=i+1}^J \left(\frac{\partial m}{\partial X_i} \right) \left(\frac{\partial m}{\partial X_k} \right) B_{X_i X_k} + \sum_{i=1}^J \left(\frac{\partial m}{\partial X_i} \right)^2 P_{X_i}^2 \\ & + \sum_{i=1}^J \sum_{k=1}^J \left(\frac{\partial m}{\partial X_i} \right) \left(\frac{\partial m}{\partial Y_k} \right) B_{X_i Y_k} \end{aligned} \quad (15)$$

where B_{Y_i} is the systematic uncertainty for the Y_i variable, B_{X_i} is the systematic uncertainty for the X_i variable, $B_{Y_i Y_k}$ is the covariance estimator for the correlated bias uncertainties in the Y_i and Y_k

variables, B_{X_i, X_k} is the covariance estimator for correlated bias uncertainties in the X_i and X_k variables, B_{X_i, Y_j} is the covariance estimator for the correlated bias uncertainties between X_i and Y_j . P_{Y_i} is the random uncertainty for the Y_i variable, and P_{X_i} is the random uncertainty for the X_i variable.

A similar expression for the uncertainty in the intercept is

$$\begin{aligned}
 U_c^2 = & \sum_{i=1}^j \left(\frac{\partial c}{\partial Y_i} \right)^2 B_{Y_i}^2 + 2 \sum_{i=1}^{j-1} \sum_{k=i+1}^j \left(\frac{\partial c}{\partial Y_i} \right) \left(\frac{\partial c}{\partial Y_k} \right) B_{Y_i, Y_k} \\
 & + \sum_{i=1}^j \left(\frac{\partial c}{\partial Y_i} \right)^2 P_{Y_i}^2 + \sum_{i=1}^j \left(\frac{\partial c}{\partial X_i} \right)^2 B_{X_i}^2 \\
 & + 2 \sum_{i=1}^{j-1} \sum_{k=i+1}^j \left(\frac{\partial c}{\partial X_i} \right) \left(\frac{\partial c}{\partial X_k} \right) B_{X_i, X_k} + \sum_{i=1}^j \left(\frac{\partial c}{\partial X_i} \right)^2 P_{X_i}^2 \\
 & + \sum_{i=1}^j \sum_{k=1}^j \left(\frac{\partial c}{\partial X_i} \right) \left(\frac{\partial c}{\partial Y_k} \right) B_{X_i, Y_k}
 \end{aligned} \quad (16)$$

The partial derivatives are

$$\frac{\partial m}{\partial Y_i} = \frac{NX_i - \sum_{i=1}^N X_i}{N \sum_{i=1}^N (X_i^2) - \left(\sum_{i=1}^N X_i \right)^2} \quad (17)$$

$$\frac{\partial c}{\partial Y_i} = \frac{\sum_{i=1}^N (X_i^2) - X_i \sum_{i=1}^N X_i}{N \sum_{i=1}^N (X_i^2) - \left(\sum_{i=1}^N X_i \right)^2} \quad (18)$$

$$\begin{aligned}
 \frac{\partial m}{\partial X_i} = & \frac{NY_i - \sum_{i=1}^N Y_i}{N \sum_{i=1}^N (X_i^2) - \left(\sum_{i=1}^N X_i \right)^2} \\
 & \frac{\left(N \sum_{i=1}^N X_i Y_i - \sum_{i=1}^N X_i \sum_{i=1}^N Y_i \right) \left(2NX_i - 2 \sum_{i=1}^N X_i \right)}{\left(N \sum_{i=1}^N (X_i^2) - \left(\sum_{i=1}^N X_i \right)^2 \right)^2}
 \end{aligned} \quad (19)$$

and

$$\begin{aligned}
 \frac{\partial m}{\partial X_i} = & \frac{2X_i \sum_{i=1}^N Y_i - \sum_{i=1}^N X_i Y_i - Y_i \sum_{i=1}^N X_i}{N \sum_{i=1}^N (X_i^2) - \left(\sum_{i=1}^N X_i \right)^2} \\
 & \frac{\left(\sum_{i=1}^N (X_i^2) \sum_{i=1}^N Y_i - \sum_{i=1}^N X_i \sum_{i=1}^N X_i Y_i \right) \left(2NX_i - 2 \sum_{i=1}^N X_i \right)}{\left(N \sum_{i=1}^N (X_i^2) - \left(\sum_{i=1}^N X_i \right)^2 \right)^2}
 \end{aligned} \quad (20)$$

The equations above show the most general form of the equations for the uncertainty in the slope and the intercept, allowing for correlation of bias errors among the different X 's, among the different Y 's and also among the X 's and Y 's. If none of the systematic error sources are common between the X variables and the Y variables, the last term of the equations, the X - Y covariance estimator, is zero. This was the form of the equations used in the simulations.

Monte Carlo Simulations

Monte Carlo-type simulations are often used in uncertainty analysis to determine the effectiveness of a particular uncertainty methodology. For this work, what is referred to as a Monte Carlo-type simulation simply means generating numbers to represent experimental data with some amount of error randomly obtained from a predefined error distribution population. Figure 1 is a schematic flowchart of the Monte Carlo simulation technique used.

The Monte Carlo simulations were conducted in the following manner. "True" values for data from a linear relationship with specified coefficients were determined. The word *true* is emphasized to indicate that it represents the actual physical quantity of the parameter if it could be measured without any bias error or precision error, which is always an unobtainable value. The two-sigma (2 standard deviation or 95% confidence) bias limits and precision limits for each X and Y were then specified. The errors in each variable were assumed to come from these normally distributed error populations with the specified standard deviations. A random value for each bias error and precision error was found from a Gaussian random deviate generator subroutine using the specified standard deviations. The Gaussian deviates have a mean of zero and an equal probability of being positive or negative. In the cases presented in this paper all of the X bias errors were defined as being correlated

and of the percent of full scale type, so the same random deviate was used for each X_i . The same held true for the Y_i variables, but with a different bias error than that in the X_i 's. Precision errors were obtained by sampling the precision error populations repeatedly to obtain independent random deviates for each X_i and Y_i . For each X_i , Y_i pair, the individual bias errors and precision errors were then summed and added to the *true* value to obtain a data point with errors from the specified error populations. These data points were then used in the linear least squares equations to obtain the value of the regression coefficients. These values represent the regression coefficients of the experiment when the bias and precision errors are present.

A 95% confidence uncertainty interval for the result was calculated from the uncertainty propagation analysis equations for m and c . A $\pm U_m$ interval was placed around the slope coefficient value, m , and if the true value of the slope was found to be within the interval a counter was incremented. A similar procedure was used with c . This procedure was repeated 10,000 times and the percent coverage, or number of times the true result was within the estimated interval, was determined. Using this procedure, the effectiveness of the uncertainty propagation equation could be investigated by checking whether or not the *true* value is within the 95% confidence uncertainty interval about the measured result 95% of the time.

A useful statistic from the simulation is the uncertainty ratio, the ratio of the average uncertainty intervals for the regression coefficients from the 10,000 iterations divided by the true 95% confidence intervals. The *true* 95% uncertainties are calculated as twice the sample standard deviations, S_m and S_c , from the 10,000 samples of the regression coefficients. The sample standard deviations from the 10,000 sample population can be expected to be good representations of the actual standard deviations of the infinite population of the coefficients with the elemental uncertainty sources as defined. An uncertainty ratio of or near unity shows that the uncertainty methodology works for the particular case, with values greater than one meaning an overprediction and values less than one meaning an underprediction.

RESULTS

Simulations were performed with errors only in Y , multiple readings of Y at each X setpoint, and with errors in both X and Y for single and multiple readings per setpoint. The coefficients m and c were

then determined with the standard linear regression equations, equations (2) and (3), and the uncertainty interval was calculated.

The simulations progressed from simple to complex, with the increasingly more complex simulations being a closer representation of an actual experimental program. Table 1 shows the input data used as the *truth*, Table 2 shows a summary of the simulations for the number of data points and the method used for the precision limits, and Table 3 shows the 2σ (95%) intervals used to determine the bias and precision errors from the Gaussian random deviate routines. The percent coverage and the uncertainty ratios were determined both with the propagation equations including the effect of correlated bias uncertainties and neglecting them.

General

A few comments and conclusions can be drawn from the results of all the simulations.

The first and third simulations are essentially verifications of the methodology. The actual 2σ (95%) confidence intervals for both the precision uncertainties and the bias uncertainties were used in the uncertainty propagation equations, including correlated bias effects. Since they yielded approximately 95% coverage the proposed methodology is demonstrated as appropriate.

In the simulations presented in this paper all of the bias uncertainties are a fixed value, or "percent of full scale." With the bias uncertainties being the same value for each data pair, the linear least squares line through the data simply translates vertically or horizontally from the true line. The value of the slope remains the same and there is no systematic uncertainty in the slope. The value of the intercept will change and will accordingly have an uncertainty. In the numerical calculation of the uncertainty of the slope when all of the bias uncertainties are correlated and there are no precision uncertainties, an error due to truncation and round-off was encountered. This problem was avoided by including a very small precision uncertainty during the cases of dominant bias uncertainties.

When the bias uncertainties are of a "percent of reading" nature, so that the bias limit is a function of the magnitude of the variable, the slope will have an associated non-zero systematic uncertainty. This case is not considered in this paper.

Simulation 1

The first simulation included a systematic error and a random error for Y only. The systematic errors were totally correlated, that is the same value of systematic error was used for each Y_i . A random error, from the same error population distribution, but with a different value was used at each data pair. The uncertainty intervals were determined using equations (15) and (16) with all X uncertainties defined as zero. The simulation was repeated for the cases of dominant systematic error, dominant random error, and for systematic error proportional to random error.

Figure 2 shows the effectiveness of the regression coefficient uncertainty propagation equation for the slope as a function of type of dominant uncertainty (bias or precision) and as a function of the number of data pairs. This figure clearly shows that the propagation equation provides the appropriate 95% coverage for all cases. Similar results yielding 94% to 96% coverage for all types of dominant uncertainties was obtained for the intercept uncertainty propagation equation. Thus, when the correct values for the precision limit and bias limit are used in the propagation equations the correct uncertainty interval is obtained. Obtaining the correct value for the precision limit is only possible if an infinite amount of previous information is available upon which to determine the precision limits.

Simulation 2

The second simulation still only included errors in the Y variable, however M additional readings of the Y variable were generated at each X variable setpoint. The same systematic error was used for all of the readings within each iteration, but a different precision error was used for each Y . The m and c coefficients for the N times M data pairs was found with the linear regression equations. The uncertainty interval was then calculated with the precision limit, P_{Y_i} , determined by calculating the standard deviation of the M Y readings at each X setpoint and using the large-sample approximation ($t=2$).

Figures 3 through 6 show the effectiveness of the regression coefficient propagation equations as a function of the number of points and for the dominant types of uncertainties. Figure 3 shows that approximately 94% to 96% coverage is obtained after the total number of data points reaches about 25 or 30. A similar result was obtained for the intercept uncertainty for dominant precision uncertainties. Figures 4 and 5 show the percent coverage for the

case of comparable magnitude bias and precision errors for the slope uncertainty and intercept uncertainty, respectively. These figures show that for even very small numbers of data points that the percent coverage is about 93%. In reference [6] it is discussed that the difference between 93% and 95% is essentially irrelevant since estimates for the bias limits cannot be made to that accuracy. When the systematic uncertainty is dominant (and the bias limit is estimated correctly) about 95% coverage is obtained, as shown in figure 6 for the intercept.

Simulation 3

The third simulation is similar to the first, but errors in both the X and Y variables are included. A single experimental (X, Y) data pair is determined at each X variable setpoint. The uncertainty intervals were determined from Equations (15) and (16). All systematic errors in the X variables are correlated and all systematic errors in the Y variables are correlated, but there is no correlation of systematic errors between the X and the Y variables. The true 95% confidence intervals for both the bias and precision uncertainties are used in the uncertainty propagation equations.

With the same three variations of dominant uncertainty types, bias, comparable, and precision, the uncertainty in the slope and the uncertainty in the Y -intercept the coverage is essentially the desired 95% and the plot appears identical to Figure 2.

Simulation 4

The fourth simulation is the most general. It includes systematic and random errors in both X and Y and there are M sets of (X, Y) experimental data at each nominal X setpoint. The uncertainty intervals were determined from Equations (15) and (16). As in the third simulation, the systematic errors in X are correlated and the systematic errors in Y are correlated, but there is no correlation of systematic errors between X and Y . The precision uncertainty is determined by calculating the standard deviation of the M readings of both variables at each X setpoint and using the large sample approximation at each setpoint.

Figure 7 shows the percent coverage for dominant precision uncertainties, for greater than about 15 total data points (3 Y data points at 5 X setpoints or 5 Y data points at 3 X setpoints) the "large-sample approximation" in the regression propagation equations provides coverage in excess of about 93%. A similar plot is obtained for the intercept. Plots essentially identical to Figures 4 and 5 for comparable bias and precision uncertainties

and Figure 6 for dominant bias uncertainty were obtained for this simulation, but not shown here.

Simulation 5

The final simulation has the same form of experimental data generation as the fourth simulation, but the linear regression is applied to the mean of the M readings at each setpoint. Accordingly, the precision uncertainty is determined using the standard deviation of the mean, S_i / \sqrt{M} , and the large-sample approximation so that the precision limits are

$$P_{X_i} = 2 \frac{S_{X_i}}{\sqrt{M}} \quad (21)$$

and

$$P_{Y_i} = 2 \frac{S_{Y_i}}{\sqrt{M}} \quad (22)$$

where the index i represents the i^{th} X setpoint.

This methodology produces a higher coverage for a smaller number of data pairs, as shown in Figures 8 through 10. In the case of dominant precision uncertainties, Figures 8 and 9, the desired coverage of about 95% is reached with only a few measurements at each X setpoint. When bias uncertainties are included and of comparable magnitude to the precision uncertainties, and the correct bias limits have been used, the percent coverage is always greater than 92% and essentially in the desired 94% to 96% range, as shown in Figure 10. When the bias uncertainties are the dominant uncertainty source the coverage is again essentially 95% for both m and c and a plot similar to Figure 6 is obtained.

Effect of Correlation

The effect of correlated bias uncertainties has been a neglected part of uncertainty analysis until relatively lately, and a new method of accounting for correlated bias uncertainties was recently presented. In many, if not most situations where a regression is performed the test data will come from the same test apparatus. Since the data is taken with the same equipment the bias errors in the experimental data will be from the same sources and will therefore be correlated. As part of the Monte Carlo simulation the percent coverage and the uncertainty ratio were determined with the regression propagation equations both including and excluding the correlated bias uncertainty terms. Figures 11 and 12

show the uncertainty interval ratio (the calculated uncertainty interval divided by the actual 95% uncertainty interval) for the slope and intercept, respectively. The data from all of the simulations and all of the experiments within a given simulation type were grouped in categories of types of dominant uncertainties: bias dominant, precision dominant, or bias and precision of comparable magnitudes. Within each of the three dominance categories the results were randomized to confound the trends within the data. Figure 11 shows the uncertainty ratio for the slope, m . In the experiments where the bias uncertainties were dominant ignoring the effect of correlation provided a dramatic overestimate of the uncertainty interval, by several orders of magnitude, since the actual uncertainty is of very small magnitude in these cases. In the experiments where the bias uncertainties and the precision uncertainties are of the same order of magnitude the uncertainty interval calculated ignoring the effect of correlated biases is still dramatically overestimated. A similar result is seen for the uncertainty ratio for the Y -intercept, although the overestimate is not quite as dramatic. Both figures also show that when precision uncertainties are dominant the appropriate uncertainty interval is obtained even if the effect of correlation is ignored in the propagation equation.

These results show quite vividly the impact of not accounting for correlated bias uncertainties when they actually exist within the data. This also demonstrates the potential error involved with using the traditional, statistically based regression uncertainty methods which ignore bias uncertainties.

Conclusion

The techniques developed in this paper provide an engineering method to determine the uncertainty in linear regression coefficients for data containing both random uncertainties, systematic uncertainties, and correlated systematic uncertainties. There are many applications of linear regression analysis uncertainty which were not studied as a part of this effort. Work is continuing in several areas.

Acknowledgments

The authors (KKB and HWC) wish to acknowledge support from NASA under contract number NAS8-38609 D.O. 106 and the Eminent Scholar in Propulsion endowment.

References

1. Montgomery, Douglas C. and Peck, Elizabeth A., *Introduction to Linear Regression*

Analysis, 2nd Ed., John Wiley & Sons, New York, 1992.

2. Dietrich, C.F., *Uncertainty, Calibration and Probability: The Statistics of Scientific and Industrial Measurements*, 2nd Ed., Adam Hilger, 1991.

3. Seber, G.A.F., *Linear Regression Analysis*, John Wiley & Sons, New York, 1977.

4. Coleman, Hugh W. and Steele, Glenn W., *Experimentation and Uncertainty Analysis for Engineers*, John Wiley & Sons, New York, 1989.

5. *Guide to the Expression of Uncertainty in Measurement*, International Organization for standardization, Beneve, Switzerland, 1993.

6. "Quality Assessment for Wind Tunnel Testing," AGARD-AR-304, 1994.

7. Brown, Kendall K., Coleman, Hugh W., Steele, W.G., and Taylor, Robert P., "Evaluation of

Correlated Bias Error Effects in Experimental Uncertainty Analysis," AIAA Paper 94-0772, presented at the 32nd Aerospace Sciences Conference, Reno, NV, Jan 1994.

8. Price, Mark L., "Uncertainty of Derived Results on X-Y Plots," Instrumentation Society of America Paper #93-107, Proceedings of the 39th International Instrumentation Symposium, Albuquerque, NM, May 1993.

9. Clark, Edward L., "Uncertainty Estimates for Derivatives and Intercepts," Sandia Report SAND90-2336 • UC-706, Sandia National Laboratories, Albuquerque, NM, September 1994.

10. Moffatt, R. J., "Describing the Uncertainties in Experimental Results," *Experimental Thermal and Fluid Science*, Vol 1, Jan. 1988, pp 3-17

3 pairs	5pairs	7 pairs	9 pairs
(90,90)	(80,80)	(70,70)	(60,60)
(100,100)	(90,90)	(80,80)	(70,70)
(110, 110)	(100, 100)	(90, 90)	(80, 80)
	(110, 110)	(100, 100)	(90, 90)
	(120, 120)	(110, 110)	(100, 100)
		(120, 120)	(110, 110)
		(130, 130)	(120, 120)
			(130, 130)
			(140, 140)

Table 1. True (X,Y) data for all simulations (true line: Y=X+0)

Sim	# of X setpoints, N	# of Y's per X, M	Precision limit determined from
1	3,5,7,9	1	2σ
2	3,5,7,9	3,5,7,9, 11,13,15	$2S_Y$
3	3,5,7,9	1	2σ
4	3,5,7,9	3,5,7,9, 11,13,15	$2S_Y, 2S_X$
5	3,5,7,9	3,5,7,9, 11,13,15	$\frac{2S_Y}{\sqrt{M}}, \frac{2S_X}{\sqrt{M}}$

Table 2. Summary of Simulations.

Sim.	Bias Dominant $B_Y, P_Y,$ B_X, P_X	Bias Precision $B_Y, P_Y,$ B_X, P_X	Precision Dominant $B_Y, P_Y,$ B_X, P_X
1	5, 0.05, n/a, n/a	2.5, 2.5, n/a, n/a	0, 5, n/a, n/a
2	5, 0.05, n/a, n/a	2.5, 2.5, n/a, n/a	0, 5, n/a, n/a
3	5, 0.05, 5, 0.05	2.5, 2.5, 2.5, 2.5	0, 5, 0, 5
4	5, 0.05, 5, 0.05	2.5, 2.5, 2.5, 2.5	0, 5, 0, 5
5	5, 0.05, 5, 0.05	2.5, 2.5, 2.5, 2.5	0, 5, 0, 5

Table 3. Simulation Uncertainty Input Data.

n/a - These simulations did not include any uncertainty in X.

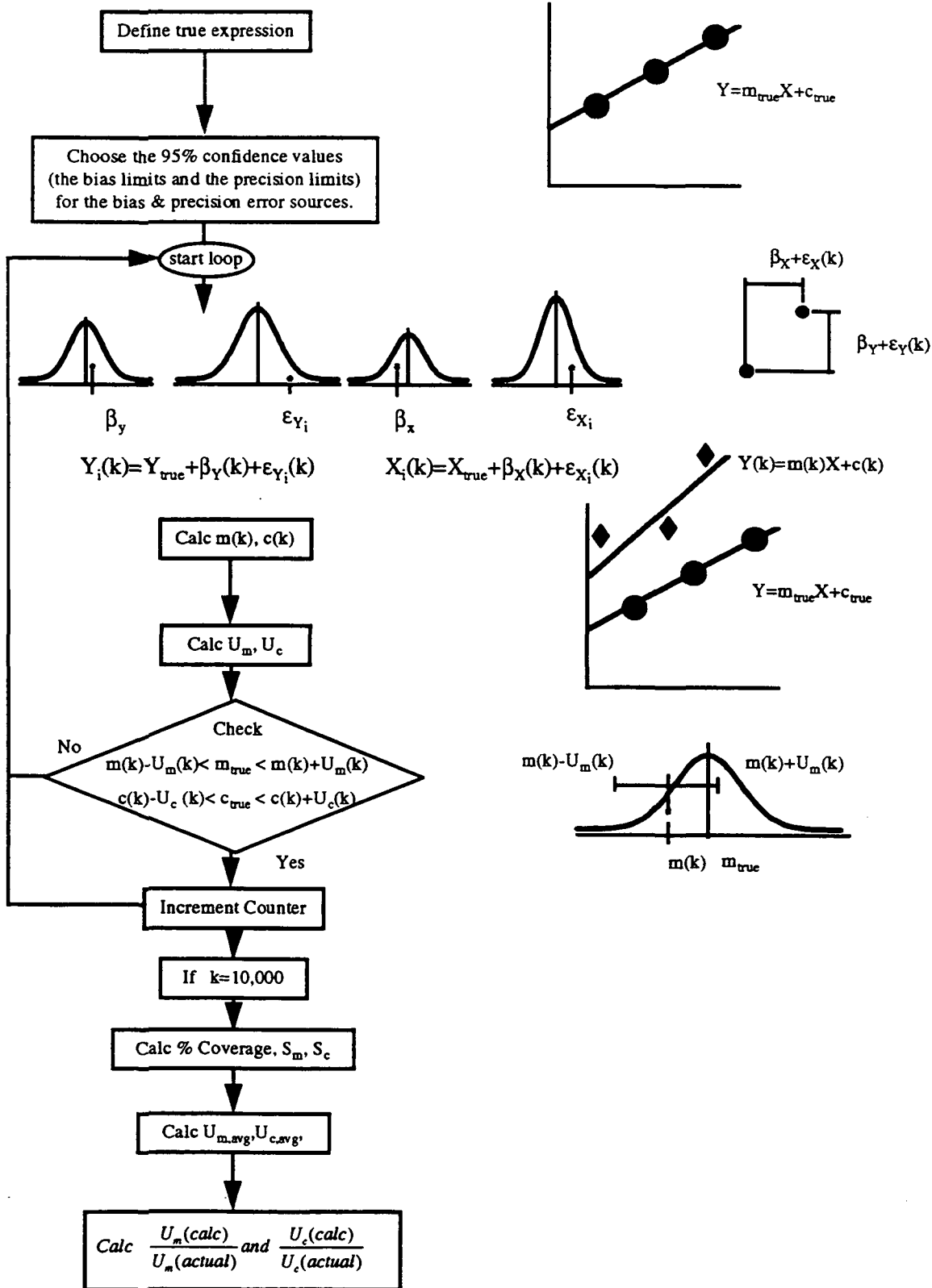


Figure 1. Monte Carlo Simulation Flowchart

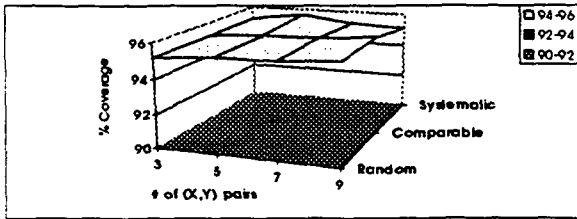


Figure 2. Simulation 1. Plot of Coverage of Slope vs Type of Dominant Uncertainty and Number of Data Uncertainties only in Y.

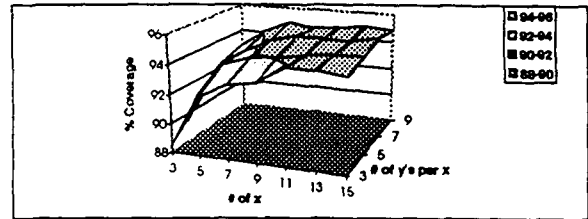


Figure 3. Simulation 2. Plot of Coverage of Slope for Dominant Precision Uncertainties vs Number of Data. Uncertainties only in Y.

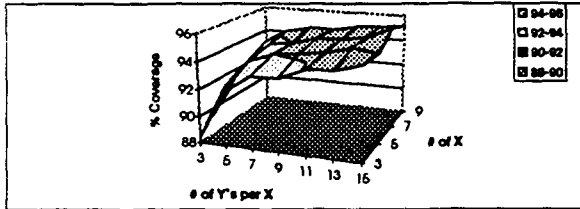


Figure 4. Simulation 2. Plot of Coverage of Slope for Comparable Bias and Precision Uncertainties vs Number of Data. Uncertainties only in Y.

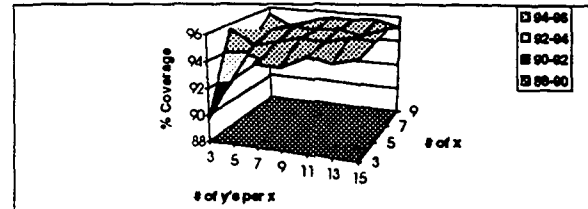


Figure 5. Simulation 2. Plot of Coverage of Intercept for Comparable Bias and Precision Uncertainties vs Number of Data. Uncertainties only in Y.

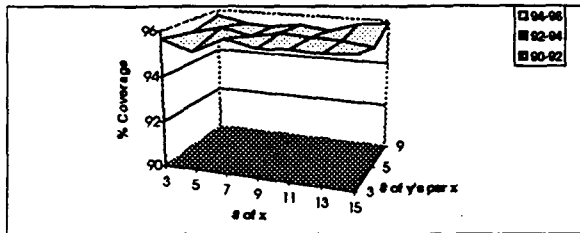


Figure 6. Simulation 2. Plot of Coverage of Intercept for Dominant Bias Uncertainties vs Number of Data. Uncertainties Only in Y.

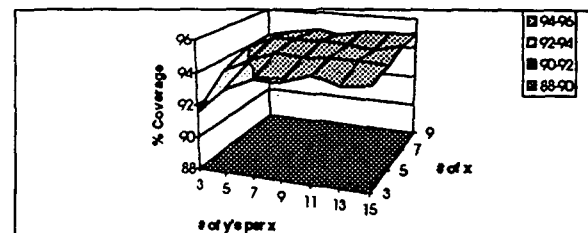


Figure 7. Simulation 4. Plot of Coverage of Slope for Dominant Precision Uncertainties vs Number of Data. Uncertainties in X and Y. Plot identical for Intercept

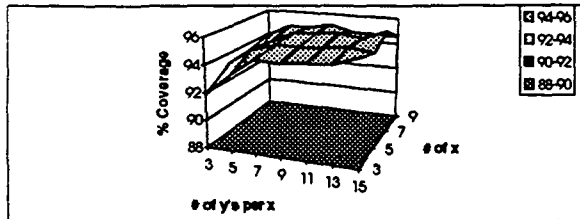


Figure 8. Simulation 5. Plot of Coverage of Intercept for Dominant Precision Uncertainties vs Number of Data. Uncertainties in X and Y

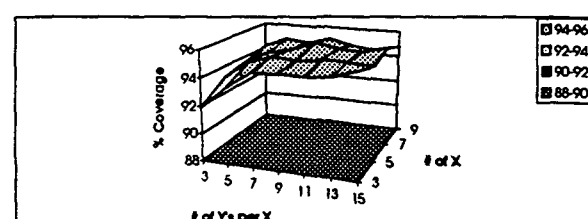


Figure 9. Simulation 5. Plot of Coverage of Slope for Dominant Precision Uncertainties vs Number of Data. Uncertainties in X and Y

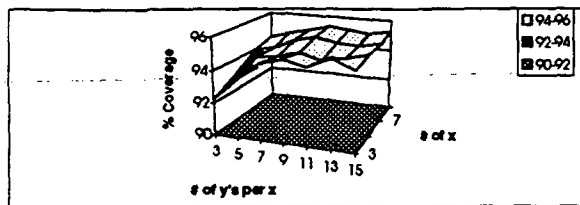


Figure 10 Simulation 5. Plot of Coverage of Slope for Comparable Bias and Precision Uncertainties vs Number of Data. Uncertainties in X and Y.

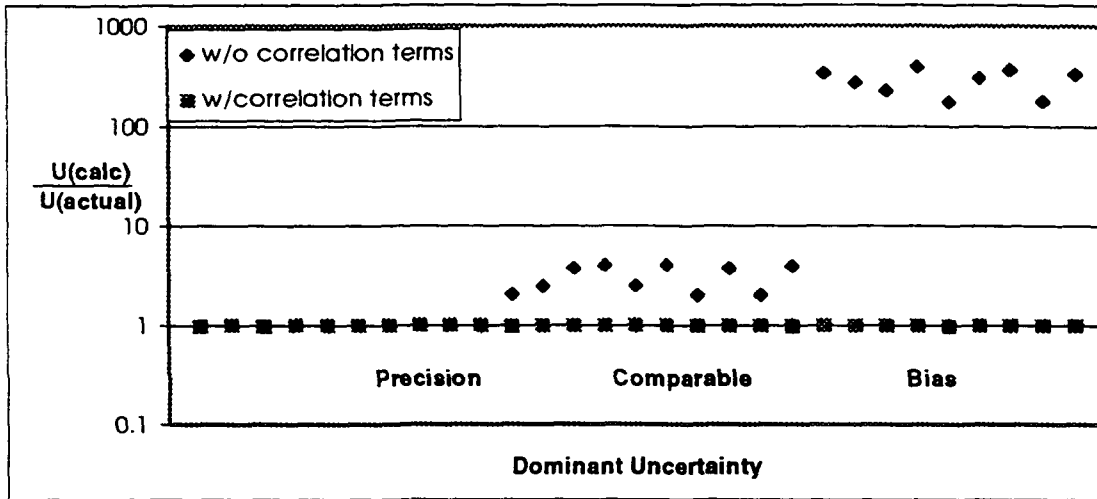


Figure 11. Plot of uncertainty ratios vs dominant uncertainty for slope uncertainty. With and without considering correlated bias uncertainties.

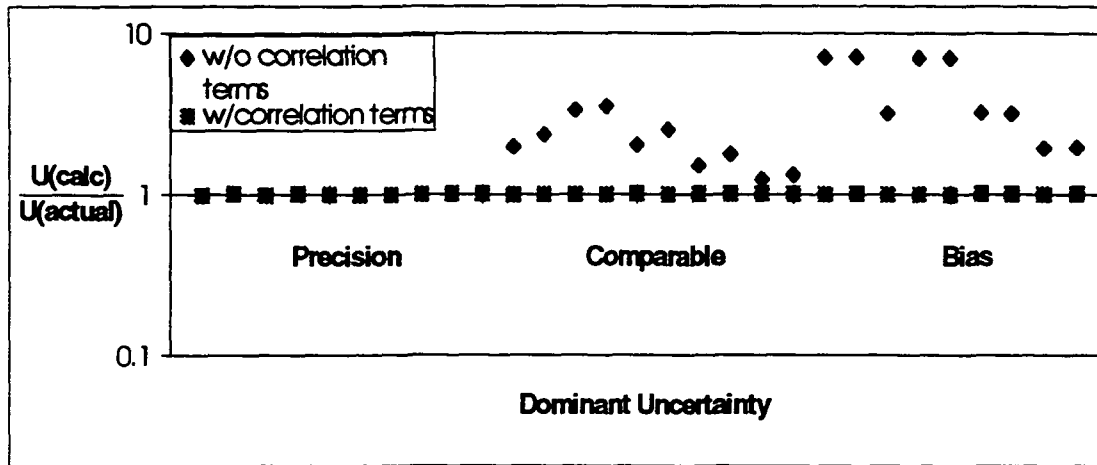


Figure 12. Plot of uncertainty ratios vs dominant uncertainty for Y-intercept uncertainty. With and without considering correlated bias uncertainties.

“PAGE MISSING FROM AVAILABLE VERSION”

Pages 12-37 missing

Appendix V
Elemental Bias Limits Used in Venturi Uncertainty Determination

Venturi # 139 (PID 8802) LPOTP Inlet	
Source	Description
$B_p=1\%$	Sverdrup Report
$B_T=1\%$	Sverdrup Report
$B_{AP}=1\%$	Engineering estimate
$B_{Cd}=0.02$	~2%, Rocketdyne report, C_D Extrapolation, Cryogenic application
$B_{D1}=0.0005$ in	Machining tolerance, Rocketdyne report
$B_{D2}=0.0005$ in	Machining tolerance, Rocketdyne report
$B_\alpha=6.5e-07$ in/in-R	~10%, Engineering estimate

Table A-V.1 LPOTP Inlet Venturi Bias Limit Inputs

Venturi # 20 (PID 8801) LPFT Inlet	
Source	Description
$B_p=1\%$	Sverdrup Report
$B_T=1\%$	Sverdrup Report
$B_{AP}=1\%$	Engineering estimate
$B_{Cd}=0.02$	~2%, 0.8% from RD report, but only cal'd at 7.6% Re
$B_{D1}=0.0005$ in	Machining tolerance, Rocketdyne report
$B_{D2}=0.0005$ in	Machining tolerance, Rocketdyne report
$B_\alpha=4.2e-07$ in/in-R	~10%, Engineering estimate

Table A-V.2 LPFT Inlet Venturi Bias Limit Inputs

Venturi # 397 (PID 8818) CCV Inlet	
Source	Description
$B_p=1\%$	Sverdrup Report
$B_T=1\%$	Sverdrup Report
$B_{AP}=1\%$	Engineering estimate
$B_{Cd}=0.031$	~3%, 2% from RD report, but only cal'd at 1.7% Re
$B_{D1}=0.0005$ in	Machining tolerance, Rocketdyne report
$B_{D2}=0.0005$ in	Machining tolerance, Rocketdyne report
$B_\alpha=5.5e-07$ in/in-R	~10%, Engineering estimate

Table A-V.3 CCV Inlet Venturi Bias Limit Inputs

Venturi # 426 (PID 8819) LPOP Discharge	
Source	Description
$B_P=1\%$	Sverdrup Report
$B_T=1\%$	Sverdrup Report
$B_{\Delta P}=1\%$	Engineering estimate
$B_{Cd}=0.020$	~2%, 1% from RD report, but only cal'd at 4.8% Re
$B_{D1}=0.0005$ in	Machining tolerance, Rocketdyne report
$B_{D2}=0.0005$ in	Machining tolerance, Rocketdyne report
$B_{\alpha}=5.5e-07$ in/in-R	~10%, Engineering estimate

Table A-V.4 LPOP Discharge Venturi Bias Limit Inputs

Venturi # 268 (PID 8804) OPB LOX	
Source	Description
$B_P=1\%$	Sverdrup Report
$B_T=1\%$	Sverdrup Report
$B_{\Delta P}=1\%$	Engineering estimate
$B_{Cd}=0.021$	~2%, .8% from RD report, but only cal'd at 18% Re
$B_{D1}=0.0005$ in	Machining tolerance, Rocketdyne report
$B_{D2}=0.0005$ in	Machining tolerance, Rocketdyne report
$B_{\alpha}=6.7e-07$ in/in-R	~10%, Engineering estimate

Table A-V.5 OPB LOX Venturi Bias Limit Inputs

Venturi # 271 (PID 8805) OPB LH₂	
Source	Description
$B_P=1\%$	Sverdrup Report
$B_T=1\%$	Sverdrup Report
$B_{\Delta P}=1\%$	Engineering estimate
$B_{Cd}=0.031$	~3%, .2.1% from RD report, but only cal'd at 1.86% Re
$B_{D1}=0.0005$ in	Machining tolerance, Rocketdyne report
$B_{D2}=0.0005$ in	Machining tolerance, Rocketdyne report
$B_{\alpha}=3.2e-07$ in/in-R	~10%, Engineering estimate

Table A-V.6 OPB LH₂ Venturi Bias Limit Inputs

Venturi # 296 (PID 8810)		FPB LOX
Source	Description	
$B_P=1\%$	Sverdrup Report	
$B_T=1\%$	Sverdrup Report	
$B_{\Delta P}=1\%$	Engineering estimate	
$B_{C_d}=0.021$	~2%, .125% from RD report, but only cal'd at 20% Re and poor curve-fit	
$B_{D_1}=0.0005$ in	Machining tolerance, Rocketdyne report	
$B_{D_2}=0.0005$ in	Machining tolerance, Rocketdyne report	
$B_{\alpha}=6.7e-07$ in/in-R	~10%, Engineering estimate	

Table A-V.7 FPB LOX Venturi Bias Limit Inputs

Venturi # 3541 (PID 8815)		Nozzle Coolant #1
Source	Description	
$B_P=1\%$	Sverdrup Report	
$B_T=1\%$	Sverdrup Report	
$B_{\Delta P}=1\%$	Engineering estimate	
$B_{C_d}=0.020$	~2%, .115% from RD report, but only cal'd at 3.40% Re	
$B_{D_1}=0.0005$	Machining tolerance, Rocketdyne report	
$B_{D_2}=0.0005$	Machining tolerance, Rocketdyne report	
$B_{\alpha}=5.5e-07$ in/in-R	~10%, Engineering estimate	

Table A-V.8 Nozzle Coolant #1 Venturi Bias Limit Inputs

Venturi # 3542 (PID 8816)		Nozzle Coolant #2
Source	Description	
$B_P=1\%$	Sverdrup Report	
$B_T=1\%$	Sverdrup Report	
$B_{\Delta P}=1\%$	Engineering estimate	
$B_{C_d}=0.020$	~2%, .115% from RD report, but only cal'd at 3.40% Re	
$B_{D_1}=0.0005$ in	Machining tolerance, Rocketdyne report	
$B_{D_2}=0.0005$ in	Machining tolerance, Rocketdyne report	
$B_{\alpha}=5.5e-07$ in/in-R	~10%, Engineering estimate	

Table A-V.9 Nozzle Coolant #2 Venturi Bias Limit Inputs

Venturi # 3543 (PID 8817)	Nozzle Coolant #3
Source	Description
$B_P=1\%$	Sverdrup Report
$B_T=1\%$	Sverdrup Report
$B_{\Delta P}=1\%$	Engineering estimate
$B_{C_d}=0.020$	~2%, .1.15% from RD report, but only cal'd at 3.40% Re
$B_{D1}=0.0005$ in	Machining tolerance, Rocketdyne report
$B_{D2}=0.0005$ in	Machining tolerance, Rocketdyne report
$B_{\alpha}=5.5e-07$ in/in-R	~10%, Engineering estimate

Table A-V.10 Nozzle Coolant #3 Venturi Bias Limit Inputs

Appendix VI
Engine Configuration and Averaged Test Data

ENGINE	TEST_NO	TESTDATE	ADUR	PWRHEAD	MAININJ	MCC	NOZZLE	LPFTPUNIT	HPFTPUNIT	LPOTPUNIT	HPOTPUNIT	LPFTP SERIAL	HPFTP SERIAL	LPOTP SERIAL	HPOTP SERIAL
3001	a50039	1/14/93	210	9	2008	6001	2026	4004R2	4406R2	2218	2722	4873079	4108675	4876205	4871900
3001	a50040	2/11/93	180	9	2008	6001	2026	4004R2	4406R2	2218	2722	4873079	4108675	4876205	4874500
3001	a50041	4/8/93	203	9	2008	6001	2026	4004R2	4406R2	2218	8105R5	4873079	4108675	4876205	BUF500
3001	a50042	4/30/93	203	9	2008	6001	2026	4004R2	8006R1	2218	8105R5	4873079	XFPW06	4876205	BUF500
3001	a50043	7/8/93	190	9	2008	6001	2026	4004R2	4406R2	2218	8202R4	4873079	4108675	4876205	XOPW02
3001	a50044	9/16/93	197	9	2008	6001	2026	4004R2	4406R2	2217	8202R5	4873079	4108675	4876390	XOPW02
3001	a50045	12/22/93	200	9	2008	6001	2026	4004R2	2227R2	2217	2315R3	4873079	4866524	4876390	4877218
3001	a50046	1/27/94	200	9	2008	6001	2026	4004R2	2227R2	4204	2315R3	4873079	4866524	4874193	4877218
3001	a50047	2/15/94	185	9	2008	6001	2026	4004R2	2227R2	4204	2315R3	4873079	4866524	4874193	4877218
3001	a50048	3/18/94	185	9	2008	6001	2026	4004R2	2227R2	4401R1	2315R3	4873079	4866524	4876580	4877218
3001	a50049	4/12/94	180	9	2008	6001	2026	4004R2	2227R2	4401R1	2315R3	4873079	4866524	4876580	4877218
3001	a50050	7/6/94	79	9	2008	6001	2026	4004R2	8106	4204	8107R10	4873079	XFPW06	4874193	XOPW07
3001	a50051	7/20/94	40	9	2008	6001	2026	4004R2	8003	4204	8107R10	4873079	XFPW03	4874193	XOPW07

Table A-VI.1 Engine Hardware Component Configuration

Input data for Venturi Calculations at 100% RPL													AVG	S	S (%)
	Venturi PID	PID	TTB039	TTB040	TTB042	TTB043	TTB044	TTB045	TTB047	TTB048	TTB049	TTB050			
P(psi)	8801	8014	4076	4116	3981	4053	4073	4022	4022	4027	4023	3999	4039.2	40.4	1.0
ΔP(psia)	"	8015	269	271	245	281	267	254	262	276	251	256	263.1	11.5	4.4
T(°R)	"	8016	472	461	467	471	481	463	463	465	466	474	468.2	6.1	1.3
P(psi)	8818	8339	5419	5512	5235	5361	5374	5309	5308	5318	5307	5224	5336.9	85.4	1.6
ΔP(psia)	"	8340	367	311	350	391	390	396	398	395	387	386	377.2	27.5	7.3
T(°R)	"	8341	94	94	91	95	95	90	91	90	91	93	92.4	1.9	2.1
P(psi)	8815	8505	5558	5613	5373	5516	5523	5460	5439	5468	5461	5384	5479.4	74.7	1.4
ΔP(psia)	"	8508	128	157	125	114	119	112	128	105	110	120	121.8	14.6	12.0
T(°R)	"	8511	108	102	100	120	93	89	90	89	89	92	97.1	10.4	10.7
P(psi)	8816	8506	5541	5605	5357	5501	5515	5440	5430	5447	5440	5385	5466.2	74.5	1.4
ΔP(psia)	"	8509	123	148	124	114	113	108	114	109	108	118	117.9	12.1	10.3
T(°R)	"	8512	96	96	93	96	95	91	91	91	91	93	93.0	2.3	2.4
P(psi)	8817	8507	5538	5604	5357	5499	5512	5430	5429	5445	5440	5392	5464.6	73.6	1.3
ΔP(psia)	"	8510	170	191	156	151	155	99	131	141	135	121	145.1	25.8	17.8
T(°R)	"	8513	98	97	94	737	92	88	89	88	88	91	156.2	204.1	130.7
P(psi)	8802	8232	3656	3642	3780	3788	3780	3687	3659	3646	3653	3796	3708.8	67.8	1.8
ΔP(psia)	"	8233	181	179	183	193	192	192	203	190	189	207	190.9	8.9	4.7
T(°R)	"	8234	193	190	188	190	189	192	192	191	193	188	190.7	1.9	1.0
P(psi)	8819	8751	3735	3717	3691	3673	3673	3739	3718	3692	3696	3718	3705.3	23.6	0.6
ΔP(psia)	"	8752	253	251	239	239	236	249	248	254	246	245	245.9	6.3	2.5
T(°R)	"	8293	194	191	190	192	192	194	194	193	194	191	192.3	1.6	0.9
P(psi)	8804	8425	6634	6695	6786	6494	6491	6856	6850	6802	6812	6621	6704.2	138.9	2.1
ΔP(psia)	"	8426	-92	100	150	152	152	114	121	113	114	134	105.8	72.1	68.1
T(°R)	"	8427	206	204	206	212	215	216	216	215	216	215	212.1	4.9	2.3
P(psi)	8805	8428	5003	5006	4846	4996	4990	4948	4945	4958	4953	4888	4953.3	52.0	1.0
ΔP(psia)	"	8429	256	260	211	267	261	231	231	247	233	261	245.8	18.4	7.5
T(°R)	"	8430	284	290	283	281	281	277	278	278	278	281	280.9	3.9	1.4
P(psi)	8810	8463	6780	6738	6848	6541	6555	6908	6897	6837	6843	6653	6760.0	134.8	2.0
ΔP(psia)	"	8464	125	130	113	113	123	117	109	101	121	97	115.0	10.4	9.0
T(°R)	"	8465	207	203	205	206	205	206	206	205	207	205	205.5	1.2	0.6

Appendix VII
Calculated Venturi Mass Flowrate Data
and Test-to-Test Standard Deviations

Calculated Venturi Mass Flow Rates (lb/sec) @ 100% RPL data														
PID	ttb050	ttb049	ttb048	ttb047	ttb045	ttb044	ttb043	ttb042	ttb040	ttb039		avg	S	S (%)
8801	26.6	26.6	27.8	27.2	26.8	27.1	27.9	26.2	28.0	27.5		27.2	0.62	2.3
8818	71.4	71.9	72.6	72.8	72.7	71.9	71.9	68.6	65.2	70.1		70.9	2.41	3.4
8815	13.1	12.6	12.4	13.6	12.8	13.1	12.2	13.2	14.8	13.2		13.1	0.72	5.5
8816	12.8	12.3	12.4	12.6	12.3	12.5	12.6	13.1	14.3	13.1		12.8	0.60	4.7
8817	13.0	13.8	14.0	13.6	11.8	14.6	7.2	14.6	16.1	15.2		13.4	2.47	18.5
8802	183	174	175	181	176	176	176	173	170	171		175	4.15	2.4
8819	910	907	924	913	914	891	897	899	921	920		910	11.0	1.2
8804	24.1	22.2	22.1	22.8	22.2	25.6	25.7	25.7	21.0	20.1		23.1	2.01	8.7
8805	34.4	32.9	33.8	32.8	32.9	34.6	35.0	31.0	34.2	34.2		33.6	1.20	3.6
8810	57.5	64.0	58.7	60.9	63.1	64.5	61.9	62.1	66.5	65.1		62.4	2.84	4.6
total	1346	1337	1352	1350	1344	1331	1327	1326	1350	1349		1341	10	0.8

Table A-VII.1 Venturi Mass Flowrates for Tests TTB 039-050 and Standard Deviations @ 100% RPL

Calculated Venturi Mass Flow Rates @ 100% RPL data (same engine components; Rocketdyne HPOTP)								
	ttb049	ttb048	ttb047	ttb045		avg	S	S (%)
8801	26.6	27.8	27.2	26.8		27.1	0.51	1.9
8818	71.9	72.6	72.8	72.7		72.5	0.41	0.6
8815	12.6	12.4	13.6	12.8		12.8	0.52	4.1
8816	12.3	12.4	12.6	12.3		12.4	0.15	1.2
8817	13.8	14.0	13.6	11.8		13.3	0.99	7.5
8802	174	175	181	176		176	3.10	1.8
8819	907	924	913	914		914	6.94	0.8
8804	22.2	22.1	22.8	22.2		22.3	0.35	1.6
8805	32.9	33.8	32.8	32.9		33.1	0.49	1.5
8810	64.0	58.7	60.9	63.1		61.6	2.39	3.9
total	1337	1352	1350	1344		1346	6.69	0.5

Table A-VII.2 Venturi Mass Flowrates for Tests TTB 045, 0048-049 and Standard Deviations @ 100% RPL

Calculated Venturi Mass Flow Rates (lb/sec) @ 104% RPL data														
PID	ttb050	ttb049	ttb048	ttb047	ttb045	ttb044	ttb043	ttb042	ttb040	ttb039		avg	S	S (%)
8801	28.0	28.1	29.2	28.5	28.3	28.4	29.3	27.4	28.6			28.4	0.59	2.1
8818	73.8	74.0	74.8	75.0	75.0	74.1	74.2	72.1	73.7			74.1	0.88	1.2
8815	13.8	13.9	13.3	13.8	13.1	13.4	12.7	13.4	13.3			13.4	0.37	2.7
8816	13.5	13.5	13.1	13.3	12.7	13.0	13.3	13.3	13.0			13.2	0.25	1.9
8817	13.6	14.5	14.6	14.0	6.0	14.3	7.3	15.0	15.2			12.7	3.49	27.4
8802	188	178	179	185	180	181	182	177	175			181	4.08	2.3
8819	948	943	962	951	949	926	932	933	953			944	11.60	1.2
8804	26.1	23.9	24.0	24.5	23.9	27.2	27.4	27.4	22.5			25.2	1.83	7.3
8805	35.7	33.7	34.8	33.5	34.0	36.1	36.2	32.3	35.8			34.7	1.39	4.0
8810	61.3	67.6	63.2	65.4	67.6	69.0	66.6	65.6	70.2			66.3	2.79	4.2
total	1402	1390	1408	1404	1389	1382	1381	1377	1401			1393	11	0.8

Table A-VII.3 Venturi Mass Flowrates for Tests TTB 040-050 and Standard Deviations @ 104% RPL

Calculated Venturi Mass Flow Rates (lb/sec) @ 104% RPL data (same engine components; Rocketdyne HPOTP)								
	ttb049	ttb048	ttb047	ttb045		avg	S	S (%)
8801	28.1	29.2	28.5	28.3		28.5	0.50	1.7
8818	74.0	74.8	75.0	75.0		74.7	0.47	0.6
8815	13.9	13.3	13.8	13.1		13.5	0.38	2.8
8816	13.5	13.1	13.3	12.7		13.1	0.32	2.4
8817	14.5	14.6	14.0	6.0		12.3	4.18	34.0
8802	178	179	185	180		180.4	3.07	1.7
8819	943	962	951	949		951.1	7.77	0.8
8804	23.9	24.0	24.5	23.9		24.1	0.27	1.1
8805	33.7	34.8	33.5	34.0		34.0	0.57	1.7
8810	67.6	63.2	65.4	67.6		65.93	2.11	3.2
total	1390	1408	1404	1389		1398	9.58	0.7

Table A-VII.2 Venturi Mass Flowrates for Tests TTB 045, 048-049 and Standard Deviations @ 100% RPL

Calculated Venturi Mass Flow Rates (lb/sec) @ 109% RPL data

PID	ttb050	ttb049	ttb048	ttb047	ttb045	ttb044	ttb043	ttb042	ttb040	ttb039		avg	S	S (%)
8801	29.8	29.9	31.0	30.3	30.0	30.1	31.1	28.6	30.4			30.1	0.73	2.4
8818	76.6	76.6	77.4	77.7	77.9	76.9	76.9	75.8	76.5			76.9	0.65	0.9
8815	14.7	14.8	14.4	14.5	13.8	14.6	13.9	13.0	14.0			14.2	0.57	4.0
8816	14.4	14.1	14.2	14.0	13.4	14.2	14.3	13.0	13.7			13.9	0.45	3.3
8817	14.3	15.4	15.5	14.9	8.3	16.2	8.4	15.4	16.0			13.8	3.15	22.8
8802	195	182	184	190	185	187	186	184	181			186	4.47	2.4
8819	993	989	1005	992	991	970	973	972	996			987	12.1	1.2
8804	28.6	26.6	26.3	27.0	26.2	29.2	29.2	29.8	25.3			27.6	1.65	6.0
8805	37.0	34.7	36.2	34.5	35.3	38.0	38.5	33.2	36.7			36.0	1.73	4.8
8810	66.0	72.6	68.5	71.0	72.9	74.6	72.6	70.0	76.3			71.6	3.13	4.4
total	1470	1455	1472	1466	1453	1450	1443	1435	1466			1457	12.68	0.9

Table A-VII.5 Venturi Mass Flowrates for Tests TTB 040-050 and Standard Deviations @ 109% RPL

Calculated Venturi Mass Flow Rates (lb/sec) @ 109% RPL data (same engine components; Rocketdyne HPOTP)

	ttb049	ttb048	ttb047	ttb045		avg	S	S (%)
8801	29.9	31.0	30.3	30.0		30.3	0.47	1.5
8818	76.6	77.4	77.7	77.9		77.4	0.55	0.7
8815	14.8	14.4	14.5	13.8		14.4	0.41	2.9
8816	14.1	14.2	14.0	13.4		13.9	0.35	2.5
8817	15.4	15.5	14.9	8.3		13.5	3.47	25.6
8802	182	184	190	185		185	3.56	1.9
8819	989	1005	992	991		994	7.37	0.7
8804	26.6	26.3	27.0	26.2		26.5	0.36	1.3
8805	34.7	36.2	34.5	35.3		35.2	0.74	2.1
8810	72.6	68.5	71.0	72.9		71.2	2.00	2.8
total	1455	1472	1466	1453		1462	8.95	0.6

Table A-VII.6 Venturi Mass Flowrates for Tests TTB 045, 048-049 and Standard Deviations @ 109% RPL

Appendix VIII
Venturi Mass Flowrate Data and Calculated Bias Limits

ttb050/100%				ttb050/104%				ttb050/109%			
	W lb/sec	Bw lb/sec	Bw (%)		W lb/sec	Bw lb/sec	Bw (%)		W lb/sec	Bw lb/sec	Bw (%)
8801	26.61	0.55	2.05	8801	28.02	0.58	2.05	8801	29.78	0.61	2.05
8818	71.41	2.17	3.04	8818	73.78	2.24	3.04	8818	76.57	2.33	3.04
8815	13.08	0.27	2.07	8815	13.77	0.29	2.07	8815	14.67	0.3	2.07
8816	12.78	0.27	2.11	8816	13.48	0.28	2.11	8816	14.37	0.3	2.11
8817	12.98	0.27	2.1	8817	13.58	0.29	2.1	8817	14.33	0.3	2.1
8802	183.29	3.8	2.07	8802	188.29	3.9	2.07	8802	195.4	4.05	2.07
8819	910.39	18.69	2.05	8819	947.63	19.43	2.05	8819	993.1	20.35	2.05
8804	24.05	0.5	2.07	8804	26.09	0.54	2.07	8804	28.55	0.59	2.07
8805	34.39	0.7	2.02	8805	35.68	0.72	2.02	8805	37.04	0.75	2.02
8810	57.47	1.19	2.07	8810	61.29	1.27	2.07	8810	66.03	1.37	2.07

Table A-VIII.1 Venturi Flowrates and Bias Limits for test TTB050

ttb049/100%				ttb049/104%				ttb049/109%			
	W lb/sec	Bw lb/sec	Bw (%)		W lb/sec	Bw lb/sec	Bw (%)		W lb/sec	Bw lb/sec	Bw (%)
8801	26.63	0.55	2.05	8801	28.12	0.58	2.05	8801	29.91	0.61	2.04
8818	71.89	2.19	3.04	8818	73.99	2.25	3.04	8818	76.63	2.33	3.04
8815	12.61	0.26	2.07	8815	13.91	0.29	2.07	8815	14.78	0.31	2.07
8816	12.31	0.26	2.11	8816	13.47	0.28	2.11	8816	14.12	0.3	2.11
8817	13.75	0.29	2.1	8817	14.45	0.3	2.1	8817	15.37	0.32	2.11
8802	173.9	3.6	2.07	8802	177.65	3.68	2.07	8802	182.2	3.77	2.07
8819	907.18	18.65	2.06	8819	943.16	19.36	2.05	8819	988.5	20.28	2.05
8804	22.16	0.46	2.07	8804	23.92	0.5	2.07	8804	26.56	0.55	2.07
8805	32.92	0.67	2.02	8805	33.74	0.68	2.02	8805	34.73	0.7	2.02
8810	64	1.33	2.07	8810	67.59	1.4	2.07	8810	72.56	1.5	2.07

Table A-VIII.2 Venturi Flowrates and Bias Limits for test TTB049

ttb048/100%				ttb048/104%				ttb048/109%			
	W lb/sec	Bw lb/sec	Bw (%)		W lb/sec	Bw lb/sec	Bw (%)		W lb/sec	Bw lb/sec	Bw (%)
8801	27.79	0.57	2.04	8801	29.23	0.6	2.04	8801	30.95	0.63	2.04
8818	72.63	2.21	3.04	8818	74.76	2.27	3.04	8818	77.37	2.35	3.04
8815	12.35	0.26	2.07	8815	13.31	0.28	2.07	8815	14.38	0.3	2.07
8816	12.37	0.26	2.11	8816	13.11	0.28	2.11	8816	14.15	0.3	2.11
8817	14.03	0.3	2.1	8817	14.64	0.31	2.11	8817	15.52	0.33	2.1
8802	174.63	3.62	2.07	8802	179.17	3.71	2.07	8802	184	3.81	2.07
8819	923.88	18.98	2.05	8819	961.66	19.73	2.05	8819	1005	20.6	2.05
8804	22.05	0.46	2.07	8804	23.97	0.5	2.07	8804	26.26	0.54	2.07
8805	33.84	0.68	2.02	8805	34.81	0.7	2.02	8805	36.19	0.73	2.02
8810	58.65	1.22	2.07	8810	63.16	1.31	2.07	8810	68.5	1.42	2.07

Table A-VIII.3 Venturi Flowrates and Bias Limits for test TTB048

ttb047/100				ttb047/104				ttb047/109			
	W lb/sec	Bw lb/sec	Bw (%)		W lb/sec	Bw lb/sec	Bw (%)		W lb/sec	Bw lb/sec	Bw (%)
8801	27.19	0.56	2.05	8801	28.52	0.58	2.05	8801	30.32	0.62	2.05
8818	72.77	2.21	3.04	8818	74.96	2.28	3.04	8818	77.74	2.36	3.04
8815	13.56	0.28	2.07	8815	13.75	0.28	2.07	8815	14.53	0.3	2.07
8816	12.64	0.27	2.11	8816	13.25	0.28	2.11	8816	14	0.3	2.11
8817	13.56	0.29	2.1	8817	14.01	0.29	2.1	8817	14.87	0.31	2.1
8802	180.74	3.75	2.07	8802	184.76	3.83	2.07	8802	190.4	3.95	2.07
8819	913.02	18.76	2.05	8819	951.13	19.52	2.05	8819	992	20.35	2.05
8804	22.83	0.47	2.07	8804	24.49	0.51	2.07	8804	26.95	0.56	2.07
8805	32.79	0.66	2.02	8805	33.5	0.68	2.02	8805	34.54	0.7	2.02
8810	60.88	1.26	2.07	8810	65.41	1.36	2.07	8810	70.95	1.47	2.07

Table A-VIII4 Venturi Flowrates and Bias Limits for test TTB047

ttb045/100				ttb045/104			
	W lb/sec	Bw lb/sec	Bw (%)		W lb/sec	Bw lb/sec	Bw (%)
8801	26.84	0.55	2.05	8801	28.25	0.58	2.05
8818	72.72	2.21	3.04	8818	75.02	2.28	3.04
8815	12.75	0.26	2.07	8815	13.08	0.27	2.07
8816	12.33	0.26	2.11	8816	12.72	0.27	2.11
8817	11.83	0.25	2.11	8817	6.03	0.13	2.11
8802	175.52	3.64	2.07	8802	179.91	3.73	2.07
8819	913.64	18.77	2.05	8819	948.5	19.47	2.05
8804	22.18	0.46	2.07	8804	23.94	0.5	2.07
8805	32.86	0.66	2.02	8805	33.95	0.69	2.02
8810	63.05	1.31	2.07	8810	67.55	1.4	2.07

Table A-VIII5 Venturi Flowrates and Bias Limits for test TTB045

ttb044/100				ttb044/104				ttb044/109			
	W lb/sec	Bw lb/sec	Bw (%)		W lb/sec	Bw lb/sec	Bw (%)		W lb/sec	Bw lb/sec	Bw (%)
8801	27.13	0.56	2.05	8801	28.42	0.58	2.05	8801	30.1	0.62	2.04
8818	71.88	2.19	3.04	8818	74.13	2.25	3.04	8818	76.91	2.34	3.04
8815	13.05	0.27	2.07	8815	13.44	0.28	2.07	8815	14.64	0.3	2.07
8816	12.52	0.26	2.11	8816	13.01	0.27	2.11	8816	14.15	0.3	2.11
8817	14.62	0.31	2.1	8817	14.32	0.3	2.1	8817	16.21	0.34	2.11
8802	176.13	3.65	2.07	8802	181.06	3.75	2.07	8802	186.5	3.86	2.07
8819	891.37	18.33	2.06	8819	925.54	19	2.05	8819	970	19.89	2.05
8804	25.55	0.53	2.07	8804	27.19	0.56	2.07	8804	29.19	0.6	2.07
8805	34.61	0.7	2.02	8805	36.12	0.73	2.02	8805	37.95	0.77	2.02
8810	64.48	1.34	2.07	8810	69	1.43	2.07	8810	74.61	1.55	2.07

Table A-VIII6 Venturi Flowrates and Bias Limits for test TTB044

ttb043/100				ttb043/104				ttb043/109			
	W lb/sec	Bw lb/sec	Bw (%)		W lb/sec	Bw lb/sec	Bw (%)		W lb/sec	Bw lb/sec	Bw (%)
8801	27.94	0.57	2.04	8801	29.27	0.6	2.05	8801	31.05	0.63	2.04
8818	71.92	2.19	3.04	8818	74.19	2.26	3.04	8818	76.87	2.34	3.04
8815	12.18	0.25	2.08	8815	12.74	0.27	2.08	8815	13.89	0.29	2.08
8816	12.59	0.27	2.11	8816	13.29	0.28	2.11	8816	14.26	0.3	2.11
8817	7.18	0.16	2.18	8817	7.27	0.16	2.18	8817	8.37	0.18	2.18
8802	176.47	3.65	2.07	8802	182.08	3.77	2.07	8802	185.5	3.84	2.07
8819	896.57	18.43	2.06	8819	932.3	19.13	2.05	8819	973.1	19.95	2.05
8804	25.67	0.53	2.07	8804	27.38	0.57	2.07	8804	29.22	0.6	2.07
8805	34.97	0.71	2.02	8805	36.22	0.73	2.02	8805	38.51	0.78	2.02
8810	61.85	1.28	2.07	8810	66.59	1.38	2.07	8810	72.6	1.51	2.07

Table A-VIII.7 Venturi Flowrates and Bias Limits for test TTB043

ttb042/100				ttb042/104				ttb042/109			
	W (lb/sec)	Bw (lb/sec)	Bw (%)		W (lb/sec)	Bw (lb/sec)	Bw (%)		W (lb/sec)	Bw lb/sec	Bw (%)
8801	26.15	0.54	2.05	8801	27.37	0.56	2.05	8801	28.58	0.59	2.05
8818	68.57	2.08	3.04	8818	72.12	2.19	3.04	8818	75.79	2.3	3.04
8815	13.17	0.27	2.07	8815	13.39	0.28	2.07	8815	13	0.27	2.07
8816	13.11	0.28	2.11	8816	13.33	0.28	2.11	8816	12.99	0.27	2.11
8817	14.59	0.31	2.11	8817	14.96	0.31	2.11	8817	15.35	0.32	2.11
8802	172.59	3.57	2.07	8802	177.16	3.67	2.07	8802	183.9	3.81	2.07
8819	898.76	18.46	2.05	8819	933.2	19.14	2.05	8819	972.3	19.93	2.05
8804	25.67	0.53	2.07	8804	27.38	0.57	2.07	8804	29.83	0.62	2.07
8805	30.98	0.63	2.03	8805	32.26	0.65	2.02	8805	33.19	0.67	2.02
8810	62.11	1.29	2.07	8810	65.58	1.36	2.07	8810	69.96	1.45	2.07

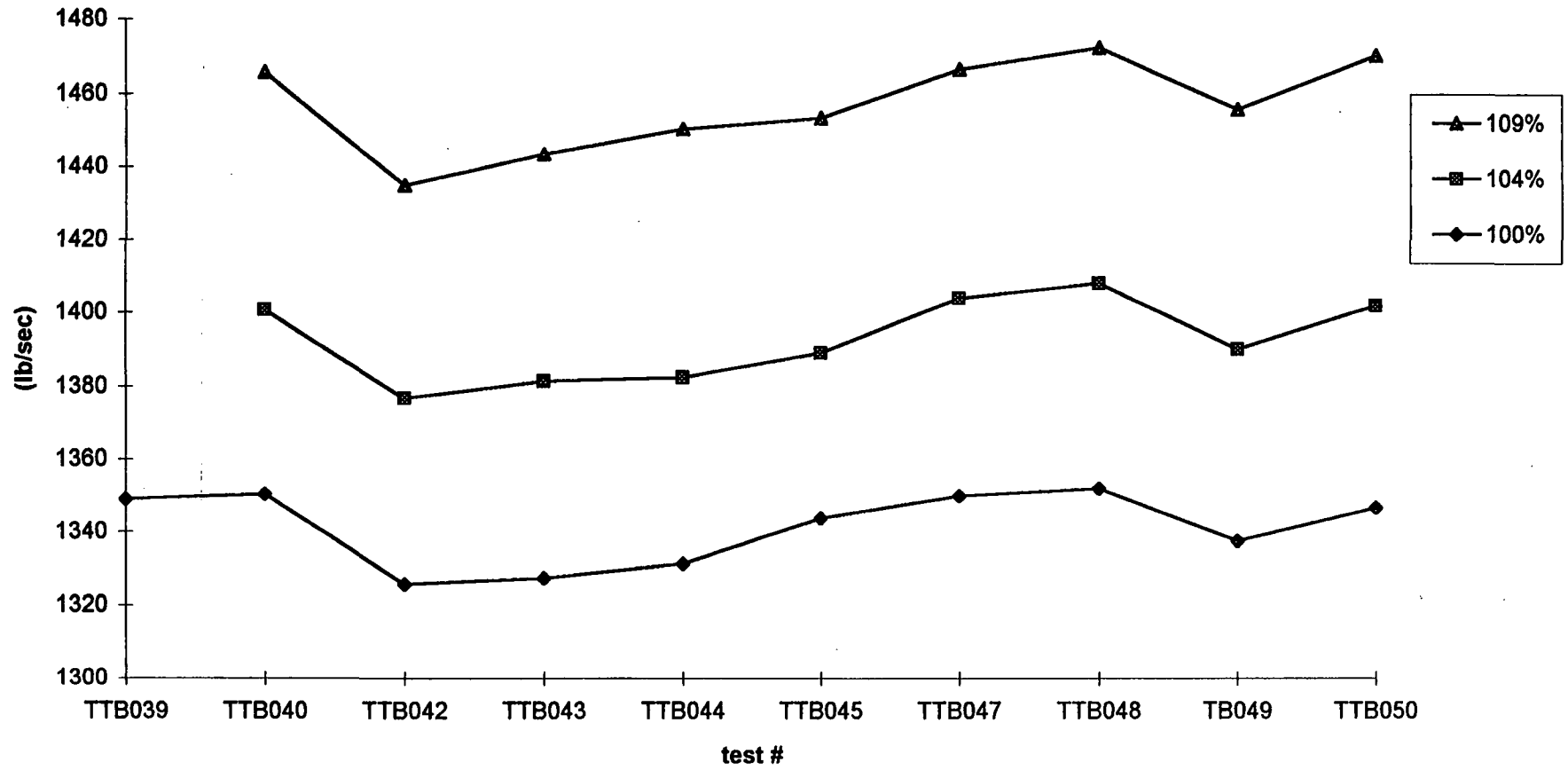
Table A-VIII.7 Venturi Flowrates and Bias Limits for test TTB042

ttb040/100				ttb040/104				ttb040/109			
	W (lb/sec)	Bw (lb/sec)	Bw (%)		W (lb/sec)	Bw (lb/sec)	Bw (%)		W (lb/sec)	Bw (lb/sec)	Bw (%)
8801	27.95	0.57	2.04	8801	28.61	0.58	2.04	8801	30.44	0.62	2.04
8818	65.15	1.98	3.04	8818	73.7	2.24	3.04	8818	76.47	2.33	3.04
8815	14.75	0.31	2.07	8815	13.34	0.28	2.07	8815	13.98	0.29	2.07
8816	14.3	0.3	2.11	8816	13	0.27	2.11	8816	13.71	0.29	2.11
8817	16.07	0.34	2.11	8817	15.22	0.32	2.11	8817	16	0.34	2.11
8802	170.03	3.52	2.07	8802	175	3.62	2.07	8802	180.8	3.75	2.07
8819	920.51	18.9	2.05	8819	953.27	19.55	2.05	8819	996	20.42	2.05
8804	20.96	0.43	2.07	8804	22.5	0.47	2.07	8804	25.27	0.52	2.07
8805	34.23	0.69	2.03	8805	35.84	0.72	2.02	8805	36.69	0.74	2.02
8810	66.52	1.38	2.07	8810	70.23	1.46	2.07	8810	76.29	1.58	2.07

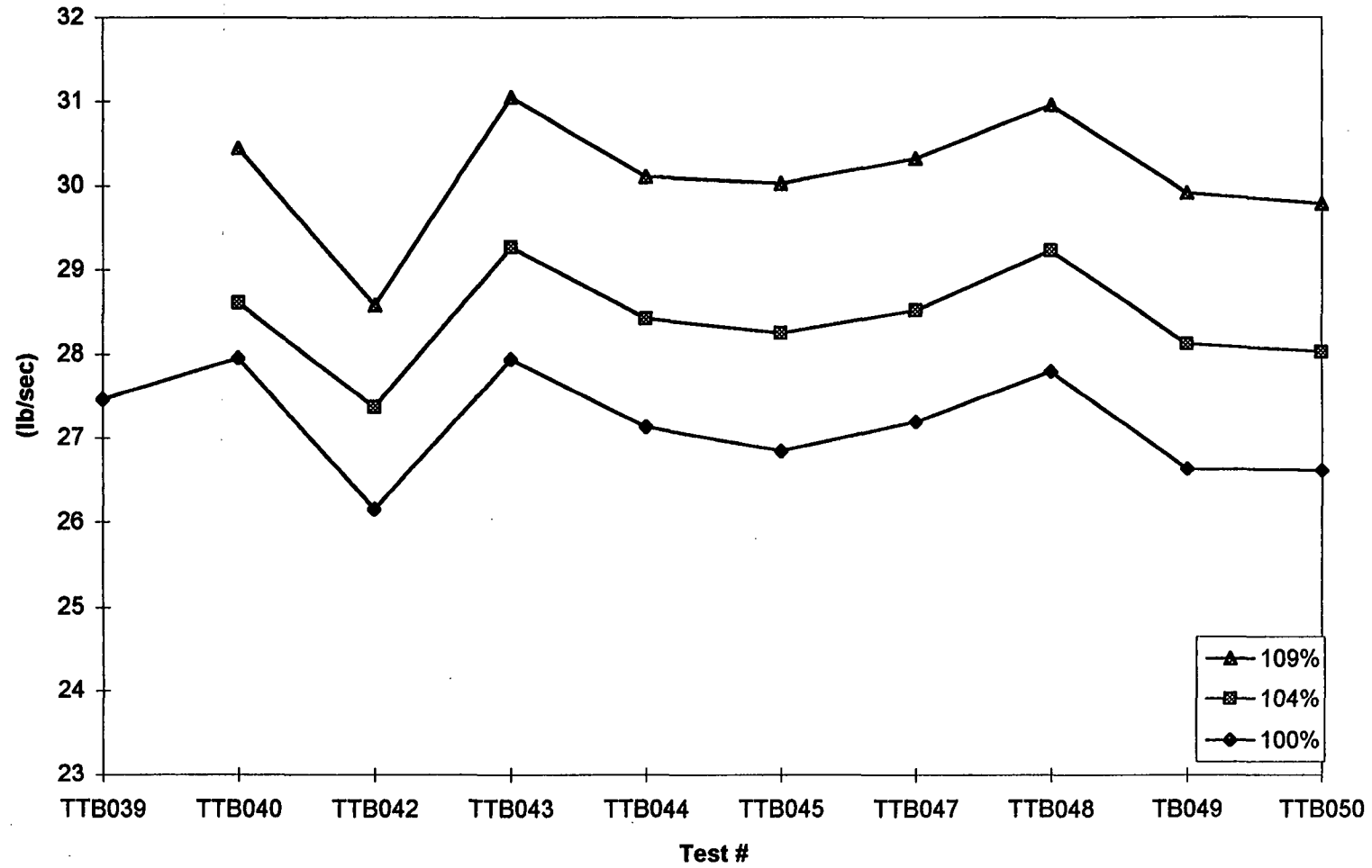
Table A-VIII.8 Venturi Flowrates and Bias Limits for test TTB040

Appendix IX
Test-to-Test Plots of Venturi Mass Flowrate

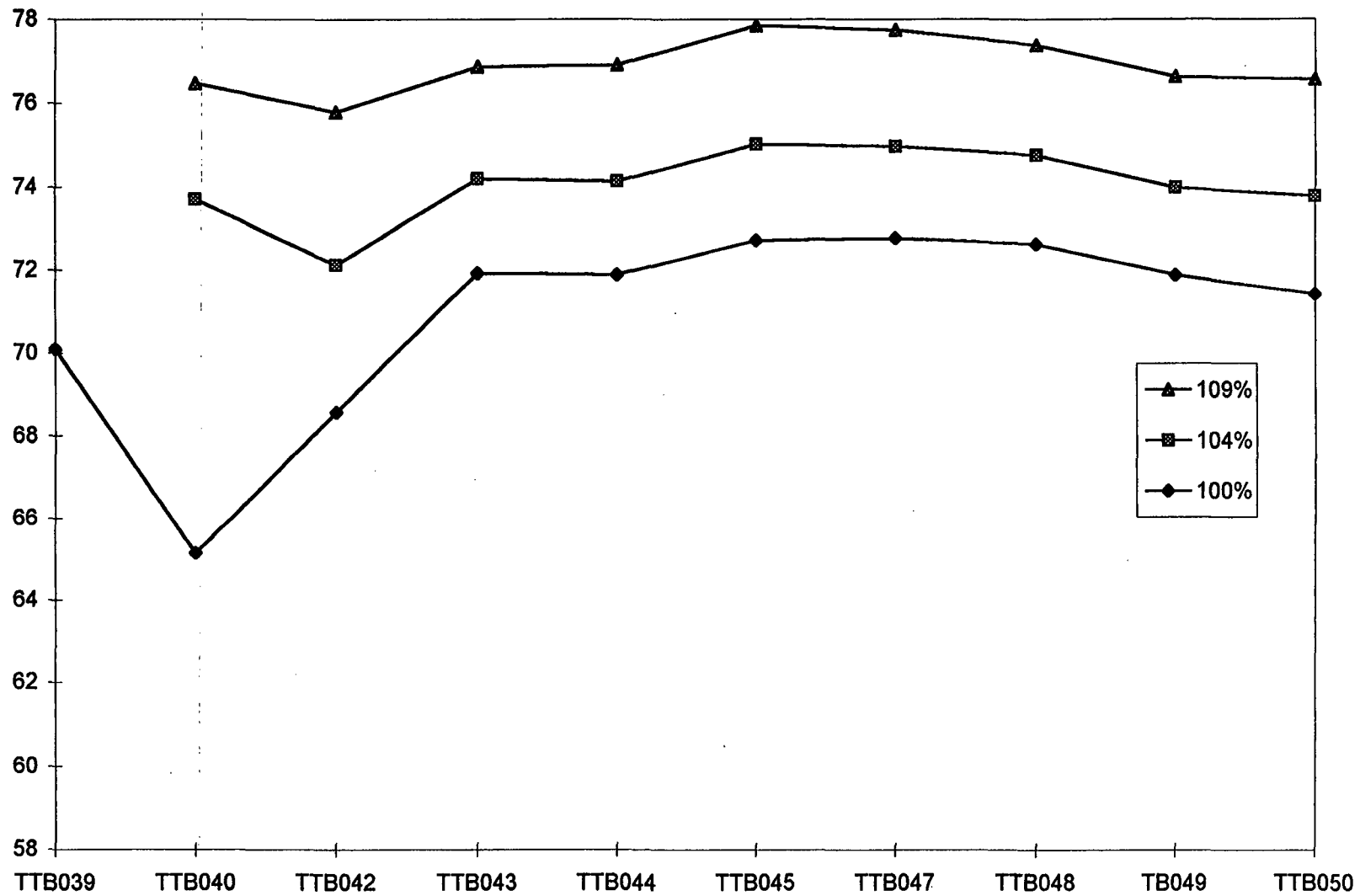
Plot of Total Flow Rate per Test



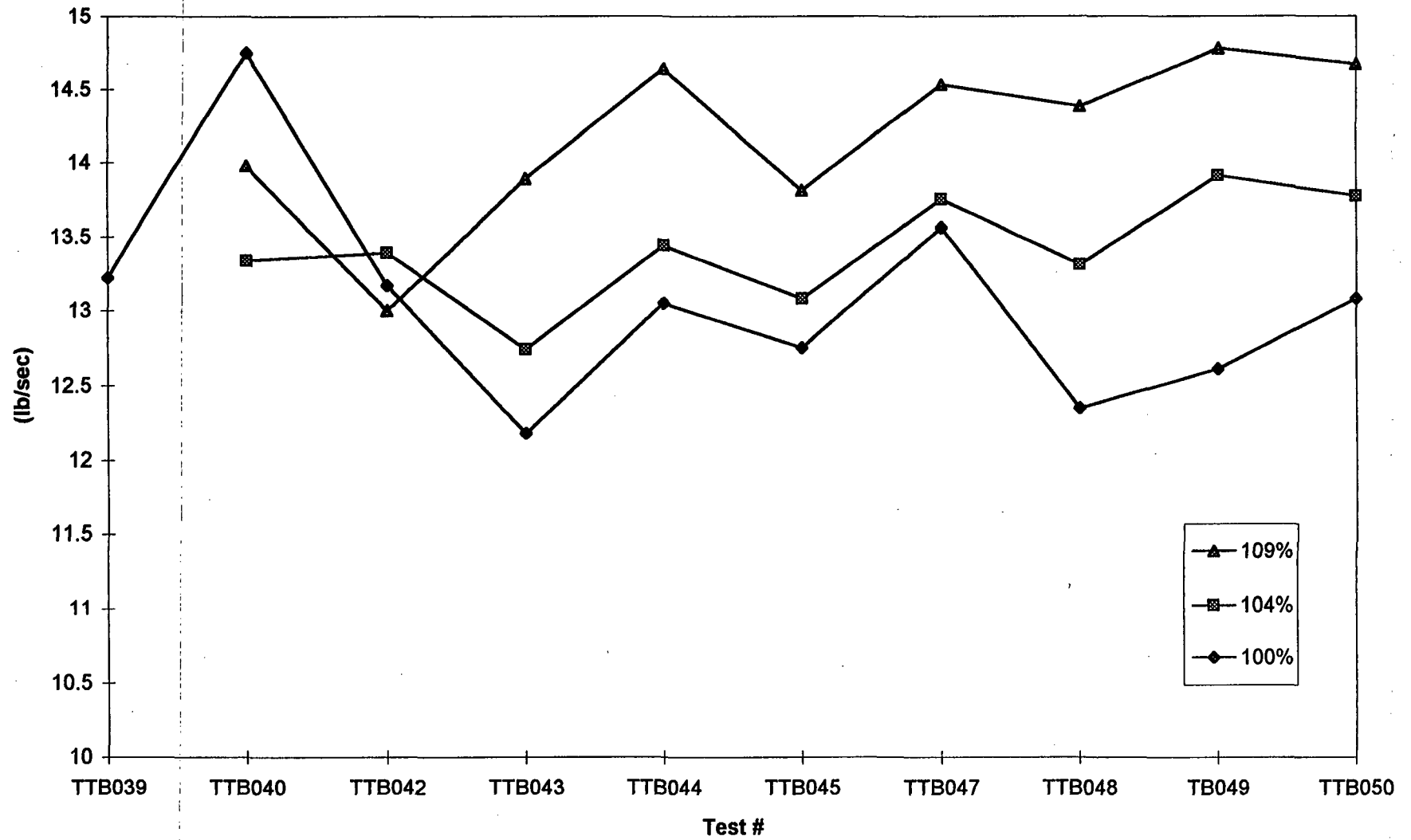
LPFT Inlet Flowrate vs Test #



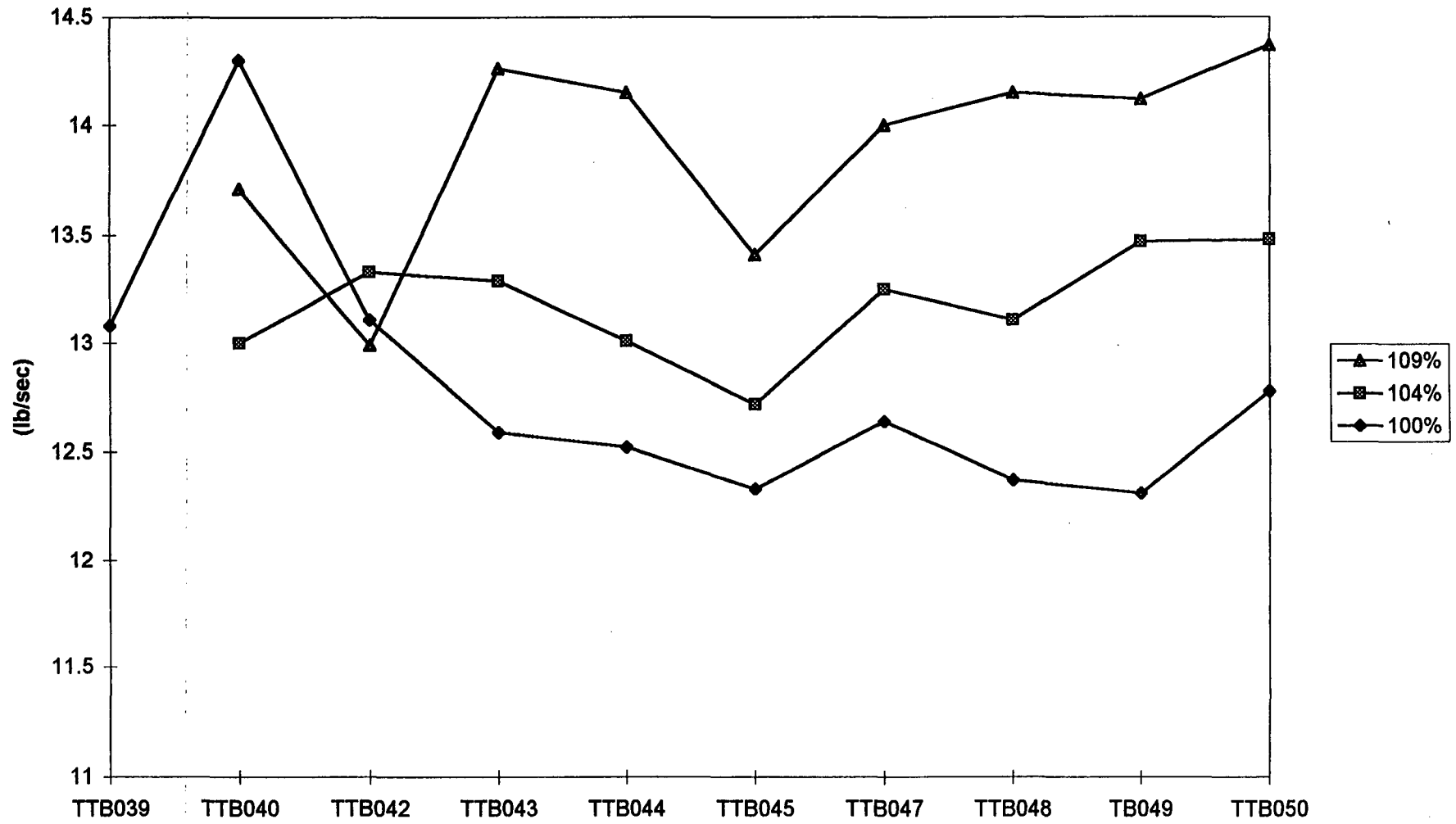
CCV Inlet Flowrate vs Test #



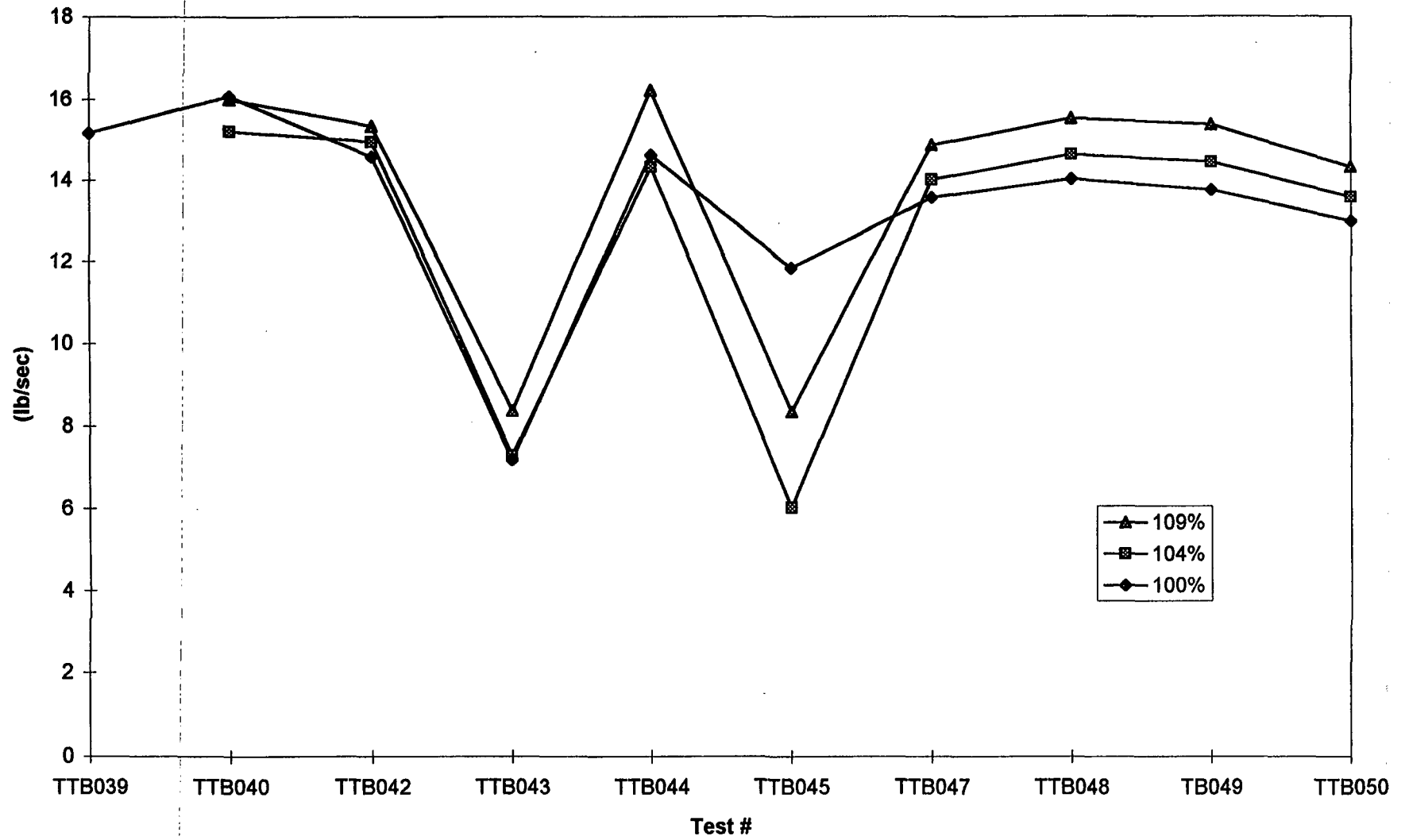
Nozzle Coolant #1 vs Test #



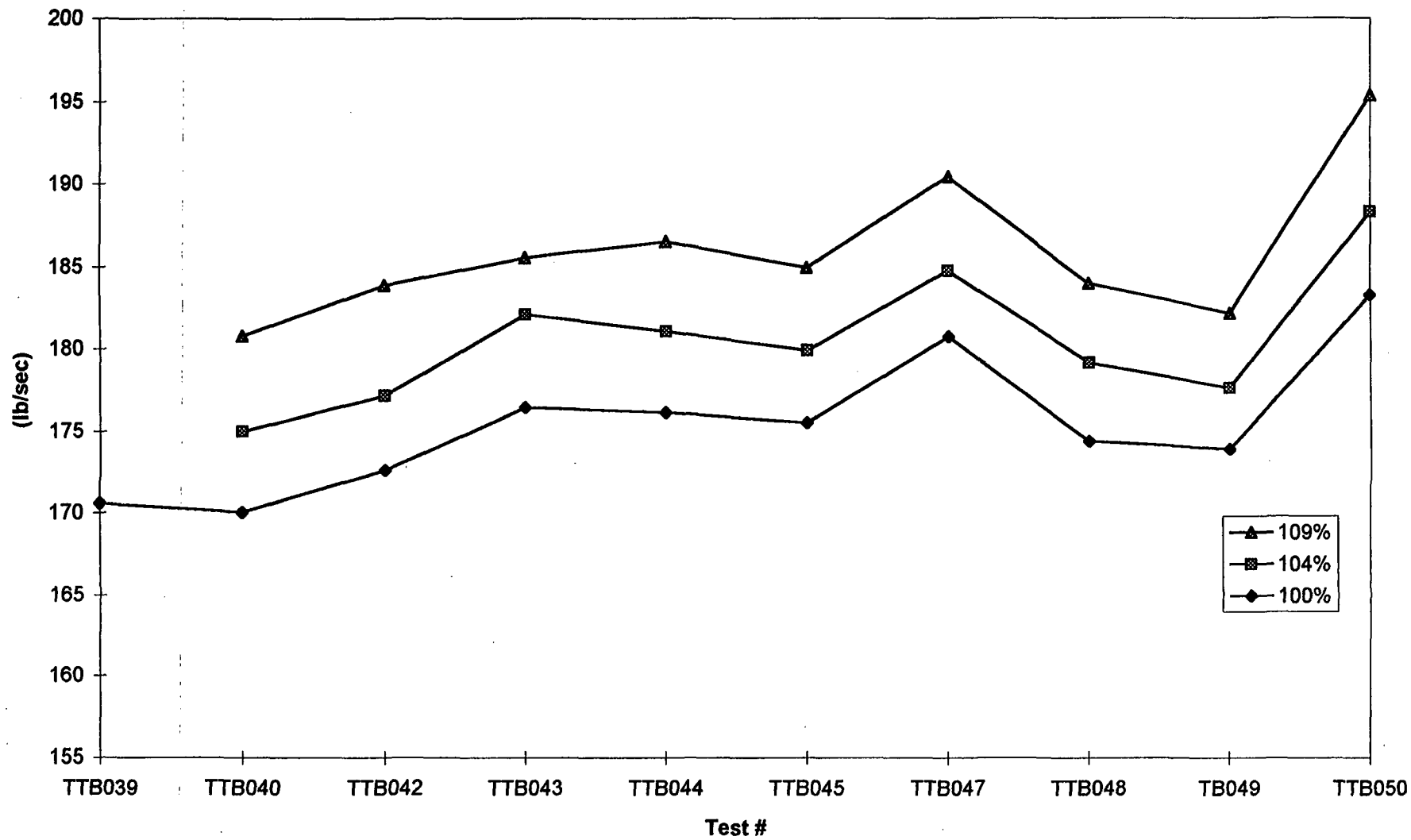
Nozzle Coolant #2 vs Test #



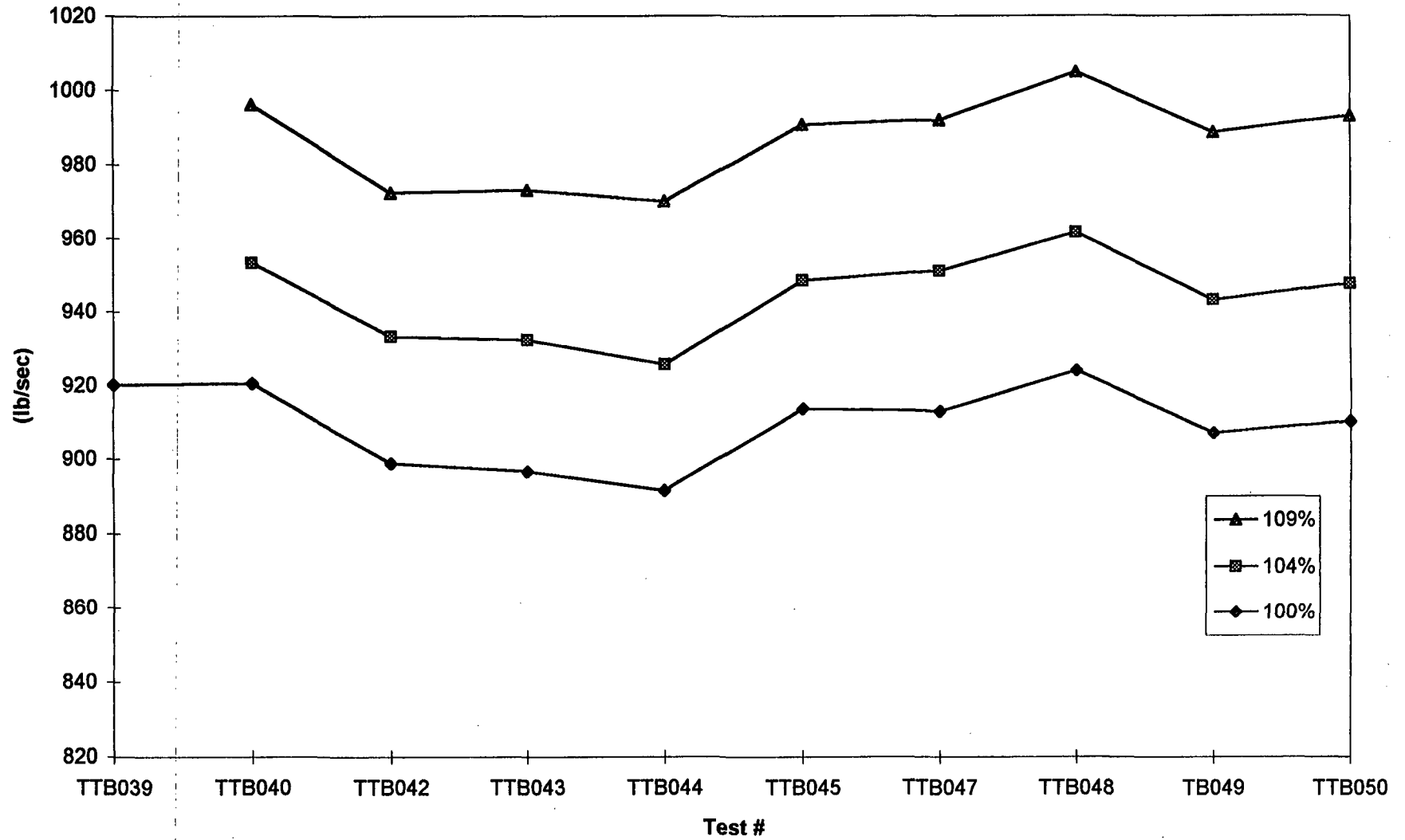
Nozzle Coolant #3 vs Test #



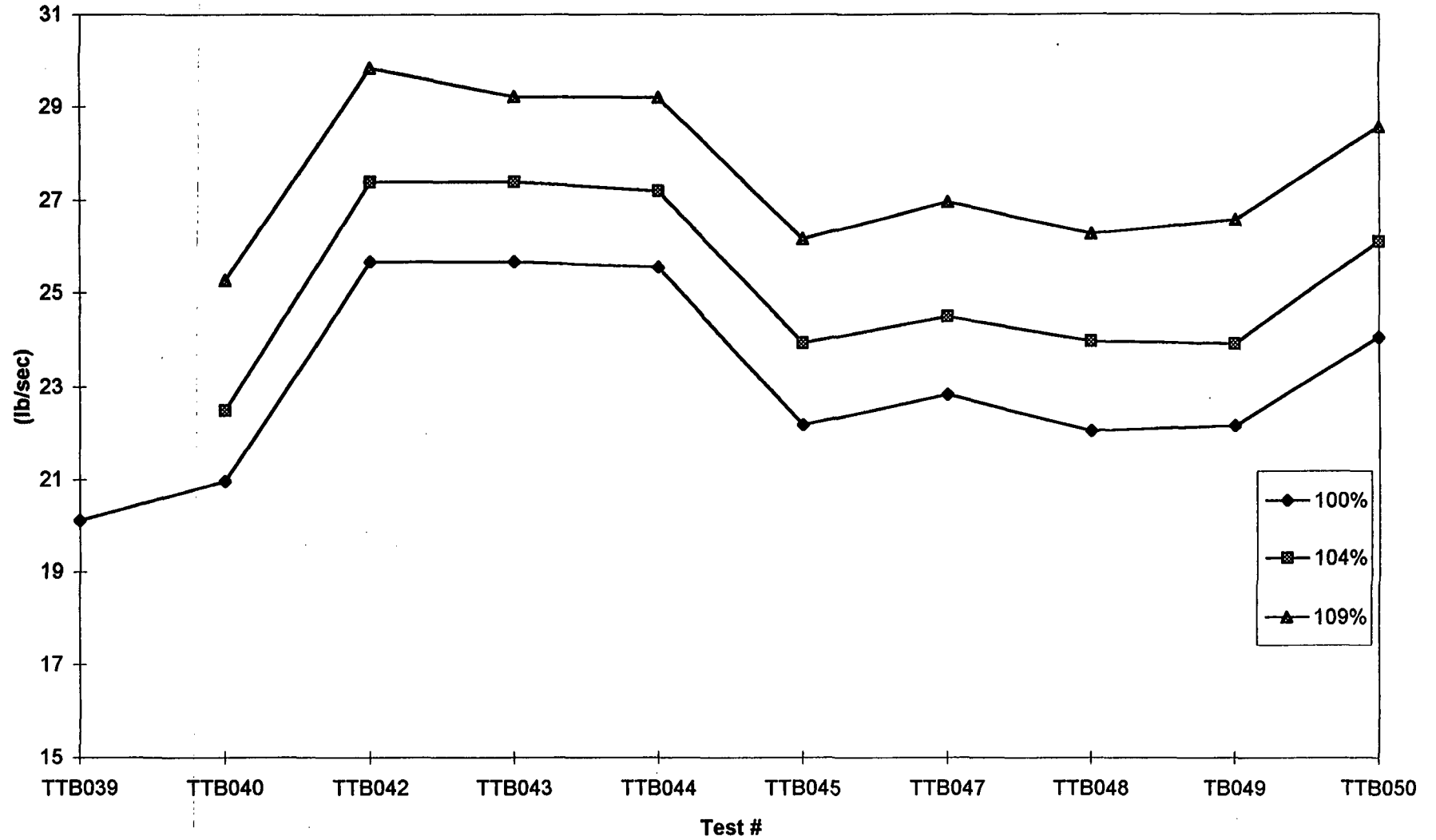
LPOT Inlet



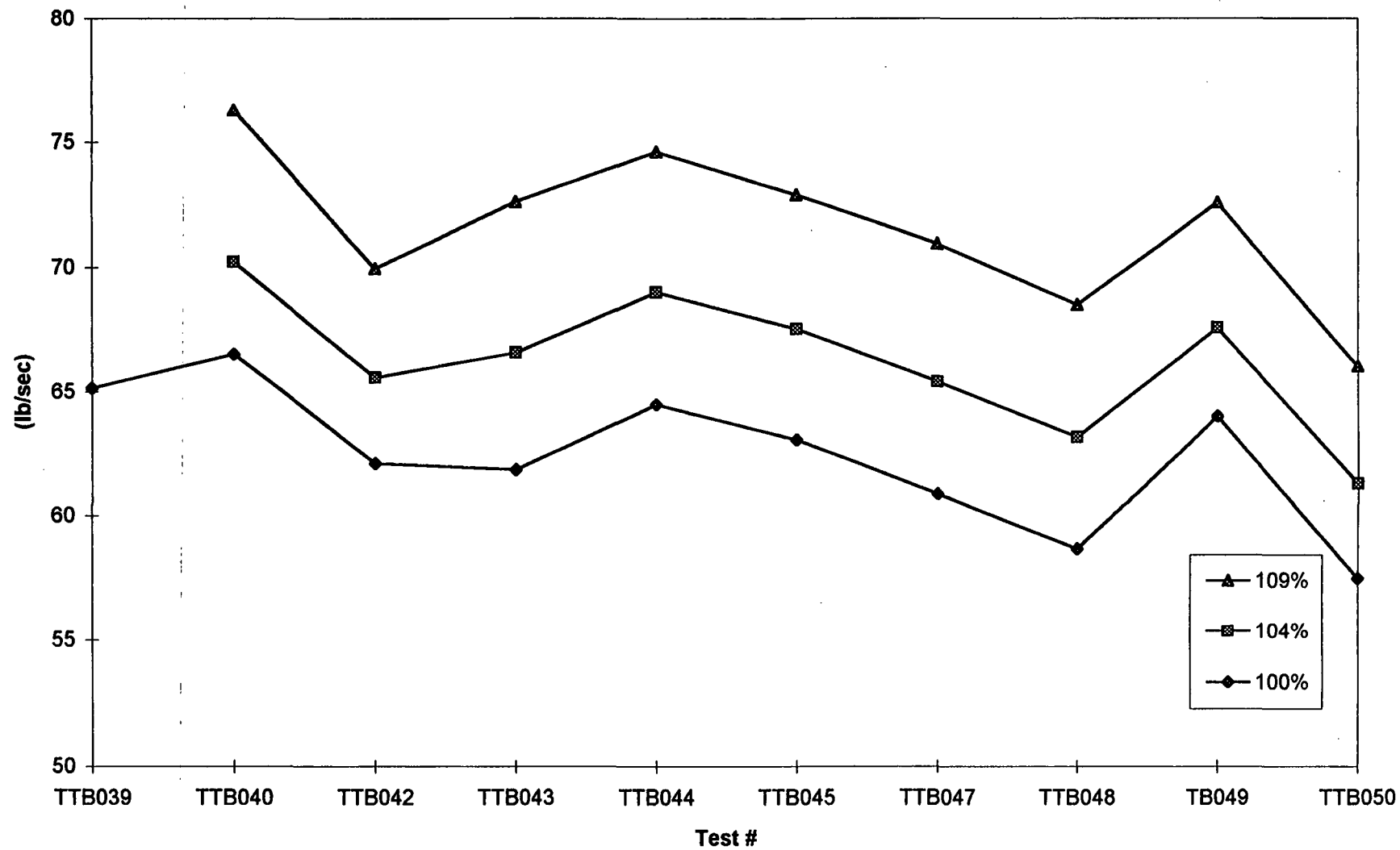
HPOP Discharge vs Test



OPB LOX flow vs Test #



FPB LOX



Appendix X

Example Output from Venturi Uncertainty Program

The output provided is from test TTB050 for 3 -5 second time slices. The definitions of the variables listed are as follows:

PID	Measurement identification
P1	Inlet pressure
DP	Differential pressure
T	Temperature
BP1	Inlet pressure bias limit
BDP	Differential pressure bias limit
BT1	Temperature bias limit
BCD	Discharge coefficient bias limit
BALP	Thermal expansion coefficient bias limit
BD1	Venturi throat diameter bias limit
BD2	Venturi inlet diameter bias limit
PW	Flowrate precision limit
W	Flowrate
UW	Uncertainty in flowrate
% UW	Percent uncertainty in flowrate

DWDP1=	$\frac{\partial W}{\partial P1}$	BWP=	$\left(\frac{\partial W}{\partial P} B_P\right)^2$
DWDDP=	$\frac{\partial W}{\partial \Delta P}$	BWDP=	$\left(\frac{\partial W}{\partial \Delta P} B_{\Delta P}\right)^2$
DWDT=	$\frac{\partial W}{\partial T}$	BWDT=	$\left(\frac{\partial W}{\partial \Delta T} B_{\Delta T}\right)^2$
DWDCD=	$\frac{\partial W}{\partial C_D}$	BWCD=	$\left(\frac{\partial W}{\partial C_D} B_{C_D}\right)^2$
DWALP=	$\frac{\partial W}{\partial \alpha}$	BWALP=	$\left(\frac{\partial W}{\partial \alpha} B_\alpha\right)^2$
DWDD1=	$\frac{\partial W}{\partial D1}$	BWD1=	$\left(\frac{\partial W}{\partial D1} B_{D1}\right)^2$
DWDD2=	$\frac{\partial W}{\partial D2}$	BWD2=	$\left(\frac{\partial W}{\partial D2} B_{D2}\right)^2$

TEST #: 8010050. ENGINE #: 3001. # OF PIDS: 43 # OF SLICES: 3

SLNUM >***** SLICE START TIME > 16.0 SLICE END TIME > 21.0

ILTTB = 1 DTTB(ILTTB) = 3998.69
ILTTB = 2 DTTB(ILTTB) = 256.49
ILTTB = 3 DTTB(ILTTB) = 473.62
ILTTB = 4 DTTB(ILTTB) = 5223.84
ILTTB = 5 DTTB(ILTTB) = 386.29
ILTTB = 6 DTTB(ILTTB) = 92.91
ILTTB = 7 DTTB(ILTTB) = 5383.70
ILTTB = 8 DTTB(ILTTB) = 119.84
ILTTB = 9 DTTB(ILTTB) = 91.82
ILTTB = 10 DTTB(ILTTB) = 5385.07
ILTTB = 11 DTTB(ILTTB) = 117.56
ILTTB = 12 DTTB(ILTTB) = 92.69
ILTTB = 13 DTTB(ILTTB) = 5392.00
ILTTB = 14 DTTB(ILTTB) = 121.34
ILTTB = 15 DTTB(ILTTB) = 90.92
ILTTB = 16 DTTB(ILTTB) = 3796.21
ILTTB = 17 DTTB(ILTTB) = 207.17
ILTTB = 18 DTTB(ILTTB) = 188.41
ILTTB = 19 DTTB(ILTTB) = 3717.76
ILTTB = 20 DTTB(ILTTB) = 245.44
ILTTB = 21 DTTB(ILTTB) = 190.50
ILTTB = 22 DTTB(ILTTB) = 6621.04
ILTTB = 23 DTTB(ILTTB) = 134.31
ILTTB = 24 DTTB(ILTTB) = 215.41
ILTTB = 25 DTTB(ILTTB) = 4887.78
ILTTB = 26 DTTB(ILTTB) = 261.37
ILTTB = 27 DTTB(ILTTB) = 280.75
ILTTB = 28 DTTB(ILTTB) = 6653.16
ILTTB = 29 DTTB(ILTTB) = 97.34
ILTTB = 30 DTTB(ILTTB) = 204.71

LPFT INLET FLOWRATE - P(8801) > 26.61 LB/S
CCV INLET FLOWRATE - P(8818) > 71.41 LB/S
NOZ CLNT FLOWRATE - P(8815) > 13.08 LB/S
NOZ CLNT FLOWRATE - P(8816) > 12.78 LB/S
NOZ CLNT FLOWRATE - P(8817) > 12.98 LB/S
LPOT INLET FLOWRATE - P(8802) > 183.29 LB/S
HPOP DISCH FLOWRATE - P(8819) > 910.39 LB/S
OPB LOX FLOWRATE - P(8804) > 24.05 LB/S
OPB FUEL FLOWRATE - W(8805) > 34.39 LB/S
FPB LOX FLOWRATE - W(8810) > 57.47 LB/S
PID 8801 LPFT INLET
VENTURI <20>

P1 3998.69 DP 256.49 T 473.62
BP1 37.9621 BDP 2.0717 BT1 1.8841
BCD 0.01992 BALP .417E-06 BD1 0.00050 BD2 0.00050
PW 0.0000
DWDP1 .3128E-02 DWDDP .4582E-01 DWDT -.243E-01
DWDCD .2624E+02 DWALP -.293E+04 DWDD1 -.120E+02 DWDD2 .5076E+02
BWP .1410E-01 BWDP .9010E-02 BWDT .2100E-02
BWCD .2731E+00 BWALP .1490E-05 BWD1 .3589E-04 BWD2 .6442E-03
W 26.6139 UW 0.54654 %UW 2.0536

PID 8818 CCV INLET
VENTURI <397>
P1 5223.84 DP 386.29 T 92.91
BP1 52.2384 BDP 3.8629 BT1 0.9291
BCD 0.03063 BALP .548E-06 BD1 0.00050 BD2 0.00050
PW 0.0000
DWDP1 .2260E-02 DWDDP .8257E-01 DWDT -.114E+00
DWDCD .6990E+02 DWALP -.612E+05 DWDD1 -.156E+02 DWDD2 .1069E+03
BWP .1394E-01 BWDP .1017E+00 BWDT .1127E-01
BWCD .4584E+01 BWALP .1126E-02 BWD1 .6050E-04 BWD2 .2855E-02
W 71.4057 UW 2.17125 %UW 3.0407

PID 8815 NOZ CLNT
VENTURI <3541>
P1 5223.84 DP 386.29 T 92.91
BP1 53.8370 BDP 1.1984 BT1 0.9182
BCD 0.02033 BALP .548E-06 BD1 0.00050 BD2 0.00050
PW 0.0000
DWDP1 .3235E-03 DWDDP .5311E-01 DWDT -.217E-01
DWDCD .1287E+02 DWALP -.110E+05 DWDD1 -.328E+01 DWDD2 .3210E+02
BWP .3033E-03 BWDP .4051E-02 BWDT .3978E-03
BWCD .6842E-01 BWALP .3607E-04 BWD1 .2688E-05 BWD2 .2575E-03
W 13.0809 UW 0.27095 %UW 2.0713

PID 8816 NOZ CLNT
VENTURI <3542>
P1 5385.07 DP 117.56 T 92.69
BP1 53.8507 BDP 1.1756 BT1 0.9269
BCD 0.02033 BALP .548E-06 BD1 0.00050 BD2 0.00050
PW 0.0000
DWDP1 .3153E-03 DWDDP .5293E-01 DWDT -.215E-01
DWDCD .1283E+02 DWALP -.110E+05 DWDD1 -.325E+01 DWDD2 .3133E+02
BWP .2882E-03 BWDP .3872E-02 BWDT .3977E-03
BWCD .6799E-01 BWALP .3607E-04 BWD1 .2639E-05 BWD2 .2453E-03
W 12.7825 UW 0.26978 %UW 2.1106

PID 8817 NOZ CLNT
VENTURI <3543>
P1 5392.00 DP 121.34 T 90.92
BP1 53.9200 BDP 1.2134 BT1 0.9092
BCD 0.02033 BALP .548E-06 BD1 0.00050 BD2 0.00050
PW 0.0000
DWDP1 .3074E-03 DWDDP .5182E-01 DWDT -.220E-01
DWDCD .1299E+02 DWALP -.134E+05 DWDD1 -.331E+01 DWDD2 .3190E+02
BWP .2747E-03 BWDP .3954E-02 BWDT .3993E-03
BWCD .6978E-01 BWALP .5388E-04 BWD1 .2740E-05 BWD2 .2544E-03
W 12.9831 UW 0.27326 %UW 2.1047

PID 8802 LPOT INLET
VENTURI <139>
P1 3796.21 DP 207.17 T 188.41
BP1 37.9621 BDP 2.0717 BT1 1.8841
BCD 0.02066 BALP .651E-06 BD1 0.00050 BD2 0.00050
PW 0.0000
DWDP1 .1137E-02 DWDDP .4420E+00 DWDT -.183E+00
DWDCD .1774E+03 DWALP -.124E+06 DWDD1 -.446E+02 DWDD2 .2986E+03
BWP .1863E-02 BWDP .8386E+00 BWDT .1195E+00
BWCD .1343E+02 BWALP .6565E-02 BWD1 .4981E-03 BWD2 .2229E-01
W 183.2910 UW 3.79655 %UW 2.0713

PID 8819 HPOP DISCH
VENTURI <426>
P1 3717.76 DP 245.44 T 190.50
BP1 37.1776 BDP 1.9050 BT1 2.4544
BCD 0.01964 BALP .549E-06 BD1 0.00050 BD2 0.00050
PW 0.0000
DWDP1 .5711E-02 DWDDP .1853E+01 DWDT -.930E+00
DWDCD .9270E+03 DWALP -.124E+06 DWDD1 -.326E+03 DWDD2 .9771E+03
BWP .4508E-01 BWDP .1247E+02 BWDT .5211E+01
BWCD .3315E+03 BWALP .1167E+00 BWD1 .2658E-01 BWD2 .2387E+00
W 910.3882 UW 18.69283 %UW 2.0533

PID 8804 OPB LOX
 VENTURI <268>
 P1 6621.04 DP 134.31 T 215.41
 BP1 66.2104 BDP 1.3431 BT1 2.1541
 BCD 0.02066 BALP 0.671E-06 BD1 0.00050 BD2 0.00050
 PW 0.0000
 DWDP1 .1475E-03 DWDDP .8961E-01 DWDT -.218E-01
 DWDCD .2318E+02 DWALP -.136E+05 DWDD1 -.635E+01 DWDD2 .8418E+02
 BWP .9539E-04 BWDP .1448E-01 BWDT .2207E-02
 BWCD .2294E+00 BWALP .8374E-04 BWD1 .1009E-04 BWD2 .1772E-02
 W 24.0457 UW 0.49778 %UW 2.0702

PID 8805 OPB FUEL
 VENTURI <271>
 P1 4887.78 DP 261.37 T 280.75
 BP1 48.8778 BDP 2.6137 BT1 2.8075
 BCD 0.01992 BALP 0.323E-06 BD1 0.00050 BD2 0.00050
 PW 0.0000
 DWDP1 .2638E-02 DWDDP .1117E-03 DWDT -.480E-01
 DWDCD .3366E+02 DWALP -.170E+05 DWDD1 -.135E+02 DWDD2 .6442E+02
 BWP .1662E-01 BWDP .8523E-07 BWDT .1812E-01
 BWCD .4495E+00 BWALP .3017E-04 BWD1 .4587E-04 BWD2 .1037E-02
 W 34.3923 UW 0.69639 %UW 2.0248

PID 8810 FPB LOX
 VENTURI <296>
 P1 6653.16 DP 97.34 T 204.71
 BP1 66.5316 BDP 0.9734 BT1 2.0471
 BCD 0.02052 BALP .671E-06 BD1 0.00050 BD2 0.00050
 PW 0.0000
 DWDP1 .3165E-03 DWDDP .2953E+00 DWDT -.508E-01
 DWDCD .5605E+02 DWALP -.371E+05 DWDD1 -.584E+01 DWDD2 .1143E+03
 BWP .4435E-03 BWDP .8260E-01 BWDT .1082E-01
 BWCD .1323E+01 BWALP .6186E-03 BWD1 .8539E-05 BWD2 .3264E-02
 W 57.4704 UW 1.19193 %UW 2.0740

SLNUM >***** SLICE START TIME > 16.0 SLICE END TIME > 21.0

8801	26.61	0.55	2.05
8818	71.41	2.17	3.04
8815	13.08	0.27	2.07
8816	12.78	0.27	2.11
8817	12.98	0.27	2.10
8802	183.29	3.80	2.07
8819	910.39	18.69	2.05
8804	24.05	0.50	2.07
8805	34.39	0.70	2.02
8810	57.47	1.19	2.07

TEST #: 8010050. ENGINE #: 3001. # OF PIDS: 43 # OF SLICES: 3

SLNUM >***** SLICE START TIME > 25.0 SLICE END TIME > 30.0

ILTTB = 1 DTTB(ILTTB) = 4185.40
ILTTB = 2 DTTB(ILTTB) = 271.89
ILTTB = 3 DTTB(ILTTB) = 468.97
ILTTB = 4 DTTB(ILTTB) = 5490.61
ILTTB = 5 DTTB(ILTTB) = 410.88
ILTTB = 6 DTTB(ILTTB) = 94.94
ILTTB = 7 DTTB(ILTTB) = 5657.44
ILTTB = 8 DTTB(ILTTB) = 132.33
ILTTB = 9 DTTB(ILTTB) = 93.74
ILTTB = 10 DTTB(ILTTB) = 5660.28
ILTTB = 11 DTTB(ILTTB) = 130.22
ILTTB = 12 DTTB(ILTTB) = 94.90
ILTTB = 13 DTTB(ILTTB) = 5666.14
ILTTB = 14 DTTB(ILTTB) = 132.12
ILTTB = 15 DTTB(ILTTB) = 92.95
ILTTB = 16 DTTB(ILTTB) = 3981.13
ILTTB = 17 DTTB(ILTTB) = 218.58
ILTTB = 18 DTTB(ILTTB) = 189.46
ILTTB = 19 DTTB(ILTTB) = 3895.58
ILTTB = 20 DTTB(ILTTB) = 265.92
ILTTB = 21 DTTB(ILTTB) = 191.59
ILTTB = 22 DTTB(ILTTB) = 6917.97
ILTTB = 23 DTTB(ILTTB) = 157.95
ILTTB = 24 DTTB(ILTTB) = 216.81
ILTTB = 25 DTTB(ILTTB) = 5138.72
ILTTB = 26 DTTB(ILTTB) = 272.94
ILTTB = 27 DTTB(ILTTB) = 281.84
ILTTB = 28 DTTB(ILTTB) = 6954.25
ILTTB = 29 DTTB(ILTTB) = 110.65
ILTTB = 30 DTTB(ILTTB) = 206.33

LPFT INLET FLOWRATE - P(8801) > 28.02 LB/S
CCV INLET FLOWRATE - P(8818) > 73.78 LB/S
NOZ CLNT FLOWRATE - P(8815) > 13.77 LB/S
NOZ CLNT FLOWRATE - P(8816) > 13.48 LB/S
NOZ CLNT FLOWRATE - P(8817) > 13.58 LB/S
LPOT INLET FLOWRATE - P(8802) > 188.29 LB/S
HPOP DISCH FLOWRATE - P(8819) > 947.63 LB/S
OPB LOX FLOWRATE - P(8804) > 26.09 LB/S
OPB FUEL FLOWRATE - W(8805) > 35.68 LB/S
FPB LOX FLOWRATE - W(8810) > 61.29 LB/S
PID 8801 LPFT INLET

VENTURI <20>

P1 4185.40 DP 271.89 T 468.97
BP1 39.8112 BDP 2.1858 BT1 1.8946
BCD 0.01992 BALP .417E-06 BD1 0.00050 BD2 0.00050
PW 0.0000
DWDP1 .3124E-02 DWDDP .4541E-01 DWDT -.256E-01
DWDCD .2763E+02 DWALP -.329E+04 DWDD1 -.126E+02 DWDD2 .5341E+02
BWP .1547E-01 BWDP .9854E-02 BWDT .2347E-02
BWCD .3030E+00 BWALP .1886E-05 BWD1 .3970E-04 BWD2 .7131E-03
W 28.0166 UW 0.57543 %UW 2.0539

PID 8818 CCV INLET

VENTURI <397>

P1 5490.61 DP 410.88 T 94.94
BP1 54.9061 BDP 4.1088 BT1 0.9494
BCD 0.03063 BALP .548E-06 BD1 0.00050 BD2 0.00050
PW 0.0000
DWDP1 .2265E-02 DWDDP .7986E-01 DWDT -.114E+00
DWDCD .7222E+02 DWALP -.668E+05 DWDD1 -.160E+02 DWDD2 .1104E+03
BWP .1546E-01 BWDP .1077E+00 BWDT .1163E-01
BWCD .4893E+01 BWALP .1340E-02 BWD1 .6425E-04 BWD2 .3044E-02
W 73.7762 UW 2.24304 %UW 3.0403

PID 8815 NOZ CLNT
VENTURI <3541>
PI 5490.61 DP 410.88 T 94.94
BP1 56.5744 BDP 1.3233 BT1 0.9374
BCD 0.02033 BALP .548E-06 BD1 0.00050 BD2 0.00050
PW 0.0000
DWDP1 .3287E-03 DWDDP .5051E-01 DWDT -.223E-01
DWDCD .1355E+02 DWALP -.117E+05 DWDD1 -.345E+01 DWDD2 .3378E+02
BWP .3459E-03 BWDP .4468E-02 BWD1 .4359E-03
BWCD .7583E-01 BWALP .4079E-04 BWD1 .2971E-05 BWD2 .2854E-03
W 13.7743 UW 0.28523 %UW 2.0707

PID 8816 NOZ CLNT
VENTURI <3542>
PI 5660.28 DP 130.22 T 94.90
BP1 56.6028 BDP 1.3022 BT1 0.9490
BCD 0.02033 BALP .548E-06 BD1 0.00050 BD2 0.00050
PW 0.0000
DWDP1 .3267E-03 DWDDP .5005E-01 DWDT -.219E-01
DWDCD .1352E+02 DWALP -.115E+05 DWDD1 -.343E+01 DWDD2 .3300E+02
BWP .3420E-03 BWDP .4247E-02 BWD1 .4308E-03
BWCD .7555E-01 BWALP .3958E-04 BWD1 .2937E-05 BWD2 .2722E-03
W 13.4754 UW 0.28430 %UW 2.1098

PID 8817 NOZ CLNT
VENTURI <3543>
PI 5666.14 DP 132.12 T 92.95
BP1 56.6614 BDP 1.3212 BT1 0.9295
BCD 0.02033 BALP .548E-06 BD1 0.00050 BD2 0.00050
PW 0.0000
DWDP1 .3195E-03 DWDDP .4951E-01 DWDT -.218E-01
DWDCD .1358E+02 DWALP -.137E+05 DWDD1 -.346E+01 DWDD2 .3335E+02
BWP .3278E-03 BWDP .4278E-02 BWD1 .4123E-03
BWCD .7624E-01 BWALP .5671E-04 BWD1 .2985E-05 BWD2 .2781E-03
W 13.5752 UW 0.28555 %UW 2.1034

PID 8802 LPOT INLET
VENTURI <139>
PI 3981.13 DP 218.58 T 189.46
BP1 39.8112 BDP 2.1858 BT1 1.8946
BCD 0.02066 BALP .651E-06 BD1 0.00050 BD2 0.00050
PW 0.0000
DWDP1 .1165E-02 DWDDP .4306E+00 DWDT -.188E+00
DWDCD .1822E+03 DWALP -.128E+06 DWDD1 -.459E+02 DWDD2 .3068E+03
BWP .2150E-02 BWDP .8860E+00 BWD1 .1264E+00
BWCD .1417E+02 BWALP .6915E-02 BWD1 .5264E-03 BWD2 .2353E-01
W 188.2875 UW 3.90044 %UW 2.0715

PID 8819 HPOP DISCH
VENTURI <426>
PI 3895.58 DP 265.92 T 191.59
BP1 38.9558 BDP 1.9159 BT1 2.6592
BCD 0.01964 BALP .549E-06 BD1 0.00050 BD2 0.00050
PW 0.0000
DWDP1 .5951E-02 DWDDP .1781E+01 DWDT -.958E+00
DWDCD .9650E+03 DWALP -.128E+06 DWDD1 -.339E+03 DWDD2 .1017E+04
BWP .5375E-01 BWDP .1165E+02 BWD1 .6488E+01
BWCD .3592E+03 BWALP .1340E+00 BWD1 .2880E-01 BWD2 .2586E+00
W 947.6333 UW 19.43365 %UW 2.0508

PID 8804 OPB LOX
 VENTURI <268>
 P1 6917.97 DP 157.95 T 216.81
 BP1 69.1797 BDP 1.5795 BT1 2.1681
 BCD 0.02066 BALP 0.671E-06 BD1 0.00050 BD2 0.00050
 PW 0.0000
 DWDP1 .1544E-03 DWDDP .8257E-01 DWDT -.234E-01
 DWDCD .2516E+02 DWALP -.159E+05 DWDD1 -.689E+01 DWDD2 .9133E+02
 BWP .1141E-03 BWDP .1701E-01 BWDT .2565E-02
 BWCD .2701E+00 BWALP .1140E-03 BWD1 .1188E-04 BWD2 .2085E-02
 W 26.0900 UW 0.54008 %UW 2.0701

PID 8805 OPB FUEL
 VENTURI <271>
 P1 5138.72 DP 272.94 T 281.84
 BP1 51.3872 BDP 2.7294 BT1 2.8184
 BCD 0.01992 BALP 0.323E-06 BD1 0.00050 BD2 0.00050
 PW 0.0000
 DWDP1 .2554E-02 DWDDP .1151E-03 DWDT -.485E-01
 DWDCD .3493E+02 DWALP -.175E+05 DWDD1 -.141E+02 DWDD2 .6684E+02
 BWP .1722E-01 BWDP .9864E-07 BWDT .1869E-01
 BWCD .4841E+00 BWALP .3187E-04 BWD1 .4949E-04 BWD2 .1117E-02
 W 35.6798 UW 0.72162 %UW 2.0225

PID 8810 FPB LOX
 VENTURI <296>
 P1 6954.25 DP 110.65 T 206.33
 BP1 69.5425 BDP 1.1065 BT1 2.0633
 BCD 0.02052 BALP .671E-06 BD1 0.00050 BD2 0.00050
 PW 0.0000
 DWDP1 .3290E-03 DWDDP .2769E+00 DWDT -.535E-01
 DWDCD .5971E+02 DWALP -.396E+05 DWDD1 -.623E+01 DWDD2 .1218E+03
 BWP .5236E-03 BWDP .9390E-01 BWDT .1219E-01
 BWCD .1501E+01 BWALP .7049E-03 BWD1 .9708E-05 BWD2 .3709E-02
 W 61.2905 UW 1.26982 %UW 2.0718

SLNUM >***** SLICE START TIME > 25.0 SLICE END TIME > 30.0

8801	28.02	0.58	2.05
8818	73.78	2.24	3.04
8815	13.77	0.29	2.07
8816	13.48	0.28	2.11
8817	13.58	0.29	2.10
8802	188.29	3.90	2.07
8819	947.63	19.43	2.05
8804	26.09	0.54	2.07
8805	35.68	0.72	2.02
8810	61.29	1.27	2.07

TEST #: 8010050. ENGINE #: 3001. # OF PIDS: 43 # OF SLICES: 3

SLNUM >***** SLICE START TIME > 34.0 SLICE END TIME > 38.0

ILTTB = 1 DTTB(ILTTB) = 4426.71
ILTTB = 2 DTTB(ILTTB) = 291.82
ILTTB = 3 DTTB(ILTTB) = 464.59
ILTTB = 4 DTTB(ILTTB) = 5838.52
ILTTB = 5 DTTB(ILTTB) = 440.25
ILTTB = 6 DTTB(ILTTB) = 97.59
ILTTB = 7 DTTB(ILTTB) = 6016.47
ILTTB = 8 DTTB(ILTTB) = 149.35
ILTTB = 9 DTTB(ILTTB) = 96.34
ILTTB = 10 DTTB(ILTTB) = 6020.90
ILTTB = 11 DTTB(ILTTB) = 147.22
ILTTB = 12 DTTB(ILTTB) = 97.43
ILTTB = 13 DTTB(ILTTB) = 6026.65
ILTTB = 14 DTTB(ILTTB) = 146.61
ILTTB = 15 DTTB(ILTTB) = 95.76
ILTTB = 16 DTTB(ILTTB) = 4233.10
ILTTB = 17 DTTB(ILTTB) = 235.31
ILTTB = 18 DTTB(ILTTB) = 190.95
ILTTB = 19 DTTB(ILTTB) = 4136.17
ILTTB = 20 DTTB(ILTTB) = 292.10
ILTTB = 21 DTTB(ILTTB) = 193.23
ILTTB = 22 DTTB(ILTTB) = 7323.87
ILTTB = 23 DTTB(ILTTB) = 189.11
ILTTB = 24 DTTB(ILTTB) = 219.42
ILTTB = 25 DTTB(ILTTB) = 5467.02
ILTTB = 26 DTTB(ILTTB) = 283.85
ILTTB = 27 DTTB(ILTTB) = 284.05
ILTTB = 28 DTTB(ILTTB) = 7369.33
ILTTB = 29 DTTB(ILTTB) = 128.39
ILTTB = 30 DTTB(ILTTB) = 208.63

LPFT INLET FLOWRATE - P(8801) > 29.78 LB/S
CCV INLET FLOWRATE - P(8818) > 76.57 LB/S
NOZ CLNT FLOWRATE - P(8815) > 14.67 LB/S
NOZ CLNT FLOWRATE - P(8816) > 14.37 LB/S
NOZ CLNT FLOWRATE - P(8817) > 14.33 LB/S
LPOT INLET FLOWRATE - P(8802) > 195.37 LB/S
HPOP DISCH FLOWRATE - P(8819) > 993.06 LB/S
OPB LOX FLOWRATE - P(8804) > 28.55 LB/S
OPB FUEL FLOWRATE - W(8805) > 37.04 LB/S
FPB LOX FLOWRATE - W(8810) > 66.03 LB/S
PID 8801 LPFT INLET
VENTURI <20>
P1 4426.71 DP 291.82 T 464.59
BP1 42.3310 BDP 2.3531 BT1 1.9095
BCD 0.01992 BALP .417E-06 BD1 0.00050 BD2 0.00050
PW 0.0000
DWDP1 .3099E-02 DWDDP .4479E-01 DWDT -.271E-01
DWDCD .2938E+02 DWALP -.403E+04 DWDD1 -.134E+02 DWDD2 .5674E+02
BWP .1721E-01 BWDP .1111E-01 BWDT .2682E-02
BWCD .3425E+00 BWALP .2817E-05 BWD1 .4467E-04 BWD2 .8049E-03
W 29.7824 UW 0.61157 %UW 2.0534

PID 8818 CCV INLET
VENTURI <397>
P1 5838.52 DP 440.25 T 97.59
BP1 58.3852 BDP 4.4025 BT1 0.9759
BCD 0.03063 BALP .548E-06 BD1 0.00050 BD2 0.00050
PW 0.0000
DWDP1 .2265E-02 DWDDP .7734E-01 DWDT -.113E+00
DWDCD .7498E+02 DWALP -.640E+05 DWDD1 -.166E+02 DWDD2 .1145E+03
BWP .1749E-01 BWDP .1159E+00 BWDT .1213E-01
BWCD .5275E+01 BWALP .1231E-02 BWD1 .6884E-04 BWD2 .3277E-02
W 76.5676 UW 2.32890 %UW 3.0416

PID 8815 NOZ CLNT
VENTURI <3541>
P1 5838.52 DP 440.25 T 97.59
BP1 60.1647 BDP 1.4935 BT1 0.9634
BCD 0.02033 BALP .548E-06 BD1 0.00050 BD2 0.00050
PW 0.0000
DWDP1 .3286E-03 DWDDP .4741E-01 DWDT -.233E-01
DWDCD .1443E+02 DWALP -.148E+05 DWDD1 -.366E+01 DWDD2 .3596E+02
BWP .3909E-03 BWDP .5014E-02 BWD1 .5045E-03
BWCD .8602E-01 BWALP .6565E-04 BWD1 .3343E-05 BWD2 .3233E-03
W 14.6686 UW 0.30373 %UW 2.0707

PID 8816 NOZ CLNT
VENTURI <3542>
P1 6020.90 DP 147.22 T 97.43
BP1 60.2090 BDP 1.4722 BT1 0.9743
BCD 0.02033 BALP .548E-06 BD1 0.00050 BD2 0.00050
PW 0.0000
DWDP1 .3289E-03 DWDDP .4701E-01 DWDT -.222E-01
DWDCD .1441E+02 DWALP -.124E+05 DWDD1 -.364E+01 DWDD2 .3517E+02
BWP .3921E-03 BWDP .4789E-02 BWD1 .4692E-03
BWCD .8588E-01 BWALP .4581E-04 BWD1 .3312E-05 BWD2 .3093E-03
W 14.3658 UW 0.30303 %UW 2.1094

PID 8817 NOZ CLNT
VENTURI <3543>
P1 6026.65 DP 146.61 T 95.76
BP1 60.2665 BDP 1.4661 BT1 0.9576
BCD 0.02033 BALP .548E-06 BD1 0.00050 BD2 0.00050
PW 0.0000
DWDP1 .3237E-03 DWDDP .4706E-01 DWDT -.222E-01
DWDCD .1435E+02 DWALP -.124E+05 DWDD1 -.363E+01 DWDD2 .3521E+02
BWP .3805E-03 BWDP .4760E-02 BWD1 .4507E-03
BWCD .8512E-01 BWALP .4581E-04 BWD1 .3302E-05 BWD2 .3099E-03
W 14.3339 UW 0.30167 %UW 2.1046

PID 8802 LPOT INLET
VENTURI <139>
P1 4233.10 DP 235.31 T 190.95
BP1 42.3310 BDP 2.3531 BT1 1.9095
BCD 0.02066 BALP .651E-06 BD1 0.00050 BD2 0.00050
PW 0.0000
DWDP1 .1179E-02 DWDDP .4150E+00 DWDT -.193E+00
DWDCD .1891E+03 DWALP -.134E+06 DWDD1 -.476E+02 DWDD2 .3183E+03
BWP .2489E-02 BWDP .9535E+00 BWD1 .1353E+00
BWCD .1526E+02 BWALP .7591E-02 BWD1 .5676E-03 BWD2 .2533E-01
W 195.3723 UW 4.04706 %UW 2.0715

PID 8819 HPOP DISCH
VENTURI <426>
P1 4136.17 DP 292.10 T 193.23
BP1 41.3617 BDP 1.9323 BT1 2.9210
BCD 0.01964 BALP .549E-06 BD1 0.00050 BD2 0.00050
PW 0.0000
DWDP1 .6197E-02 DWDDP .1701E+01 DWDT -.993E+00
DWDCD .1012E+04 DWALP -.134E+06 DWDD1 -.356E+03 DWDD2 .1066E+04
BWP .6570E-01 BWDP .1081E+02 BWD1 .8408E+01
BWCD .3947E+03 BWALP .1340E+00 BWD1 .3161E-01 BWD2 .2841E+00
W 993.0620 UW 20.35188 %UW 2.0494

PID 8804 OPB LOX
 VENTURI <268>
 P1 7323.87 DP 189.11 T 219.42
 BP1 73.2387 BDP 1.8911 BT1 2.1943
 BCD 0.02066 BALP 0.671E-06 BD1 0.00050 BD2 0.00050
 PW 0.0000
 DWDP1 .1687E-03 DWDDP .7550E-01 DWDT -.250E-01
 DWDCD .2754E+02 DWALP -.159E+05 DWDD1 -.755E+01 DWDD2 .9995E+02
 BWP .1527E-03 BWDP .2038E-01 BWDT .3015E-02
 BWCD .3237E+00 BWALP .1140E-03 BWD1 .1424E-04 BWD2 .2497E-02
 W 28.5502 UW 0.59121 %UW 2.0708

PID 8805 OPB FUEL
 VENTURI <271>
 P1 5467.02 DP 283.85 T 284.05
 BP1 54.6702 BDP 2.8385 BT1 2.8405
 BCD 0.01992 BALP 0.323E-06 BD1 0.00050 BD2 0.00050
 PW 0.0000
 DWDP1 .2442E-02 DWDDP .1226E-03 DWDT -.490E-01
 DWDCD .3627E+02 DWALP -.184E+05 DWDD1 -.146E+02 DWDD2 .6944E+02
 BWP .1782E-01 BWDP .1211E-06 BWDT .1941E-01
 BWCD .5221E+00 BWALP .3541E-04 BWD1 .5352E-04 BWD2 .1206E-02
 W 37.0400 UW 0.74839 %UW 2.0205

PID 8810 FPB LOX
 VENTURI <296>
 P1 7369.33 DP 128.39 T 208.63
 BP1 73.6933 BDP 1.2839 BT1 2.0863
 BCD 0.02052 BALP .671E-06 BD1 0.00050 BD2 0.00050
 PW 0.0000
 DWDP1 .3540E-03 DWDDP .2572E+00 DWDT -.565E-01
 DWDCD .6434E+02 DWALP -.425E+05 DWDD1 -.675E+01 DWDD2 .1312E+03
 BWP .6805E-03 BWDP .1091E+00 BWDT .1390E-01
 BWCD .1743E+01 BWALP .8142E-03 BWD1 .1138E-04 BWD2 .4305E-02
 W 66.0350 UW 1.36820 %UW 2.0719

SLNUM >***** SLICE START TIME > 34.0 SLICE END TIME > 38.0

8801	29.78	0.61	2.05
8818	76.57	2.33	3.04
8815	14.67	0.30	2.07
8816	14.37	0.30	2.11
8817	14.33	0.30	2.10
8802	195.37	4.05	2.07
8819	993.06	20.35	2.05
8804	28.55	0.59	2.07
8805	37.04	0.75	2.02
8810	66.03	1.37	2.07

Appendix XI

Venturi Uncertainty Analysis Computer Program

This program is written in FORTRAN and resides in the EADS10 computer system as program VENJB2 in the following directory, SIMPSSP.MSFC.VENKB.

```

PROGRAM VENJB
C
C THIS PROGRAM HAS BEEN MODIFIED BY K. BROWN TO CALCULATE THE
C UNCERTAINTIES IN THE VENTURI CALCULATIONS.
C
DOUBLE PRECISION DTTB(40),DH
INTEGER PNSLC,PBTIME,PETIME
DIMENSION PIDTTB(40),WW(10),UNW(10),PER(10),NPID(10)
C
NPID(1)=8801
NPID(2)=8818
NPID(3)=8815
NPID(4)=8816
NPID(5)=8817
NPID(6)=8802
NPID(7)=8819
NPID(8)=8804
NPID(9)=8805
NPID(10)=8810
C
C READ IN TEST DATA
C
READ(36,100) TEST,ENGNUM,IPIDN,ISLCN
READ(36,110) PNSLC,PBTIME,PETIME,
& (PIDTTB(ITTB),ITTB=1,40)
1 READ(36,120,END=999) NSLC,BTIME,ETIME,
& (DTTB(ITTB),ITTB=1,40)
100 FORMAT(T11,F8.0,T32,F5.0,T51,I3,T70,I3/)
110 FORMAT(15(1X,I4))
120 FORMAT(5(1X,E14.8E2))
C
WRITE(6,150) TEST,ENGNUM,IPIDN,ISLCN
WRITE(6,160) PNSLC,PBTIME,PETIME,
& (PIDTTB(ITTB),ITTB=1,40)
WRITE(55,150) TEST,ENGNUM,IPIDN,ISLCN
WRITE(6,170) NSLC,BTIME,ETIME,
& (DTTB(ITTB),ITTB=1,40)
150 FORMAT(/2X,TEST #: ',F8.0,3X,ENGINE #: ',F5.0,3X,
& # OF PIDS: ',I3,3X,# OF SLICES: ',I3/)
160 FORMAT(15(1X,I4))
170 FORMAT(5(1X,E14.8E2))
C DO 700, ILTTB=1,30
C700 READ(10,702) DTTB(ILTTB)
C READ(10,*)
C801 FORMAT( )
C702 FORMAT(4X,F9.2)
C
WRITE(55,205) NSLC,BTIME,ETIME
205 FORMAT(2X,SLNUM > ',I5,2X,SLICE START TIME > ',F5.1,
$ 2X,SLICE END TIME > ',F5.1)
DO 209, ILTTB=1,30
WRITE(55,210) ILTTB,DTTB(ILTTB)
210 FORMAT(2X,ILTTB =',I5,4X,DTTB(ILTTB) = ',F9.2)
209 CONTINUE
WRITE(55,*)
C
H=1.0
CALL FLOWOR(20,DTTB(1),DTTB(2),DTTB(3),9,H,DH,W,WG,RO,VDPT)
WRITE(55,320) WG
320 FORMAT(2X,LPFT INLET FLOWRATE - P(8801) > ',F9.2,' LB/S')
CALL FLOWOR(397,DTTB(4),DTTB(5),DTTB(6),9,H,DH,W,WG,RO,VDPT)
WRITE(55,330) WG
330 FORMAT(2X,CCV INLET FLOWRATE - P(8818) > ',F9.2,' LB/S')
CALL FLOWOR(3541,DTTB(7),DTTB(8),DTTB(9),9,H,DH,W,WG,RO,VDPT)
WRITE(55,340) WG
340 FORMAT(2X,NOZ CLNT FLOWRATE - P(8815) > ',F9.2,' LB/S')
CALL FLOWOR(3542,DTTB(10),DTTB(11),DTTB(12),9,H,DH,W,WG,RO,VDPT)
WRITE(55,350) WG
350 FORMAT(2X,NOZ CLNT FLOWRATE - P(8816) > ',F9.2,' LB/S')
CALL FLOWOR(3543,DTTB(13),DTTB(14),DTTB(15),9,H,DH,W,WG,RO,VDPT)
WRITE(55,360) WG

```

```

360  FORMAT(2X,'NOZ CLNT FLOWRATE - P(8817) >',F9.2,' LB/S')
      CALL FLOWOR(139,DTTB(16),DTTB(17),DTTB(18),9,H,DH,W,WG,RO,VDPT)
      WRITE(55,370) W
370  FORMAT(2X,'LPOT INLET FLOWRATE - P(8802) >',F9.2,' LB/S')
      CALL FLOWOR(426,DTTB(19),DTTB(20),DTTB(21),9,H,DH,W,WG,RO,VDPT)
      WRITE(55,380) W
380  FORMAT(2X,'HPOP DISCH FLOWRATE - P(8819) >',F9.2,' LB/S')
      CALL FLOWOR(268,DTTB(22),DTTB(23),DTTB(24),9,H,DH,W,WG,RO,VDPT)
      WRITE(55,390) W
390  FORMAT(2X,'OPB LOX FLOWRATE - P(8804) >',F9.2,' LB/S')
      CALL FLOWOR(271,DTTB(25),DTTB(26),DTTB(27),9,H,DH,W,WG,RO,VDPT)
      WRITE(55,400) WG
400  FORMAT(2X,'OPB FUEL FLOWRATE - W(8805) >',F9.2,' LB/S')
      CALL FLOWOR(296,DTTB(28),DTTB(29),DTTB(30),9,H,DH,W,WG,RO,VDPT)
      WRITE(55,410) W
410  FORMAT(2X,'FPB LOX FLOWRATE - W(8810) >',F9.2,' LB/S')
C
C THE TIME STEP - H - FOR THE PARTIAL DERIVATIVES IS
      H=1.001
C CALCULATE VENTURI FLOW FOR VENTURI 20 AND THE
C ASSOCIATED VENTURI UNCERTAINTY, THE UNCERTAINTY DATA IS
      BP1=0.01*DTTB(16)
      BT=0.01*DTTB(18)
      BDP=0.01*DTTB(17)
      BCD=0.01992
      BALPHA=4.17E-07
      BD1=0.0005
      BD2=0.0005
      PW=0.0
      CALL FLOWOR(20,DTTB(1),DTTB(2),DTTB(3),9,H,DH,W,WG,RO,VDPT)
C      WRITE(55,720) WG
C720  FORMAT(2X,'LPFT INLET FLOWRATE - P(8801) >',F9.2,' LB/S')
C CALCULATE THE PARTIAL DERIVATIVES
C PARTIAL DERIVATIVE FOR P1 IS
      HP1=DTTB(1)*H
      CALL FLOWOR(20,HP1,DTTB(2),DTTB(3),9,H,DH,W,HW,RO,VDPT)
      DWDP1=(HW-WG)/(HP1-DTTB(1))
C PARTIAL DERIVATIVE FOR DP
      HDP=DTTB(2)*H
      CALL FLOWOR(20,DTTB(1),HDP,DTTB(3),9,H,DH,W,HW,RO,VDPT)
      DWDDP=(HW-WG)/(HDP-DTTB(2))
C PARTIAL DERIVATIVE FOR T1
      HT1=DTTB(3)*H
      CALL FLOWOR(20,DTTB(1),DTTB(2),HT1,9,H,DH,W,HW,RO,VDPT)
      DWDT=(HW-WG)/(HT1-DTTB(3))
C PARTIAL DERIVATIVE FOR D1
      CALL FLOWOR(20,DTTB(1),DTTB(2),DTTB(3),1,H,DH,W,HW,RO,VDPT)
      DWDD1=(HW-WG)/DH
C PARTIAL DERIVATIVE FOR D2
      CALL FLOWOR(20,DTTB(1),DTTB(2),DTTB(3),2,H,DH,W,HW,RO,VDPT)
      DWDD2=(HW-WG)/DH
C PARTIAL DERIVATIVE FOR CD
      CALL FLOWOR(20,DTTB(1),DTTB(2),DTTB(3),3,H,DH,W,HW,RO,VDPT)
      DWDCD=(HW-WG)/DH
C PARTIAL DERIVATIVE FOR ALPHA
      CALL FLOWOR(20,DTTB(1),DTTB(2),DTTB(3),5,H,DH,W,HW,RO,VDPT)
      DWDALP=(HW-WG)/DH
C CALCULATE THE SQUARED TERMS FOR THE PARTIALS TIMES THE
C UNCERTAINTY IN THE VARIABLES
      BWP=(BP1*DWDP1)**2
      BWT=(BT*DWDT)**2
      BWDP=(BDP*DWDDP)**2
      BWCD=(BCD*DWDCD)**2
      BWALPHA=(BALPHA*DWDALP)**2
      BWD1=(BD1*DWDD1)**2
      BWD2=(BD2*DWDD2)**2
C CALCULATE THE FLOW UNCERTAINTY
C CALCULATE THE CORRELATED BIAS TERMS, SWAG FOR CORRELATION
C COEFFICIENT USED AT THIS POINT
      BD1BD2=DWDD1*DWDD2*BD1*BD2*1.00
      BTBDP=DWDT*DWDDP*(BT*BDP)*0.00

```



```

BTBP1=DWDT*DWDPI*(BT*BP1)*0.00
BDPBP1=DWDDP*DWDPI*(BDP*BP1)*0.00
C VENTURI 20 UNCERTAINTY IS
UW=SQRT(BWP+BWT+BWDP+BWCD+BWALPHA+2.*BD1BD2+BWD1+BWD2
&+2.*BTBDP+2*BDPBP1+PW**2)
PERCENT=100.*UW/WG
WW(1)=WG
UNW(1)=UW
PER(1)=PERCENT
C VENTURI 20 OUTPUT
WRITE (55,*)'PID 8801 LPFT INLET'
WRITE (55,*)' VENTURI <20>'
WRITE (55,721) DTTB(1),DTTB(2),DTTB(3)
WRITE (55,722) BP1,BDP,BT
WRITE (55,723) BCD,BALPHA,BD1,BD2
WRITE (55,724) PW
WRITE (55,725) DWDPI,DWDDP,DWDT
WRITE (55,726) DWDCD,DWDALP,DWDD1,DWDD2
WRITE (55,727) BWP,BWDP,BWT
WRITE (55,728) BWCD,BWALPHA,BWD1,BWD2
WRITE (55,729) WG,UW,PERCENT
721 FORMAT(3X,'P1',4X,F8.2,5X,'DP',3X,F8.2,5X,'T',3X,F8.2)
722 FORMAT(3X,'BP1',3X,F8.4,5X,'BDP',3X,F8.4,4X,'BT1',1X,F8.4)
723 FORMAT(3X,'BCD',3X,F8.5,5X,'BALP',3X,E8.3,3X,'BD1',2X,F8.5,
&6X,'BD2',2X,F8.5)
724 FORMAT(3X,'PW',4X,F8.4)
725 FORMAT(2X,'DWDPI',3X,E9.4,2X,'DWDDP',3X,E9.4,2X,'DWDT',3X,E9.3)
726 FORMAT(2X,'DWDCD',3X,E9.4,2X,'DUALP',3X,E9.3,2X,'DWDD1',3X,E9.3,
&2X,'DWDD2',2X,E9.4)
727 FORMAT(2X,'BWP',5X,E9.4,3X,'BWDP',3X,E9.4,3X,'BWD1',2X,E9.4)
728 FORMAT(2X,'BWCD',4X,E9.4,3X,'BWALP',3X,E9.4,2X,'BWD1',2X,E9.4,
&4X,'BWD2',2X,E9.4)
729 FORMAT(2X,' W ',3X,F9.4,4X,'UW',5X,F9.5,2X,'% UW',2X,F8.4)
WRITE (55,*)'***** ***** ***** ***** *****'
WRITE (55,*)
C
C CALCULATE THE FLOWRATE AND FLOWRATE UNCERTAINTY FOR VENTURI 397
CALL FLOWOR(397,DTTB(4),DTTB(5),DTTB(6),9,H,DH,W,WG,RO,VDPT)
C WRITE(55,730) WG
C730 FORMAT(2X,'CCV INLET FLOWRATE - P(8818) >',F9.2,' LB/S')
BP1=0.01*DTTB(4)
BT=0.01*DTTB(6)
BDP=0.01*DTTB(5)
BCD=0.03063
BALPHA=5.48E-07
BD1=0.0005
BD2=0.0005
PW=0.0
C CALCULATE THE PARTIAL DERIVATIVES
C PARTIAL DERIVATIVE FOR P1 IS
HP1=DTTB(4)*H
CALL FLOWOR(397,HP1,DTTB(5),DTTB(6),9,H,DH,W,HW,RO,VDPT)
DWDPI=(HW-WG)/(HP1-DTTB(4))
C PARTIAL DERIVATIVE FOR DP
HDP=DTTB(5)*H
CALL FLOWOR(397,HDP,DTTB(4),DTTB(6),9,H,DH,W,HW,RO,VDPT)
DWDDP=(HW-WG)/(HDP-DTTB(5))
C PARTIAL DERIVATIVE FOR T1
HT1=DTTB(6)*H
CALL FLOWOR(397,DTTB(4),DTTB(5),HT1,9,H,DH,W,HW,RO,VDPT)
DWD1=(HW-WG)/(HT1-DTTB(6))
C PARTIAL DERIVATIVE FOR D1
CALL FLOWOR(397,DTTB(4),DTTB(5),DTTB(6),1,H,DH,W,HW,RO,VDPT)
DWDD1=(HW-WG)/DH
C PARTIAL DERIVATIVE FOR D2
CALL FLOWOR(397,DTTB(4),DTTB(5),DTTB(6),2,H,DH,W,HW,RO,VDPT)
DWDD2=(HW-WG)/DH
C PARTIAL DERIVATIVE FOR CD
CALL FLOWOR(397,DTTB(4),DTTB(5),DTTB(6),3,H,DH,W,HW,RO,VDPT)
DWDCD=(HW-WG)/DH
C PARTIAL DERIVATIVE FOR ALPHA

```

```

CALL FLOWOR(397,DTTB(4),DTTB(5),DTTB(6),4,H, DH, W, HW, RO, VDPT)
DWDALP=(HW-WG)/DH
C CALCULATE THE SQUARED TERMS FOR THE PARTIALS TIMES THE
C UNCERTAINTY IN THE VARIABLES
BWP=(BP1*DWDP1)**2
BWT=(BT*DWDT)**2
BWDP=(BDP*DWDDP)**2
BWCD=(BCD*DWDCD)**2
BWALPHA=(BALPHA*DWDALP)**2
BWD1=(BD1*DWDD1)**2
BWD2=(BD2*DWDD2)**2
C CALCULATE THE FLOW UNCERTAINTY
C CALCULATE THE CORRELATED BIAS TERMS, SWAG FOR CORRELATION
C COEFFICIENT USED AT THIS POINT
BD1BD2=DWDD1*DWDD2*BD1*BD2*1.0
BTBDP=DWDT*DWDDP*(BT*BDP)*0.00
BTBP1=DWDT*DWDP1*(BT*BP1)*0.00
BDPBP1=DWDDP*DWDP1*(BDP*BP1)*0.00
C VENTURI 397 UNCERTAINTY IS
UW=SQRT(BWP+BWT+BWDP+BWCD+BWALPHA+2.*BD1BD2+BWD1+BWD2
&+2.*BTBDP+2*BDPBP1+PW**2)
PERCENT=100.*UW/WG
WW(2)=WG
UNW(2)=UW
PER(2)=PERCENT
C VENTURI 397 OUTPUT
WRITE (55,*) 'PID 8818 CCV INLET'
WRITE (55,*) ' VENTURI <397>'
WRITE (55,731) DTTB(4),DTTB(5),DTTB(6)
WRITE (55,732) BP1,BDP,BT
WRITE (55,733) BCD,BALPHA,BD1,BD2
WRITE (55,734) PW
WRITE (55,735) DWDP1,DWDDP,DWDT
WRITE (55,736) DWDCD,DWDALP,DWDD1,DWDD2
WRITE (55,737) BWP,BWDP,BWT
WRITE (55,738) BWCD,BWALPHA,BWD1,BWD2
WRITE (55,739) WG,UW,PERCENT
731 FORMAT(3X,'P1',4X,F8.2,5X,'DP',3X,F8.2,5X,'T',3X,F8.2)
732 FORMAT(3X,'BP1',3X,F8.4,5X,'BDP',3X,F8.4,4X,'BT1',1X,F8.4)
733 FORMAT(3X,'BCD',3X,F8.5,5X,'BALP',3X,E8.3,3X,'BD1',2X,F8.5,
&6X,'BD2',2X,F8.5)
734 FORMAT(3X,'PW',4X,F8.4)
735 FORMAT(2X,'DWDP1',3X,E9.4,2X,'DWDDP',3X,E9.4,2X,'DWDT',3X,E9.3)
736 FORMAT(2X,'DWDCD',3X,E9.4,2X,'DWDALP',3X,E9.3,2X,'DWDD1',3X,E9.3,
&2X,'DWDD2',2X,E9.4)
737 FORMAT(2X,'BWP',5X,E9.4,3X,'BWDP',3X,E9.4,3X,'BWDT',2X,E9.4)
738 FORMAT(2X,'BWCD',4X,E9.4,3X,'BWALP',3X,E9.4,2X,'BWD1',2X,E9.4,
&4X,'BWD2',2X,E9.4)
739 FORMAT(2X,' W ',3X,F9.4,4X,'UW',5X,F9.5,2X,'% UW',2X,F8.4)
WRITE (55,*) '***** ***** ***** ***** ***** *****'
WRITE (55,*)
C
C CALCULATE THE FLOWRATE AND FLOWRATE UNCERTAINTY FOR VENTURI 3541
CALL FLOWOR(3541,DTTB(7),DTTB(8),DTTB(9),9,H, DH, W, WG, RO, VDPT)
C WRITE(55,740) WG
C740 FORMAT(2X,'NOZ CLNT FLOWRATE - P(8815) >',F9.2,' LB/S')
BP1=0.01*DTTB(7)
BT=0.01*DTTB(9)
BDP=0.01*DTTB(8)
BCD=0.02033
BALPHA=5.48E-07
BD1=0.0005
BD2=0.0005
PW=0.00
C CALCULATE THE PARTIAL DERIVATIVES
C PARTIAL DERIVATIVE FOR P1 IS
HP1=DTTB(7)*H
CALL FLOWOR(3541,HP1,DTTB(8),DTTB(9),9,H, DH, W, HW, RO, VDPT)
DWDP1=(HW-WG)/(HP1-DTTB(7))
C PARTIAL DERIVATIVE FOR DP
HDP=DTTB(8)*H

```

```

CALL FLOWOR(3541,DTTB(7),HDP,DTTB(9),9,H,DH,W,HW,RO,VDPT)
DWDDP=(HW-WG)/(HDP-DTTB(8))
C PARTIAL DERIVATIVE FOR T1
HT1=DTTB(9)*H
CALL FLOWOR(3541,DTTB(7),DTTB(8),HT1,9,H,DH,W,HW,RO,VDPT)
DWDT=(HW-WG)/(HT1-DTTB(9))
C PARTIAL DERIVATIVE FOR D1
CALL FLOWOR(3541,DTTB(7),DTTB(8),DTTB(9),1,H,DH,W,HW,RO,VDPT)
DWDD1=(HW-WG)/DH
C PARTIAL DERIVATIVE FOR D2
CALL FLOWOR(3541,DTTB(7),DTTB(8),DTTB(9),2,H,DH,W,HW,RO,VDPT)
DWDD2=(HW-WG)/DH
C PARTIAL DERIVATIVE FOR CD
CALL FLOWOR(3541,DTTB(7),DTTB(8),DTTB(9),3,H,DH,W,HW,RO,VDPT)
DWDCD=(HW-WG)/DH
C PARTIAL DERIVATIVE FOR ALPHA
CALL FLOWOR(3541,DTTB(7),DTTB(8),DTTB(9),4,H,DH,W,HW,RO,VDPT)
DWDALP=(HW-WG)/DH
C CALCULATE THE SQUARED TERMS FOR THE PARTIALS TIMES THE
C UNCERTAINTY IN THE VARIABLES
BWP=(BP1*DWDP1)**2
BWT=(BT*DWDT)**2
BWDP=(BDP*DWDDP)**2
BWCD=(BCD*DWDCD)**2
BWALPHA=(BALPHA*DWDALP)**2
BWD1=(BD1*DWDD1)**2
BWD2=(BD2*DWDD2)**2
C CALCULATE THE FLOW UNCERTAINTY
C CALCULATE THE CORRELATED BIAS TERMS, SWAG FOR CORRELATION
C COEFFICIENT USED AT THIS POINT
BD1BD2=DWDD1*DWDD2*BD1*BD2*1.00
BTBDP=DWDT*DWDDP*(BT*BDP)*0.00
BTBP1=DWDT*DWDP1*(BT*BP1)*0.00
BDPBP1=DWDDP*DWDP1*(BDP*BP1)*0.00
C VENTURI 3541 UNCERTAINTY IS
UW=SQRT(BWP+BWT+BWDP+BWCD+BWALPHA+2.*BD1BD2+BWD1+BWD2
&+2.*BTBDP+2*BDPBP1+PW**2)
PERCENT=100.*UW/WG
WW(3)=WG
UNW(3)=UW
PER(3)=PERCENT
C VENTURI 3541 OUTPUT
WRITE (55,*)
WRITE (55,*)'PID 8815 NOZ CLNT'
WRITE (55,*)' VENTURI <3541>'
WRITE (55,741) DTTB(4),DTTB(5),DTTB(6)
WRITE (55,742) BP1,BDP,BT
WRITE (55,743) BCD,BALPHA,BD1,BD2
WRITE (55,744) PW
WRITE (55,745) DWDP1,DWDDP,DWDT
WRITE (55,746) DWDCD,DWDALP,DWDD1,DWDD2
WRITE (55,747) BWP,BWDP,BWT
WRITE (55,748) BWCD,BWALPHA,BWD1,BWD2
WRITE (55,749) WG,UW,PERCENT
741 FORMAT(3X,'P1',4X,F8.2,5X,'DP',3X,F8.2,5X,'T',3X,F8.2)
742 FORMAT(3X,'BP1',3X,F8.4,5X,'BDP',3X,F8.4,4X,'BT1',1X,F8.4)
743 FORMAT(3X,'BCD',3X,F8.5,5X,'BALP',3X,E8.3,3X,'BD1',2X,F8.5,
&6X,'BD2',2X,F8.5)
744 FORMAT(3X,'PW',4X,F8.4)
745 FORMAT(2X,'DWDP1',3X,E9.4,2X,'DWDDP',3X,E9.4,2X,'DWDT',3X,E9.3)
746 FORMAT(2X,'DWDCD',3X,E9.4,2X,'DWDALP',3X,E9.3,2X,'DWDD1',3X,E9.3,
&2X,'DWDD2',2X,E9.4)
747 FORMAT(2X,'BWP',5X,E9.4,3X,'BWDP',3X,E9.4,3X,'BWDT',2X,E9.4)
748 FORMAT(2X,'BWCD',4X,E9.4,3X,'BWALP',3X,E9.4,2X,'BWD1',2X,E9.4,
&4X,'BWD2',2X,E9.4)
749 FORMAT(2X,' W ',3X,F9.4,4X,'UW',5X,F9.5,2X,'% UW',2X,F8.4)
WRITE (55,*)'*****'
WRITE (55,*)
C
C
C CALCULATE THE FLOWRATE AND FLOWRATE UNCERTAINTY FOR VENTURI 3541

```

```

CALL FLOWOR(3542,DTTB(10),DTTB(11),DTTB(12),9,H,DH,W,WG,RO,VDPT)
C WRITE(55,750) WG
C750 FORMAT(2X,NOZ CLNT FLOWRATE - P(8816) >,'F9.2,' LB/S)
BP1=0.01*DTTB(10)
BT=0.01*DTTB(12)
BDP=0.01*DTTB(11)
BCD=0.02033
BALPHA=5.48E-07
BD1=0.0005
BD2=0.0005
PW=0.0
C CALCULATE THE PARTIAL DERIVATIVES
C PARTIAL DERIVATIVE FOR P1 IS
HP1=DTTB(10)*H
CALL FLOWOR(3542,HP1,DTTB(11),DTTB(12),9,H,DH,W,HW,RO,VDPT)
DWDPI=(HW-WG)/(HP1-DTTB(10))
C PARTIAL DERIVATIVE FOR DP
HDP=DTTB(11)*H
CALL FLOWOR(3542,DTTB(10),HDP,DTTB(12),9,H,DH,W,HW,RO,VDPT)
DWDDP=(HW-WG)/(HDP-DTTB(11))
C PARTIAL DERIVATIVE FOR T1
HT1=DTTB(12)*H
CALL FLOWOR(3542,DTTB(10),DTTB(11),HT1,9,H,DH,W,HW,RO,VDPT)
DWDTI=(HW-WG)/(HT1-DTTB(12))
C PARTIAL DERIVATIVE FOR D1
CALL FLOWOR(3542,DTTB(10),DTTB(11),DTTB(12),1,H,DH,W,HW,RO,VDPT)
DWDD1=(HW-WG)/DH
C PARTIAL DERIVATIVE FOR D2
CALL FLOWOR(3542,DTTB(10),DTTB(11),DTTB(12),2,H,DH,W,HW,RO,VDPT)
DWDD2=(HW-WG)/DH
C PARTIAL DERIVATIVE FOR CD
CALL FLOWOR(3542,DTTB(10),DTTB(11),DTTB(12),3,H,DH,W,HW,RO,VDPT)
DWDCD=(HW-WG)/DH
C PARTIAL DERIVATIVE FOR ALPHA
CALL FLOWOR(3542,DTTB(10),DTTB(11),DTTB(12),4,H,DH,W,HW,RO,VDPT)
DWDALP=(HW-WG)/DH
C CALCULATE THE SQUARED TERMS FOR THE PARTIALS TIMES THE
C UNCERTAINTY IN THE VARIABLES
BWP=(BP1*DWDPI)**2
BWT=(BT*DWDTI)**2
BWDP=(BDP*DWDDP)**2
BWCD=(BCD*DWDCD)**2
BWALPHA=(BALPHA*DWDALP)**2
BWD1=(BD1*DWDD1)**2
BWD2=(BD2*DWDD2)**2
C CALCULATE THE FLOW UNCERTAINTY
C CALCULATE THE CORRELATED BIAS TERMS, SWAG FOR CORRELATION
C COEFFICIENT USED AT THIS POINT
BD1BD2=DWDD1*DWDD2*BD1*BD2*1.0
BTBDP=DWDTI*DWDDP*(BT*BDP)*0.0
BTBP1=DWDTI*DWDPI*(BT*BP1)*0.0
BDPBP1=DWDDP*DWDPI*(BDP*BP1)*0.0
C VENTURI 3542 UNCERTAINTY IS
UW=SQRT(BWP+BWT+BWDP+BWCD+BWALPHA+2.*BD1BD2+BWD1+BWD2
&+2.*BTBDP+2*BDPBP1+PW**2)
PERCENT=100.*UW/WG
WW(4)=WG
UNW(4)=UW
PER(4)=PERCENT
C VENTURI 3542 OUTPUT
WRITE (55,*)
WRITE (55,*) 'PID' 8816 NOZ CLNT
WRITE (55,*) ' VENTURI <3542>'
WRITE (55,751) DTTB(10),DTTB(11),DTTB(12)
WRITE (55,752) BP1,BDP,BT
WRITE (55,753) BCD,BALPHA,BD1,BD2
WRITE (55,754) PW
WRITE (55,755) DWDPI,DWDDP,DWDTI
WRITE (55,756) DWDCD,DWDALP,DWDD1,DWDD2
WRITE (55,757) BWP,BWDP,BWT
WRITE (55,758) BWCD,BWALPHA,BWD1,BWD2

```

```

WRITE (55,759) WG,UW,PERCENT
751 FORMAT(3X,'P1',4X,F8.2,5X,'DP',3X,F8.2,5X,'T',3X,F8.2)
752 FORMAT(3X,'BP1',3X,F8.4,5X,'BDP',3X,F8.4,4X,'BT1',1X,F8.4)
753 FORMAT(3X,'BCD',3X,F8.5,5X,'BALP',3X,E8.3,3X,'BD1',2X,F8.5,
&6X,'BD2',2X,F8.5)
754 FORMAT(3X,'PW',4X,F8.4)
755 FORMAT(2X,'DWDP1',3X,E9.4,2X,'DWDDP',3X,E9.4,2X,'DWD1',3X,E9.3)
756 FORMAT(2X,'DWDCD',3X,E9.4,2X,'DWALP',3X,E9.3,2X,'DWDD1',3X,E9.3,
&2X,'DWDD2',2X,E9.4)
757 FORMAT(2X,'BWP',5X,E9.4,3X,'BWDP',3X,E9.4,3X,'BWD1',2X,E9.4)
758 FORMAT(2X,'BWCD',4X,E9.4,3X,'BWALP',3X,E9.4,2X,'BWD1',2X,E9.4,
&4X,'BWD2',2X,E9.4)
759 FORMAT(2X,' W ',3X,F9.4,4X,'UW',5X,F9.5,2X,'% UW',2X,F8.4)
WRITE (55,*) '***** ***** ***** ***** *****'
WRITE (55,*)

C
C CALCULATE THE FLOWRATE AND FLOWRATE UNCERTAINTY FOR VENTURI 3543
CALL FLOWOR(3543,DTTB(13),DTTB(14),DTTB(15),9,H,DH,W,WG,RO,VDPT)
C WRITE(55,760) WG
C760 FORMAT(2X,'NOZ CLNT FLOWRATE - P(8817) >,'F9.2,' LB/S')
BP1=0.01*DTTB(13)
BT=0.01*DTTB(15)
BDP=0.01*DTTB(14)
BCD=0.02033
BALPHA=5.48E-07
BD1=0.0005
BD2=0.0005
PW=0.00
C CALCULATE THE PARTIAL DERIVATIVES
C PARTIAL DERIVATIVE FOR P1 IS
HP1=DTTB(13)*H
CALL FLOWOR(3543,HP1,DTTB(14),DTTB(15),9,H,DH,W,HW,RO,VDPT)
DWDP1=(HW-WG)/(HP1-DTTB(13))
C PARTIAL DERIVATIVE FOR DP
HDP=DTTB(14)*H
CALL FLOWOR(3543,DTTB(13),HDP,DTTB(15),9,H,DH,W,HW,RO,VDPT)
DWDDP=(HW-WG)/(HDP-DTTB(14))
C PARTIAL DERIVATIVE FOR T1
HT1=DTTB(15)*H
CALL FLOWOR(3543,DTTB(13),DTTB(14),HT1,9,H,DH,W,HW,RO,VDPT)
DWD1=(HW-WG)/(HT1-DTTB(15))
C PARTIAL DERIVATIVE FOR D1
CALL FLOWOR(3543,DTTB(13),DTTB(14),DTTB(15),1,H,DH,W,HW,RO,VDPT)
DWDD1=(HW-WG)/DH
C PARTIAL DERIVATIVE FOR D2
CALL FLOWOR(3543,DTTB(13),DTTB(14),DTTB(15),2,H,DH,W,HW,RO,VDPT)
DWDD2=(HW-WG)/DH
C PARTIAL DERIVATIVE FOR CD
CALL FLOWOR(3543,DTTB(13),DTTB(14),DTTB(15),3,H,DH,W,HW,RO,VDPT)
DWDCD=(HW-WG)/DH
C PARTIAL DERIVATIVE FOR ALPHA
CALL FLOWOR(3543,DTTB(13),DTTB(14),DTTB(15),4,H,DH,W,HW,RO,VDPT)
DWDALP=(HW-WG)/DH
C CALCULATE THE SQUARED TERMS FOR THE PARTIALS TIMES THE
C UNCERTAINTY IN THE VARIABLES
BWP=(BP1*DWDP1)**2
BWT=(BT*DWD1)**2
BWDP=(BDP*DWDDP)**2
BWCD=(BCD*DWDCD)**2
BWALPHA=(BALPHA*DWDALP)**2
BWD1=(BD1*DWDD1)**2
BWD2=(BD2*DWDD2)**2
C CALCULATE THE FLOW UNCERTAINTY
C CALCULATE THE CORRELATED BIAS TERMS, SWAG FOR CORRELATION
C COEFFICIENT USED AT THIS POINT
BD1BD2=DWDD1*DWDD2*BD1*BD2*1.0
BTBDP=DWD1*DWDDP*(BT*BDP)*0.0
BTBP1=DWD1*DWDP1*(BT*BP1)*0.0
BDPBP1=DWDDP*DWDP1*(BDP*BP1)*0.0
C VENTURI 3543 UNCERTAINTY IS
UW=SQRT(BWP+BWT+BWDP+BWCD+BWALPHA+2.*BD1BD2+BWD1+BWD2

```

```

&+2.*BTBDP+2*BDPBP1+PW**2)
PERCENT=100.*UW/WG
WW(5)=WG
UNW(5)=UW
PER(5)=PERCENT
C VENTURI 3543 OUTPUT
WRITE (55,*)
WRITE (55,*)'PID 8817 NOZ CLNT'
WRITE (55,*)' VENTURI <3543>'
WRITE (55,761) DTTB(13),DTTB(14),DTTB(15)
WRITE (55,762) BP1,BDP,BT
WRITE (55,763) BCD,BALPHA,BD1,BD2
WRITE (55,764) PW
WRITE (55,765) DWDP1,DWDDP,DWDT
WRITE (55,766) DWDCD,DWDALP,DWDD1,DWDD2
WRITE (55,767) BWP,BWDP,BWT
WRITE (55,768) BWCD,BWALPHA,BWD1,BWD2
WRITE (55,769) WG,UW,PERCENT
761 FORMAT(3X,'P1',4X,F8.2,5X,'DP',3X,F8.2,5X,'T',3X,F8.2)
762 FORMAT(3X,'BP1',3X,F8.4,5X,'BDP',3X,F8.4,4X,'BT1',1X,F8.4)
763 FORMAT(3X,'BCD',3X,F8.5,5X,'BALP',3X,E8.3,3X,'BD1',2X,F8.5,
&6X,'BD2',2X,F8.5)
764 FORMAT(3X,'PW',4X,F8.4)
765 FORMAT(2X,'DWDP1',3X,E9.4,2X,'DWDDP',3X,E9.4,2X,'DWDT',3X,E9.3)
766 FORMAT(2X,'DWDCD',3X,E9.4,2X,'DWDALP',3X,E9.3,2X,'DWDD1',3X,E9.3,
&2X,'DWDD2',2X,E9.4)
767 FORMAT(2X,'BWP',5X,E9.4,3X,'BWDP',3X,E9.4,3X,'BWDT',2X,E9.4)
768 FORMAT(2X,'BWCD',4X,E9.4,3X,'BWALP',3X,E9.4,2X,'BWD1',2X,E9.4,
&4X,'BWD2',2X,E9.4)
769 FORMAT(5X,' W ',3X,F9.4,4X,'UW',5X,F9.5,2X,'% UW',2X,F8.4)
WRITE (55,*)'*****'
WRITE (55,*)
C
C CALCULATE VENTURI FLOW FOR VENTURI 139 AND THE
C ASSOCIATED VENTURI UNCERTAINTY, THE UNCERTAINTY DATA IS
BP1=0.01*DTTB(16)
BT=0.01*DTTB(18)
BDP=0.01*DTTB(17)
BCD=0.02066
BALPHA=6.51E-07
BD1=0.0005
BD2=0.0005
PW=0.0
CALL FLOWOR(139,DTTB(16),DTTB(17),DTTB(18),9,H,DH,W,WG,RO,VDPT)
C WRITE(55,770) W
C770 FORMAT(2X,'POT INLET FLOWRATE - P(8802) >',F9.2,' LB/S')
C CALCULATE THE PARTIAL DERIVATIVES
C PARTIAL DERIVATIVE FOR P1 IS
HP1=DTTB(16)*H
CALL FLOWOR(139,HP1,DTTB(17),DTTB(18),9,H,DH,HW,WG,RO,VDPT)
DWDP1=(HW-W)/(HP1-DTTB(16))
C WRITE(55,*) 'H,H,DH,DH,HW,HW,DWDP1,DWDP1'
C PARTIAL DERIVATIVE FOR DP
C H=1.0001
HDP=DTTB(17)*H
CALL FLOWOR(139,DTTB(16),HDP,DTTB(18),9,H,DH,HW,WG,RO,VDPT)
DWDDP=(HW-W)/(HDP-DTTB(17))
C WRITE(55,*) 'H,H,DH,DH,HW,HW,DWDDP,DWDDP'
C PARTIAL DERIVATIVE FOR T1
C H=1.0001
HT1=DTTB(18)*H
CALL FLOWOR(139,DTTB(16),DTTB(17),HT1,9,H,DH,HW,WG,RO,VDPT)
DWDT=(HW-W)/(HT1-DTTB(18))
C WRITE(55,*) 'H,H,DH,DH,HW,HW,DWDT,DWDT'
C PARTIAL DERIVATIVE FOR D1
C H=1.0001
CALL FLOWOR(139,DTTB(16),DTTB(17),DTTB(18),1,H,DH,HW,WG,RO,VDPT)
DWDD1=(HW-W)/DH
C WRITE(55,*) 'H,H,DH,DH,HW,HW,DWDD1,DWDD1'
C PARTIAL DERIVATIVE FOR D2
C H=1.0001

```

```

CALL FLOWOR(139,DTTB(16),DTTB(17),DTTB(18),2,H,DH,HW,WG,RO,VDPT)
DWDD2=(HW-W)/DH
CALL FLOWOR(139,DTTB(16),DTTB(17),DTTB(18),7,H,DH,HW,WG,RO,VDPT)
DWDCD=(HW-W)/DH
C PARTIAL DERIVATIVE FOR ALPHA
C H=1.0001
CALL FLOWOR(139,DTTB(16),DTTB(17),DTTB(18),4,H,DH,HW,WG,RO,VDPT)
DWDALP=(HW-W)/DH
C WRITE(55,*) H,H,DH,DH,HW,HW,DWDALP,DWDALP
C CALCULATE THE SQUARED TERMS FOR HTE PARTIALS TIMES THE
C UNCERTAINTY IN THE VARIABLES
BWP=(BP1*DWDP1)**2
BWT=(BT*DWDT)**2
BWDP=(BDP*DWDDP)**2
BWCD=(BCD*DWDCD)**2
BWALPHA=(BALPHA*DWDALP)**2
BWD1=(BD1*DWDD1)**2
BWD2=(BD2*DWDD2)**2
C CALCULATE THE FLOW UNCERTAINTY
C CALCULATE THE CORRELATED BIAS TERMS, SWAG FOR CORRELATION
C COEFFICIENT USED AT THIS POINT
BD1BD2=DWDD1*DWDD2*BD1*BD2*1.0
BTBDP=DWDT*DWDDP*(BT*BDP)*0.0
BTBP1=DWDT*DWDP1*(BT*BP1)*0.0
BDPBP1=DWDDP*DWDP1*(BDP*BP1)*0.0
C VENTURI 139 UNCERTAINTY IS
UW=SQRT(BWP+BWT+BWDP+BWCD+BWALPHA+BWD1+BWD2
&+2.*BTBDP+2.*BDPBP1+2.*BD1BD2+PW*PW)
PERCENT=100.*UW/W
WW(6)=W
UNW(6)=UW
PER(6)=PERCENT
C VENTURI 139 OUTPUT
WRITE (55,*)
WRITE (55,*) 'PID 8802 LPOT INLET'
WRITE (55,*) ' VENTURI <139>'
WRITE (55,771) DTTB(16),DTTB(17),DTTB(18)
WRITE (55,772) BP1,BDP,BT
WRITE (55,773) BCD,BALPHA,BD1,BD2
WRITE (55,774) PW
WRITE (55,775) DWDP1,DWDDP,DWDT
WRITE (55,776) DWDCD,DWDALP,DWDD1,DWDD2
WRITE (55,777) BWP,BWDP,BWT
WRITE (55,778) BWCD,BWALPHA,BWD1,BWD2
WRITE (55,779) W,UW,PERCENT
771 FORMAT(3X,'P1',4X,F8.2,5X,'DP',3X,F8.2,5X,'T',3X,F8.2)
772 FORMAT(3X,'BP1',3X,F8.4,5X,'BDP',3X,F8.4,4X,'BT1',1X,F8.4)
773 FORMAT(3X,'BCD',3X,F8.5,5X,'BALP',3X,E8.3,3X,'BD1',2X,F8.5,
&6X,'BD2',2X,F8.5)
774 FORMAT(3X,'PW',4X,F8.4)
775 FORMAT(2X,'DWDP1',3X,E9.4,2X,'DWDDP',3X,E9.4,2X,'DWDT',3X,E9.3)
776 FORMAT(2X,'DWDCD',3X,E9.4,2X,'DWDALP',3X,E9.3,2X,'DWDD1',3X,E9.3,
&2X,'DWDD2',2X,E9.4)
777 FORMAT(2X,'BWP',5X,E9.4,3X,'BWDP',3X,E9.4,3X,'BWDT',2X,E9.4)
778 FORMAT(2X,'BWCD',4X,E9.4,3X,'BWALP',3X,E9.4,2X,'BWD1',2X,E9.4,
&4X,'BWD2',2X,E9.4)
779 FORMAT(5X,' W ',3X,F9.4,4X,' UW ',5X,F9.5,2X,'% UW',2X,F8.4)
WRITE (55,*) '***** ***** ***** ***** ***** *****'
WRITE (55,*)
C
C CALCULATE THE FLOWRATE AND FLOWRATE UNCERTAINTY FOR VENTURI 426
CALL FLOWOR(426,DTTB(19),DTTB(20),DTTB(21),9,H,DH,W,WG,RO,VDPT)
BP1=0.01*DTTB(19)
BT=0.01*DTTB(20)
BDP=0.01*DTTB(21)
BCD=0.01964
BALPHA=5.49E-07
BD1=0.0005
BD2=0.0005
PW=0.0
C CALCULATE THE PARTIAL DERIVATIVES

```

C PARTIAL DERIVATIVE FOR PI IS
 HP1=DTTB(19)*H
 CALL FLOWOR(426,HP1,DTTB(20),DTTB(21),9,H,DH,HW,WG,RO,VDPT)
 DWDP1=(HW-W)/(HP1-DTTB(19))

C PARTIAL DERIVATIVE FOR DP
 HDP=DTTB(20)*H
 CALL FLOWOR(426,DTTB(19),HDP,DTTB(21),9,H,DH,HW,WG,RO,VDPT)
 DWDDP=(HW-W)/(HDP-DTTB(20))

C PARTIAL DERIVATIVE FOR T1
 HT1=DTTB(21)*H
 CALL FLOWOR(426,DTTB(19),DTTB(20),HT1,9,H,DH,HW,WG,RO,VDPT)
 DWDT=(HW-W)/(HT1-DTTB(21))

C PARTIAL DERIVATIVE FOR D1
 CALL FLOWOR(426,DTTB(19),DTTB(20),DTTB(21),1,H,DH,HW,WG,RO,VDPT)
 DWDD1=(HW-W)/DH

C PARTIAL DERIVATIVE FOR D2
 CALL FLOWOR(426,DTTB(19),DTTB(20),DTTB(21),2,H,DH,HW,WG,RO,VDPT)
 DWDD2=(HW-W)/DH

C PARTIAL DERIVATIVE FOR CD
 CALL FLOWOR(426,DTTB(19),DTTB(20),DTTB(21),7,H,DH,HW,WG,RO,VDPT)
 DWDCD=(HW-W)/DH

C PARTIAL DERIVATIVE FOR ALPHA
 CALL FLOWOR(426,DTTB(19),DTTB(20),DTTB(21),4,H,DH,HW,WG,RO,VDPT)
 DWDALPHA=(HW-W)/DH

C CALCULATE THE SQUARED TERMS FOR THE PARTIALS TIMES THE
 C UNCERTAINTY IN THE VARIABLES
 BWP=(BP1*DWDP1)**2
 BWT=(BT*DWDT)**2
 BWDP=(BDP*DWDDP)**2
 BWCD=(BCD*DWDCD)**2
 BWALPHA=(BALPHA*DWDALPHA)**2
 BWD1=(BD1*DWDD1)**2
 BWD2=(BD2*DWDD2)**2

C CALCULATE THE FLOW UNCERTAINTY
 C CALCULATE THE CORRELATED BIAS TERMS, SWAG FOR CORRELATION
 C COEFFICIENT USED AT THIS POINT
 BD1BD2=DWDD1*DWDD2*BD1*BD2*1.0
 BTBDP=DWDT*DWDDP*(BT*BDP)*0.0
 BTBP1=DWDT*DWDP1*(BT*BP1)*0.0
 BTBP1=DWDDP*DWDP1*(BDP*BP1)*0.0

C VENTURI 426 UNCERTAINTY IS
 UW=SQRT(BWP+BWT+BWDP+BWCD+BWALPHA+2.*BD1BD2+BWD1+BWD2
 &+2.*BTBDP+2.*BDPBP1+PW**2)
 PERCENT=100.*UW/W
 WW(7)=W
 UNW(7)=UW
 PER(7)=PERCENT

C VENTURI 426 OUTPUT
 WRITE (55,*)
 WRITE (55,*)'PID 8819 HPOP DISCH'
 WRITE (55,*)' VENTURI <426>'
 WRITE (55,781) DTTB(19),DTTB(20),DTTB(21)
 WRITE (55,782) BP1,BDP,BT
 WRITE (55,783) BCD,BALPHA,BD1,BD2
 WRITE (55,784) PW
 WRITE (55,785) DWDP1,DWDDP,DWDT
 WRITE (55,786) DWDCD,DWDALP,DWDD1,DWDD2
 WRITE (55,787) BWP,BWDP,BWT
 WRITE (55,788) BWCD,BWALPHA,BWD1,BWD2
 WRITE (55,789) W,UW,PERCENT

781 FORMAT(3X,'P1',4X,F8.2,5X,'DP',3X,F8.2,5X,'T',3X,F8.2)
 782 FORMAT(3X,'BP1',3X,F8.4,5X,'BDP',3X,F8.4,4X,'BT1',1X,F8.4)
 783 FORMAT(3X,'BCD',3X,F8.5,5X,'BALP',3X,E8.3,3X,'BD1',2X,F8.5,
 &6X,'BD2',2X,F8.5)
 784 FORMAT(3X,'PW',4X,F8.4)
 785 FORMAT(2X,'DWDP1',3X,E9.4,2X,'DWDDP',3X,E9.4,2X,'DWDT',3X,E9.3)
 786 FORMAT(2X,'DWDCD',3X,E9.4,2X,'DWDALP',3X,E9.3,2X,'DWDD1',3X,E9.3,
 &2X,'DWDD2',2X,E9.4)
 787 FORMAT(2X,'BWP',5X,E9.4,3X,'BWDP',3X,E9.4,3X,'BWD1',2X,E9.4)
 788 FORMAT(2X,'BWCD',4X,E9.4,3X,'BWALP',3X,E9.4,2X,'BWD1',2X,E9.4,
 &4X,'BWD2',2X,E9.4)


```

789 FORMAT(5X,' W ',3X,F9.4,4X,'UW',5X,F9.5,2X,'% UW',2X,F8.4)
WRITE (55,*) '***** ***** ***** ***** ***** *****'
WRITE (55,*)
C
C
C CALCULATE THE FLOWRATE AND FLOWRATE UNCERTAINTY FOR VENTURI 268
CALL FLOWOR(268,DTTB(22),DTTB(23),DTTB(24),9,H,DH,W,WG,RO,VDPT)
BP1=0.01*DTTB(22)
BT=0.01*DTTB(24)
BDP=0.01*DTTB(23)
BCD=0.02066
BALPHA=6.71E-07
BD1=0.0005
BD2=0.0005
PW=0.0
C CALCULATE THE PARTIAL DERIVATIVES
C PARTIAL DERIVATIVE FOR P1 IS
HP1=DTTB(22)*H
CALL FLOWOR(268,HP1,DTTB(23),DTTB(24),9,H,DH,H,W,WG,RO,VDPT)
DWDP1=(HW-W)/(HP1-DTTB(22))
C PARTIAL DERIVATIVE FOR DP
HDP=DTTB(23)*H
CALL FLOWOR(268,HDP,DTTB(22),DTTB(24),9,H,DH,H,W,WG,RO,VDPT)
DWDDP=(HW-W)/(HDP-DTTB(23))
C PARTIAL DERIVATIVE FOR T1
HT1=DTTB(24)*H
CALL FLOWOR(268,HT1,DTTB(22),DTTB(23),DTTB(24),9,H,DH,H,W,WG,RO,VDPT)
DWDT=(HW-W)/(HT1-DTTB(24))
C PARTIAL DERIVATIVE FOR D1
CALL FLOWOR(268,DTTB(22),DTTB(23),DTTB(24),1,H,DH,H,W,WG,RO,VDPT)
DWDD1=(HW-W)/DH
C PARTIAL DERIVATIVE FOR D2
CALL FLOWOR(268,DTTB(22),DTTB(23),DTTB(24),2,H,DH,H,W,WG,RO,VDPT)
DWDD2=(HW-W)/DH
C PARTIAL DERIVATIVE FOR CD
CALL FLOWOR(268,DTTB(22),DTTB(23),DTTB(24),7,H,DH,H,W,WG,RO,VDPT)
DWDCD=(HW-W)/DH
C PARTIAL DERIVATIVE FOR ALPHA
CALL FLOWOR(268,DTTB(22),DTTB(23),DTTB(24),4,H,DH,H,W,WG,RO,VDPT)
DWDALP=(HW-W)/DH
C CALCULATE THE SQUARED TERMS FOR THE PARTIALS TIMES THE
C UNCERTAINTY IN THE VARIABLES
BWP=(BP1*DWDP1)**2
BWT=(BT*DWDT)**2
BWDP=(BDP*DWDDP)**2
BWCD=(BCD*DWDCD)**2
BWALPHA=(BALPHA*DWDALP)**2
BWD1=(BD1*DWDD1)**2
BWD2=(BD2*DWDD2)**2
C CALCULATE THE FLOW UNCERTAINTY
C CALCULATE THE CORRELATED BIAS TERMS, SWAG FOR CORRELATION
C COEFFICIENT USED AT THIS POINT
BD1BD2=DWDD1*DWDD2*BD1*BD2
BTBDP=DWDT*DWDDP*(BT*BDP)*0.00
BTBP1=DWDT*DWDP1*(BT*BP1)*0.00
BTBP1=DWDDP*DWDP1*(BDP*BP1)*0.00
UW=SQRT(BWP+BWT+BWDP+BWCD+BWALPHA+2.*BD1BD2+BWD1+BWD2
&+2.*BTBDP+2.*BDPBP1+PW**2)
PERCENT=100.*UW/W
WW(8)=W
UNW(8)=UW
PER(8)=PERCENT
C VENTURI 268 OUTPUT
WRITE (55,*)
WRITE (55,*) 'PID 8804 OPB LOX'
WRITE (55,*) ' VENTURI <268>'
WRITE (55,791) DTTB(22),DTTB(23),DTTB(24)
WRITE (55,792) BP1,BDP,BT
WRITE (55,793) BCD,BALPHA,BD1,BD2
WRITE (55,794) PW
WRITE (55,795) DWDP1,DWDDP,DWDT

```

```

WRITE (55,796) DWDCD,DWDALP,DWDD1,DWDD2
WRITE (55,797) BWP,BWDP,BWT
WRITE (55,798) BWCD,BWALPHA,BWD1,BWD2
WRITE (55,799) W,UW,PERCENT
791 FORMAT(3X,'P1',4X,F8.2,5X,'DP',3X,F8.2,5X,'T',3X,F8.2)
792 FORMAT(3X,'BP1',3X,F8.4,5X,'BDP',3X,F8.4,4X,'BT1',1X,F8.4)
793 FORMAT(3X,'BCD',3X,F8.5,5X,'BALP',3X,E9.3,3X,'BD1',2X,F8.5,
&6X,'BD2',2X,F8.5)
794 FORMAT(3X,'PW',4X,F8.4)
795 FORMAT(2X,'DWDP1',3X,E9.4,2X,'DWDDP',3X,E9.4,2X,'DWDT',3X,E9.3)
796 FORMAT(2X,'DWDCD',3X,E9.4,2X,'DWALP',3X,E9.3,2X,'DWDD1',3X,E9.3,
&2X,'DWDD2',2X,E9.4)
797 FORMAT(2X,'BWP',5X,E9.4,3X,'BWDP',3X,E9.4,3X,'BWDT',2X,E9.4)
798 FORMAT(2X,'BWCD',4X,E9.4,3X,'BWALP',3X,E9.4,2X,'BWD1',2X,E9.4,
&4X,'BWD2',2X,E9.4)
799 FORMAT(5X,' W ',3X,F9.4,4X,' UW ',5X,F9.5,2X,' % UW ',2X,F8.4)
WRITE (55,*) '***** ***** ***** ***** *****'
WRITE (55,*)

C
C
C CALCULATE THE FLOWRATE AND FLOWRATE UNCERTAINTY FOR VENTURI 271
CALL FLOWOR(271,DTTB(25),DTTB(26),DTTB(27),9,H,DH,W,WG,RO,VDPT)
C WRITE(55,800) WG
C800 FORMAT(2X,'OPB FUEL FLOWRATE - W(8805) >',F9.2,' LB/S')
BP1=0.01*DTTB(25)
BT=0.01*DTTB(27)
BDP=0.01*DTTB(26)
BCD=0.01992
BALPHA=3.23E-07
BD1=0.0005
BD2=0.0005
PW=0.0
C CALCULATE THE PARTIAL DERIVATIVES
C PARTIAL DERIVATIVE FOR P1 IS
HP1=DTTB(25)*H
CALL FLOWOR(271,HP1,DTTB(26),DTTB(27),9,H,DH,W,HW,RO,VDPT)
DWDP1=(HW-WG)/(HP1-DTTB(25))
C PARTIAL DERIVATIVE FOR DP
HDP=DTTB(26)*H
CALL FLOWOR(271,DTTB(25),HDP,DTTB(27),9,H,DH,W,HW,RO,VDPT)
DWDDP=(HW-WG)/(HDP-DTTB(14))
C PARTIAL DERIVATIVE FOR T1
HT1=DTTB(27)*H
CALL FLOWOR(271,DTTB(25),DTTB(26),HT1,9,H,DH,W,HW,RO,VDPT)
DWDT=(HW-WG)/(HT1-DTTB(27))
C PARTIAL DERIVATIVE FOR D1
CALL FLOWOR(271,DTTB(25),DTTB(26),DTTB(27),1,H,DH,W,HW,RO,VDPT)
DWDD1=(HW-WG)/DH
C PARTIAL DERIVATIVE FOR D2
CALL FLOWOR(271,DTTB(25),DTTB(26),DTTB(27),2,H,DH,W,HW,RO,VDPT)
DWDD2=(HW-WG)/DH
C PARTIAL DERIVATIVE FOR CD
CALL FLOWOR(271,DTTB(25),DTTB(26),DTTB(27),7,H,DH,W,HW,RO,VDPT)
DWDCD=(HW-WG)/DH
C PARTIAL DERIVATIVE FOR ALPHA
CALL FLOWOR(271,DTTB(25),DTTB(26),DTTB(27),4,H,DH,W,HW,RO,VDPT)
DWDALP=(HW-WG)/DH
C CALCULATE THE SQUARED TERMS FOR THE PARTIALS TIMES THE
C UNCERTAINTY IN THE VARIABLES
BWP=(BP1*DWDP1)**2
BWT=(BT*DWDT)**2
BWDP=(BDP*DWDDP)**2
BWCD=(BCD*DWDCD)**2
BWALPHA=(BALPHA*DWDALP)**2
BWD1=(BD1*DWDD1)**2
BWD2=(BD2*DWDD2)**2
C CALCULATE THE FLOW UNCERTAINTY
C CALCULATE THE CORRELATED BIAS TERMS, SWAG FOR CORRELATION
C COEFFICIENT USED AT THIS POINT
BD1BD2=DWDD1*DWDD2*BD1*BD2*1.0
BTBDP=DWDT*DWDDP*(BT*BDP)*0.00

```

```

BTBP1=DWDT*DWDPI*(BT*BP1)*0.00
BTBP1=DWDDP*DWDPI*(BDP*BP1)*0.00
C VENTURI 271 UNCERTAINTY IS
UW=SQRT(BWP+BWT+BWDP+BWCD+BWALPHA+2.*BD1BD2+BWD1+BWD2
&+2.*BTBDP+2*BDPBP1+PW**2)
PERCENT=100.*UW/WG
WW(9)=WG
UNW(9)=UW
PER(9)=PERCENT
C VENTURI 271 OUTPUT
WRITE (55,*)
WRITE (55,*)'PID 8805 OPB FUEL'
WRITE (55,*)'VENTURI <271>'
WRITE (55,801) DTTB(25),DTTB(26),DTTB(27)
WRITE (55,802) BP1,BDP,BT
WRITE (55,803) BCD,BALPHA,BD1,BD2
WRITE (55,804) PW
WRITE (55,805) DWDPI,DWDDP,DWDT
WRITE (55,806) DWDCD,DWDALP,DWDD1,DWDD2
WRITE (55,807) BWP,BWDP,BWT
WRITE (55,808) BWCD,BWALPHA,BWD1,BWD2
WRITE (55,809) WG,UW,PERCENT
801 FORMAT(3X,'P1',4X,F8.2,5X,'DP',3X,F8.2,5X,'T',3X,F8.2)
802 FORMAT(3X,'BP1',3X,F8.4,5X,'BDP',3X,F8.4,4X,'BT1',1X,F8.4)
803 FORMAT(3X,'BCD',3X,F8.5,5X,'BALP',3X,E9.3,2X,'BD1',2X,F8.5,
&6X,'BD2',2X,F8.5)
804 FORMAT(3X,'PW',4X,F8.4)
805 FORMAT(2X,'DWDPI',3X,E9.4,2X,'DWDDP',3X,E9.4,2X,'DWDT',3X,E9.3)
806 FORMAT(2X,'DWDCD',3X,E9.4,2X,'DWDALP',3X,E9.3,2X,'DWDD1',3X,E9.3,
&2X,'DWDD2',2X,E9.4)
807 FORMAT(2X,'BWP',5X,E9.4,3X,'BWDP',3X,E9.4,3X,'BWDT',2X,E9.4)
808 FORMAT(2X,'BWCD',4X,E9.4,3X,'BWALP',3X,E9.4,2X,'BWD1',2X,E9.4,
&4X,'BWD2',2X,E9.4)
809 FORMAT(5X,' W ',3X,F9.4,4X,'UW',5X,F9.5,2X,'% UW',2X,F8.4)
WRITE (55,*)'*****'
WRITE (55,*)
C
C CALCULATE THE FLOWRATE AND FLOWRATE UNCERTAINTY FOR VENTURI 296
CALL FLOWOR(296,DTTB(28),DTTB(29),DTTB(30),9,H, DH,W,WG,RO,VDPT)
BP1=0.01*DTTB(28)
BT=0.01*DTTB(30)
BDP=0.01*DTTB(29)
BCD=0.02052
BALPHA=6.71E-07
BD1=0.0005
BD2=0.0005
PW=0.0
C CALCULATE THE PARTIAL DERIVATIVES
C PARTIAL DERIVATIVE FOR P1 IS
HP1=DTTB(28)*H
CALL FLOWOR(296,HP1,DTTB(29),DTTB(30),9,H, DH,HW,WG,RO,VDPT)
DWDP1=(HW-W)/(HP1-DTTB(28))
C PARTIAL DERIVATIVE FOR DP
HDP=DTTB(29)*H
CALL FLOWOR(296,DTTB(28),HDP,DTTB(30),9,H, DH,HW,WG,RO,VDPT)
DWDDP=(HW-W)/(HDP-DTTB(29))
C PARTIAL DERIVATIVE FOR T1
HT1=DTTB(30)*H
CALL FLOWOR(296,DTTB(28),DTTB(29),HT1,9,H, DH,HW,WG,RO,VDPT)
DWDT=(HW-W)/(HT1-DTTB(30))
C PARTIAL DERIVATIVE FOR D1
CALL FLOWOR(296,DTTB(28),DTTB(29),DTTB(30),1,H, DH,HW,WG,RO,VDPT)
DWDD1=(HW-W)/DH
C PARTIAL DERIVATIVE FOR D2
CALL FLOWOR(296,DTTB(28),DTTB(29),DTTB(30),2,H, DH,HW,WG,RO,VDPT)
DWDD2=(HW-W)/DH
C PARTIAL DERIVATIVE FOR CD
CALL FLOWOR(296,DTTB(28),DTTB(29),DTTB(30),7,H, DH,HW,WG,RO,VDPT)
DWDCD=(HW-W)/DH
C PARTIAL DERIVATIVE FOR ALPHA
CALL FLOWOR(296,DTTB(28),DTTB(29),DTTB(30),4,H, DH,HW,WG,RO,VDPT)

```

```

DWDALP=(HW-W)/DH
C CALCULATE THE SQUARED TERMS FOR THE PARTIALS TIMES THE
C UNCERTAINTY IN THE VARIABLES
  BWP=(BP1*DWDPI)**2
  BWT=(BT*DWDI)**2
  BWDP=(BDP*DWDPI)**2
  BWCD=(BCD*DWDI)**2
  BWALPHA=(BALPHA*DWDALP)**2
  BWD1=(BD1*DWDI)**2
  BWD2=(BD2*DWDI)**2
C CALCULATE THE FLOW UNCERTAINTY
C CALCULATE THE CORRELATED BIAS TERMS, SWAG FOR CORRELATION
C COEFFICIENT USED AT THIS POINT
  BD1BD2=DWDD1*DWDI**2*BD1*BD2*0.0
  BTBDP=DWDI*DWDPI*(BT*BDP)*0.00
  BTBP1=DWDI*DWDPI*(BT*BP1)*0.00
  BTBP1=DWDPI*DWDPI*(BDP*BP1)*0.00
C VENTURI 296 UNCERTAINTY IS
  UW=SQRT(BWP+BWT+BWDP+BWCD+BWALPHA+2.*BD1BD2+BWD1+BWD2
  &+2.*BTBDP+2.*BDFBP1+PW**2)
  PERCENT=100.*UW/W
  WW(10)=W
  UNW(10)=UW
  PER(10)=PERCENT
C VENTURI 296 OUTPUT
  WRITE (55,*)
  WRITE (55,*) 'PID 8810 FPB LOX'
  WRITE (55,*) ' VENTURI <296>'
  WRITE (55,811) DTTB(28),DTTB(29),DTTB(30)
  WRITE (55,812) BP1,BDP,BT
  WRITE (55,813) BCD,BALPHA,BD1,BD2
  WRITE (55,814) PW
  WRITE (55,815) DWDPI,DWDPI,DWDI
  WRITE (55,816) DWDCD,DWDALP,DWDD1,DWDD2
  WRITE (55,817) BWP,BWDP,BWT
  WRITE (55,818) BWCD,BWALPHA,BWD1,BWD2
  WRITE (55,819) W,UW,PERCENT
811 FORMAT(3X,'P1',4X,F8.2,5X,'DP',3X,F8.2,5X,'T',3X,F8.2)
812 FORMAT(3X,'BP1',3X,F8.4,5X,'BDP',3X,F8.4,4X,'BT1',1X,F8.4)
813 FORMAT(3X,'BCD',3X,F8.5,5X,'BALP',3X,E8.3,3X,'BD1',2X,F8.5,
  &6X,'BD2',2X,F8.5)
814 FORMAT(3X,'PW',4X,F8.4)
815 FORMAT(2X,'DWDPI',3X,E9.4,2X,'DWDPI',3X,E9.4,2X,'DWDI',3X,E9.3)
816 FORMAT(2X,'DWDCD',3X,E9.4,2X,'DWDALP',3X,E9.3,2X,'DWDD1',3X,E9.3,
  &2X,'DWDD2',2X,E9.4)
817 FORMAT(2X,'BWP',5X,E9.4,3X,'BWDP',3X,E9.4,3X,'BWDI',2X,E9.4)
818 FORMAT(2X,'BWCD',4X,E9.4,3X,'BWALP',3X,E9.4,2X,'BWD1',2X,E9.4,
  &4X,'BWD2',2X,E9.4)
819 FORMAT(5X,' W ',3X,F9.4,4X,' UW ',5X,F9.5,2X,'% UW ',2X,F8.4)
  WRITE (55,*) '***** ***** ***** ***** *****'
  WRITE (55,*)
C
C CALL FLOWOR(247,DTTB(1),DTTB(2),DTTB(3),9,H,DH,W,WG,RO,VDPT)
C WRITE(55,911) W
C911 FORMAT(2X,'HTX INLET FLOWRATE - P(8803) >',F9.2,' LB/S')
C
  WRITE (55,*)
  WRITE(55,915) NSLC,BTIME,ETIME
915 FORMAT(2X,'SLNUM >',I5,2X,'SLICE START TIME >',F5.1,
  $ 2X,'SLICE END TIME >',F5.1)
  WRITE (55,*)
  DO 925 I=1,10
  WRITE (55,920) NPID(I),WW(I),UNW(I),PER(I)
920 FORMAT(2X,4(I4,2X,F7.2,2X,F6.2,2X,F6.2))
925 CONTINUE
  WRITE (55,*)
C
C
  GO TO 1
C
999 STOP

```

```

END
C
C-----00310099
C AUTHOR: J. BUTAS / J. LEAHY / R. NEUMEYER - DEC 1990      00320099
C          00330099
C DATED REVISIONS: NONE      00340099
C          00350099
C PURPOSE:   TO CALCULATE FLOW VENTURI FLOWS IN LBM/SEC    00360099
C          00370099
C FORM OF CALL: CALL FLOWOR      00380099
C          00390099
C INPUT:   ID      FLOW ORIFICE ID NUMBER      00400099
C          ICD     SWITCH TO ITERATE ON CD=F(REYNOLDS) 00401099
C          P1      UPSTREAM PRESSURE      PSIA    00410099
C          T1      UPSTREAM TEMPERATURE    DEG R  00420099
C          DP      ORIFICE DELTA PRESSURE  PSIA    00430099
C          00440099
C OUTPUT:  WL      FLOWRATE, LIQ CALCULATION  LBM/SEC 00450099
C          WG      FLOWRATE, GAS CALCULATION  LBM/SEC 00460099
C          RHO     DENSITY      LBM/FT**3 00470099
C          00480099
C METHOD:   00490099
C          00500099
C RESTRICTIONS: FORT77      00510099
C          00520099
C NOTES:   00530099
C          00540099
C          GASEOUS FLOW EQ REQUIREMENTS :      00550099
C          00560099
C          DP = MEASURED DELTA PRESSURE  PSID    00570099
C          P1 = MEASURED INLET PRESSURE  PSIA    00580099
C          T1 = MEASURED INLET TEMPERATURE DEG R  00590099
C          D1 = VENTURI INLET DIAMETER  IN      00600099
C          D2 = VENTURI THROAT DIAMETER  IN     00610099
C          CDFV = DISCHARGE COEFFICIENT MEASURED VIA WATER/AIR 00620099
C          TESTS AT RKDN ENGINEERING DEV LAB IN CANOGA PK 00630099
C          Z = COMPRESSIBILITY = F(P1,T1)      00640099
C          GAM = GAMMA      = F(P1,T1)      00650099
C          RHO = DENSITY    = F(P1,T1) LBM/FT3 00660099
C          00670099
C          LIQUID FLOW EQ REQUIREMENTS :      00680099
C          00690099
C          DP = MEASURED DELTA PRESSURE  PSID    00700099
C          P1 = MEASURED INLET PRESSURE  PSIA    00710099
C          T1 = MEASURED INLET TEMPERATURE DEG R  00720099
C          D1 = VENTURI INLET DIAMETER  IN     00730099
C          D2 = VENTURI THROAT DIAMETER  IN     00740099
C          CDFV = DISCHARGE COEFFICIENT MEASURED VIA WATER/AIR 00750099
C          TESTS AT RKDN ENGINEERING DEV LAB IN CANOGA PK 00760099
C          CDFVT= THEORETICAL DISCH. COEFFICIENT FOR ID = 247. 00770099
C          GAM = GAMMA      = F(P1,T1)      00780099
C          RHO = DENSITY    = F(P1,T1) LBM/FT3 00790099
C          00800099
C REVISIONS:      00810099
C NONE          00820099
C-----00830099
SUBROUTINE FLOWOR(ID,P1,DP,T1,NVAR,H,DH,WL,WG,RHO,VDPT) 00840199
IMPLICIT REAL (A-H,O-Z)      00841199
COMMON/PROPTY/KU,DL,DV,HL,HV,S,SL,SV,CV,CVL,CVV,CP,CPL,CPV,GAMMA,
X GAMMAL,GAMMAV,C,CL,CVP,MU,MUL,MUV,K,KL,KV,SIGMA,EXCESK,EXCL,EXCV
REAL BETA,C,CD,CDFVA,CDFVC,CPH2,CVH2,CPHE,CVHE,FV,K1,K2,MACHCOR
REAL KM,KVDI,MUH2,MUHE,PCOOL,PHE,RD,TE,TEQU,X,YCOOL,YHE
REAL WH2_203,WHEH_203,MWH2,MWHE,MWMIX,CPMIX,CVMIX,KMIX,C1,C2
REAL MU,MUL,MUV,K,KL,KV,A1,A2,MUMIX,MWO2,MWN2,P203RAT,RHE,RCOOL
C
REAL*8 PFLUID,TFLUID,ROFLUID,VFLUID,HFLUID,SFLUID,CVFLUID, 00841399
* CPFLUID,WFLUID,EFLUID,THFLUID,V2FLUID,ERFLUID,TSFLUID 00841499
REAL*4 XMW      00890099
CHARACTER*3 FLD      00870099
CHARACTER*2 TYPE    00880099
C          00910099

```

```

DATA NAMOX/2HO2/
DATA NAMHY/2HH2/
C_____ 00920099
C CHECK TO SEE IF ZERO. IF SO, SET WL TO VERY 00930099
C SMALL NUMBER AND EXIT. 00940099
C_____ 00950099
WRITE(6,*) 'VENTURI #,ID,P1,DP,T1
C WRITE (55,*) 'ENTERING SUBROUTINE FLOWOR'
C WRITE (55,*) 'ID',ID,'NVAR',NVAR
C IF (1.EQ.1) RETURN
C_____ 00950099
IF ((P1 .LE. 0) .OR. (T1 .LE. 0) .OR. (DP .EQ. 0)) THEN 00960099
  WL = -10002.0 00970099
  WRITE(86,*) 'INSTRUMENTATION INADEQUATE TO CALC. FLOWRATE'
  GOTO 999 00990099
END IF 01000099
C 01010099
C SET A DUMMY VALUE FOR THE RETURNED STEP SIZE
DH=9999.
C DH IS SET UNREASONABLY HIGH TO BE VISIBLE IN OUTPUT
TYPE = 'RO' 01020099
C_____ 01030099
C VENTURI CONSTANTS AS A FUNCTION OF VENTURI NUMBER (IMRL ITEM NO.) 01040099
C_____ 01050099
MACHCOR = 1.0
IF (ID .EQ. 20) THEN 01130099
C *** LPFTP TURBINE DRIVE DUCT (ALL COMMENTED VARIABLES IN THIS SECTION) 01140099
C REFER TO WATER FLOW CHARACTERISTICS. ALL CURRENT VARIABLES ARE FROM 01140099
C AIR FLOW TEST DATA. (LPFT VENTURI WAS RE-CALIBRATED WITH AIR DUE TO: 01140099
C E0215(A1666) AND LOW REYNOLDS NUMBER H2O CAL. JC LEAHY 3-4-92 01140099
IOP1 = 2 01150099
FLD = 'H2' 01160099
D1 = 1.9920 01170099
IF (NVAR.EQ.1) THEN
  D1=D1*H
  DH=D1-D1/H
ENDIF
D2 = 1.5225 01180099
IF (NVAR.EQ.2) THEN
  D2=D2*H
  DH=D2-D2/H
ENDIF
C CDFV = 0.99610 01190099
CDFV = 1.0125 01190099
IF (NVAR.EQ.3) THEN
  CDFV=CDFV*H
  DH=CDFV-CDFV/H
ENDIF
XK = 0.448 01200099
RP = 1.948 01210099
ALPHA=0.00000417 01220099
IF (NVAR.EQ.5) THEN
  ALPOLD=ALPHA
  ALPHA=ALPHA*1.01
  DH=ALPHA-ALPOLD
ENDIF
TYPE = 'RO' 01230099
C AO = 0.99522 01240099
AO = 1.0213183 01240099
C BO = 0.000626 01250099
BO = 0.01503 01250099
C REDT = 2.50E+06 01260099
REDT = 5.00E+06 01260099
C AA = 1.80 01270099
AA = 0.20 01270099
TREF = 480.0 01280099
MACHCOR = 1.00246
C 01290099
ELSEIF (ID .EQ. 139) THEN 01300099
C *** LPOTP TURBINE DRIVE DUCT 01310099
IOP1 = 1 01320099

```

```

FLD = 'O2'                                01330099
D1 = 2.2998                                01340099
IF (NVAR.EQ.1) THEN
  D1=D1*H
  DH=D1-D1/H
ENDIF
D2 = 1.5743                                01350099
IF (NVAR.EQ.2) THEN
  D2=D2*H
  DH=D2-D2/H
ENDIF
CDFV = 1.03332                              01360099
IF (NVAR.EQ.7) THEN
  CDOLD=CDFV
  CDFV=CDFV*H
  DH=CDFV-CDOLD
C WRITE (55,*) 'ID',ID,'NVAR',NVAR
C WRITE(55,*) 'CDFV',CDFV,'CDOLD',CDOLD,'DH',DH
  ENDF
XK = 0.316                                  01370099
RP = 2.441                                  01380099
ALPHA= 0.00000651                          01390099
IF (NVAR.EQ.4) THEN
  ALPOLD=ALPHA
  ALPHA=ALPHA*1.01
  DH=ALPHA-ALPOLD
ENDIF
AO = 1.04232                                01400099
BO = 0.01258                                01410099
REDT = 4.00E+05                             01420099
AA = 1.00                                    01430099
TREF = 190.0                                01440099
C                                             01450099
ELSEIF(ID .EQ. 247) THEN                    01460099
C *** HEX OXIDIZER SUPPLY ***** NOTE: CDFV IS AN ESTIMATE ***** 01470099
  IOP1 = 1                                  01480099
  FLD = 'O2'                                01490099
  D1 = 0.5535                                01500099
  IF (NVAR.EQ.1) THEN
    D1=D1*H
    DH=D1-D1/H
  ENDF
  D2 = 0.1745                                01510099
  IF (NVAR.EQ.2) THEN
    D2=D2*H
    DH=D2-D2/H
  ENDF
  CDFV = 0.9850                              01520099
  IF (NVAR.EQ.3) THEN
    CDFV=CDFV*H
    DH=CDFV-CDFV/H
  ENDF
  ALPHA= 0.00000569                          01530099
  IF (NVAR.EQ.4) THEN
    ALPHA=ALPHA*H
    DH=ALPHA*(1.-(1/H))
  ENDF
  TREF = 185.0                               01540099
C                                             01550099
ELSEIF(ID .EQ. 268) THEN                    01560099
C *** OPB OXIDIZER SUPPLY                   01570099
  IOP1 = 1                                  01580099
  FLD = 'O2'                                01590099
  D1 = 1.0972                                01600099
  IF (NVAR.EQ.1) THEN
    D1=D1*H
    DH=D1-D1/H
  ENDF
  D2 = 0.6551                                01610099
  IF (NVAR.EQ.2) THEN
    D2=D2*H

```

DH=D2-D2/H		
ENDIF		
CDFV = 1.03717		01620099
IF (NVAR.EQ.7) THEN		
CDOLD=CDFV		
CDFV=CDFV*H		
DH=CDFV-CDOLD		
ENDIF		
ALPHA= 0.00000671		01630099
IF (NVAR.EQ.4) THEN		
ALPHA=ALPHA*H		
DH=ALPHA*(1.-(1./H))		
ENDIF		
AO = 1.04585		01640099
BO = 0.009103		01650099
REDT = 6.00E+05		01660099
AA = 1.10		01670099
TREF = 200.0		01680099
C	01690099	
ELSEIF(ID .EQ. 271) THEN		01700099
C *** OPB FUEL SUPPLY		01710099
IOP1 = 2		01720099
FLD = 'H2'		01730099
D1 = 2.0060		01740099
IF (NVAR.EQ.1) THEN		
D1=D1*H		
DH=D1-D1/H		
ENDIF		
D2 = 1.4931		01750099
IF (NVAR.EQ.2) THEN		
D2=D2*H		
DH=D2-D2/H		
ENDIF		
CDFV = 1.02162		01760099
IF (NVAR.EQ.7) THEN		
CDOLD=CDFV		
CDFV=CDFV*H		
DH=CDFV-CDOLD		
ENDIF		
XK = 0.276		01770099
RP = 1.233		01780099
ALPHA= 0.00000323		01790099
IF (NVAR.EQ.4) THEN		
ALPOLD=ALPHA		
ALPHA=ALPHA*1.01		
DH=ALPHA-ALPOLD		
ENDIF		
AO = 1.02163		01800099
BO = 0.003231		01810099
REDT = 7.00E+05		01820099
AA = 1.50		01830099
TREF = 280.0		01840099
C	01850099	
ELSEIF(ID .EQ. 275) THEN		01860099
C *** OPB ASI OXIDIZER SUPPLY		01870099
IOP1 = 1		01880099
FLD = 'O2'		01890099
D1 = 0.3030		01900099
D2 = 0.0818		01910099
CDFV = 1.05226		01920099
ALPHA= 0.00000549		01930099
AO = 1.05499		01940099
BO = 0.02565		01950099
REDT = 8.00E+05		01960099
AA = 1.75		01970099
TREF = 280.0		01980099
C	01990099	
ELSEIF(ID .EQ. 274) THEN		02000099
C *** OPB ASI IGNITOR OXIDIZER SUPPLY		02010099
IOP1 = 1		02020099
FLD = 'O2'		02030099

D1 = 0.3030	02040099
D2 = 0.0561	02050099
CDFV = 0.99143	02060099
ALPHA= 0.00000549	02070099
AO = 0.99656	02080099
BO = 0.007346	02090099
REDT = 5.00E+05	02100099
AA = 0.20	02110099
TREF = 200.0	02120099
C	02130099
ELSEIF(ID .EQ. 277) THEN	02140099
C *** OPB ASI FUEL SUPPLY	02150099
IOP1 = 2	02160099
FLD = 'H2'	02170099
D1 = 0.4000	02180099
D2 = 0.1870	02190099
CDFV = 0.99061	02200099
ALPHA= 0.00000536	02210099
AO = 0.99086	02220099
BO = 0.002473	02230099
REDT = 1.00E+06	02240099
AA = 1.00	02250099
TREF = 90.0	02260099
C	02270099
ELSEIF(ID .EQ. 296) THEN	02280099
C *** FPB OXIDIZER SUPPLY	02290099
IOP1 = 1	02300099
FLD = 'O2'	02310099
D1 = 2.0090	02320099
IF (NVAR.EQ.1) THEN	
D1=D1*H	
DH=D1-D1/H	
ENDIF	
D2 = 1.1090	02330099
IF (NVAR.EQ.2) THEN	
D2=D2*H	
DH=D2-D2/H	
ENDIF	
CDFV = 1.02573	02340099
IF (NVAR.EQ.7) THEN	
CDOLD=CDFV	
CDFV=CDFV*H	
DH=CDFV-CDOLD	
ENDIF	
ALPHA= 0.00000671	02350099
IF (NVAR.EQ.4) THEN	
ALPOLD=ALPHA	
ALPHA=ALPHA*1.01	
DH=ALPHA-ALPOLD	
ENDIF	
AO = 1.02633	02360099
BO = 0.0006843	02370099
REDT = 1.80E+06	02380099
AA = 1.50	02390099
TREF = 200.0	02400099
C	02410099
ELSEIF(ID .EQ. 303) THEN	02420099
C *** FPB ASI OXIDIZER SUPPLY	02430099
IOP1 = 1	02440099
FLD = 'O2'	02450099
D1 = 0.3030	02460099
D2 = 0.0928	02470099
CDFV = 1.08156	02480099
ALPHA= 0.00000549	02490099
AO = 1.08269	02500099
BO = 0.02121	02510099
REDT = 6.50E+05	02520099
AA = 2.00	02530099
TREF = 280.0	02540099
C	02550099
ELSEIF(ID .EQ. 302) THEN	02560099

```

C *** FPB ASI IGNITER OXIDIZER SUPPLY                                02570099
  IOP1 = 1                                                            02580099
  FLD = 'O2'                                                            02590099
  D1 = 0.3030                                                            02600099
  D2 = 0.0502                                                            02610099
  CDFV = .98288                                                            02620099
  ALPHA= 0.00000549                                                    02630099
  AO = 0.98296                                                            02640099
  BO = 0.00161                                                            02650099
  REDT = 4.00E+05                                                        02660099
  AA = 1.50                                                                02670099
  TREF = 200.0                                                            02680099
C
C 02690099
  ELSEIF(ID.EQ.305) THEN                                                02700099
C *** FPB ASI FUEL SUPPLY                                            02710099
  IOP1 = 2                                                            02720099
  FLD = 'H2'                                                            02730099
  D1 = 0.4000                                                            02740099
  D2 = 0.1811                                                            02750099
  CDFV = 0.96581                                                            02760099
  ALPHA= 0.00000536                                                    02770099
  AO = 0.96835                                                            02780099
  BO = 0.008258                                                            02790099
  REDT = 1.00E+06                                                        02800099
  AA = 0.50                                                                02810099
  TREF = 90.0                                                            02820099
C
C 02830099
  ELSEIF(ID.EQ.3541) THEN                                              02840099
C *** FLIGHT NOZZLE COOLANT SUPPLY NO. 1                            02850099
  IOP1 = 2                                                            02860099
  FLD = 'H2'                                                            02870099
  D1 = 1.5241                                                            02880099
  IF (NVAR.EQ.1) THEN
    D1=D1*H
    DH=D1-D1/H
  ENDIF
  D2 = 0.9726                                                            02890099
  IF (NVAR.EQ.2) THEN
    D2=D2*H
    DH=D2-D2/H
  ENDIF
  CDFV = 1.01644                                                            02900099
  IF (NVAR.EQ.3) THEN
    CDFV=CDFV*H
    DH=CDFV-CDFV/H
  ENDIF
  XK = 1.123                                                            02910099
  RP = 1.656                                                            02920099
  ALPHA= 0.00000548                                                    02930099
  IF (NVAR.EQ.4) THEN
    ALPHA=ALPHA*H
    DH=ALPHA*(1.-(1./H))
  ENDIF
  AO = 1.01645                                                            02940099
  BO = 0.002959                                                            02950099
  REDT = 5.00E+05                                                        02960099
  AA = 1.50                                                                02970099
  TREF = 90.0                                                            02980099
C
C 02990099
  ELSEIF(ID.EQ.3542) THEN                                              03000099
C *** FLIGHT NOZZLE COOLANT SUPPLY NO. 2                            03010099
  IOP1 = 2                                                            03020099
  FLD = 'H2'                                                            03030099
  D1 = 1.5250                                                            03040099
  IF (NVAR.EQ.1) THEN
    D1=D1*H
    DH=D1-D1/H
  ENDIF
  D2 = 0.9760                                                            03050099
  IF (NVAR.EQ.2) THEN
    D2=D2*H

```

```

DH=D2-D2/H
ENDIF
CDFV = 0.99590                                03060099
IF (NVAR.EQ.3) THEN
  CDFV=CDFV*H
  DH=CDFV-CDFV/H
ENDIF
XK = 1.141                                    03070099
RP = 1.702                                    03080099
ALPHA= 0.00000548                             03090099
IF (NVAR.EQ.4) THEN
  ALPHA=ALPHA*H
  DH=ALPHA*(1.-(1/H))
ENDIF
AO = 0.9959                                  03100099
BO = 0.002620                                03110099
REDT = 5.00E+05                               03120099
AA = 1.50                                     03130099
TREF = 90.0                                  03140099
C                                               03150099
ELSEIF(ID.EQ.3543) THEN                       03160099
C *** FLIGHT NOZZLE COOLANT SUPPLY NO. 3     03170099
IOP1 = 2                                      03180099
FLD = 'H2'                                   03190099
D1 = 1.5205                                  03200099
IF (NVAR.EQ.1) THEN
  D1=D1*H
  DH=D1-D1/H
ENDIF
D2 = 0.9730                                  03210099
IF (NVAR.EQ.2) THEN
  D2=D2*H
  DH=D2-D2/H
ENDIF
CDFV = 0.99918                               03220099
IF (NVAR.EQ.3) THEN
  CDFV=CDFV*H
  DH=CDFV-CDFV/H
ENDIF
XK = 1.217                                    03230099
RP = 1.795                                    03240099
ALPHA= 0.00000548                             03250099
IF (NVAR.EQ.4) THEN
  ALPHA=ALPHA*H
  DH=ALPHA*(1.-(1/H))
ENDIF
AO = 0.99919                                  03260099
BO = 0.002990                                03270099
REDT = 5.00E+05                               03280099
AA = 1.50                                     03290099
TREF = 90.0                                  03300099
C                                               03310099
ELSEIF(ID.EQ.397) THEN                       03320099
C *** CCV FLIGHT NOZZLE COOLANT SUPPLY     03330099
IOP1 = 2                                      03340099
FLD = 'H2'                                   03350099
D1 = 2.4382                                  03360099
IF (NVAR.EQ.1) THEN
  D1=D1*H
  DH=D1-D1/H
ENDIF
D2 = 1.6939                                  03370099
IF (NVAR.EQ.2) THEN
  D2=D2*H
  DH=D2-D2/H
ENDIF
CDFV = 1.02091                               03380099
IF (NVAR.EQ.3) THEN
  CDFV=CDFV*H
  DH=CDFV-CDFV/H
ENDIF

```

```

XK = 0.196                                03390099
RP = 1.913                                03400099
ALPHA= 0.00000548                          03410099
IF (NVAR.EQ.4) THEN
  ALPHA=ALPHA*H
  DH=ALPHA*(1.-(1./H))
ENDIF
AO = 1.02106                               03420099
BO = 0.01152                               03430099
REDT = 5.00E+05                            03440099
AA = 1.00                                   03450099
TREF = 90.0                                03460099
C                                           03470099
ELSEIF(ID.EQ.426) THEN                      03480099
C *** HPOTP PUMP DISCHARGE                 03490099
  IOP1 = 1                                  03500099
  FLD = 'O2'                                03510099
  D1 = 3.9910                               03520099
  IF (NVAR.EQ.1) THEN
    D1=D1*H
    DH=D1-D1/H
  ENDIF
  D2 = 3.2090                               03530099
  IF (NVAR.EQ.2) THEN
    D2=D2*H
    DH=D2-D2/H
  ENDIF
  CDFV = 0.98195                            03540099
  IF (NVAR.EQ.7) THEN
    CDOLD=CDFV
    CDFV=CDFV*H
    DH=CDFV-CDOLD
  ENDIF
  ALPHA= 0.00000549                         03550099
  IF (NVAR.EQ.4) THEN
    ALPHA=ALPHA*H
    DH=ALPHA*(1.-(1./H))
  ENDIF
  AO = 0.98091                              03560099
  BO = 7340.0                               03570099
  REDT = 1.00E+05                           03580099
  AA = 5.00                                 03590099
  TREF = 200.0                              03600099
C                                           03610099
ELSE                                         03620099
  GOTO 999                                  03630099
ENDIF                                       03640099
IF (IOP1.EQ.1) THEN                        03761199
  WRITE (6,*) 'FLOW ORIFICE OUTPUT-LIQUID' 03761299
  WRITE (6,*) 'ID, ID,P1,P1,T1,T1,DP,DP'    03761399
  WRITE (6,*) 'FLD,FLD'                     03761499
  WRITE (6,*) 'D1,D1,D2,D2,CDFV,CDFV,XK,XK' 03763099
  WRITE (6,*) 'RP,RP,ALPHA,ALPHA,AO,AO,BO,BO' 03763199
  WRITE (6,*) 'REDT,REDT,AA,AA,TREF,TREF'    03763199
  WRITE (6,*) 'NVAR,NVAR,H,H,DH,DH'
  WRITE (6,*)
C   WRITE (55,*) 'ID,ID,NVAR,NVAR,H,H,DH,DH'
ELSE                                         03764099
  WRITE (6,*) 'FLOW ORIFICE OUTPUT-GAS'      03770099
  WRITE (6,*) 'ID, ID,P1,P1,T1,T1,DP,DP'    03770199
  WRITE (6,*) 'FLD,FLD'                     03761499
  WRITE (6,*) 'D1,D1,D2,D2,CDFV,CDFV,XK,XK' 03763099
  WRITE (6,*) 'RP,RP,ALPHA,ALPHA,AO,AO,BO,BO' 03763199
  WRITE (6,*) 'REDT,REDT,AA,AA,TREF,TREF'    03763199
  WRITE (6,*) 'NVAR,NVAR,H,H,DH,DH'
C   WRITE (55,*) 'ID,ID,NVAR,NVAR,H,H,DH,DH'
ENDIF                                       03781099
C                                           03790099
WRITE(6,*) 'BEGIN PROPERTY LOOKUP'
C_____ 02770099

```

```

C PROPERTY LOOK-UPS FOR GAMMA AND DENSITY                                02780099
C_____ 02790099
IF (FLD.EQ. H2) THEN 02800099
  XMW = 2.016 02810099
WRITE(6,*) 'CALL - SETUP(NAMHY)'
CALL SETUP(NAMHY)
WRITE(6,*) 'RETURN - SETUP(NAMHY)'
  KU = 3
C *** KS = 1 RETURNS DENSITY, KP = 1+2+4+8=15 RETURNS CP,CV AND MU...
WRITE(6,*) 'CALL - GASP2 H2'
CALL GASP2(1,15,T1,P1,DH2,HH2,3)
WRITE(6,*) 'RETURN - GASP2 H2'
  RHO = DH2
  CP1 = CP
  CV1 = CV
  VU = MU
  GAM = CP1/CV1 02920099
ELSEIF(FLD.EQ. 'O2') THEN 02940099
  XMW = 32.00 02950099
WRITE(6,*) 'CALL - SETUP(NAMOX)'
CALL SETUP(NAMOX)
WRITE(6,*) 'RETURN - SETUP(NAMOX)'
  KU = 3
C *** KS = 1 RETURNS DENSITY, KP = 1+2+4+8=15 RETURNS CP,CV AND MU...
WRITE(6,*) 'CALL - GASP2 O2'
CALL GASP2(1,15,T1,P1,DO2,HO2,3)
WRITE(6,*) 'RETURN - GASP2 O2'
  RHO = DO2
  CP1 = CP
  CV1 = CV
  VU = MU
  GAM = CP1/CV1 02920099
ENDIF 03070099
WRITE(6,*) 'END PROPERTY LOOKUP'
C 03080099
WRITE(6,*) 'BEGIN FLOW CALCULATIONS'
C_____ 03090099
C FLOW CALCULATIONS 03100099
C_____ 03110099
C *** B IS F/M BETA RATIO (DIAMETER RATIO) WHERE D1 IS INLET DIA. & *** 03120099
C *** D2 IS THE THROAT DIAMETER *** 03130099
C *** TE IS THE THERMAL EXPANSION FACTOR *** 03140099
C *** CW IS THE CALIBRATION COEFFICIENT *** 03150099
  B = D2 / D1 03160099
  A2 = D2**2.*3.14159/4. 03161099
  B2 = B**2 03170099
  B4 = B**4 03180099
  T4 = TREF - 528. 03180099
  TE = 1.0 + (2 * ALPHA * (T1 - 528.)) 03190099
C TE = 1.0 + (2 * (ALPHA / T4) * (T1 - 528.)) 03190099
  CW = D2**2.*CDFV / (SQRT(1. - B4)) 03200099
  XP = 1 - DP/P1 03201099
  P2 = P1 - DP 03201199
  P2OP1 = P2/P1 03202099
  G2 = 2./GAM 03203099
  GAM1 = GAM/(GAM-1) 03204099
  GAM2 = (GAM-1)/GAM 03205099
  GAM3 = (GAM+1)/GAM 03205199
  YA = (XP**G2*GAM1)*((1-XP**GAM2)/(1-XP))*((1-B4)/(1-B4*XP**G2)) 03206099
  YA = SQRT(YA) 03207099
  CONST = 2.*32.174/144. 03208099
  AREAC = 3.14159/4.00 03210099
  CDSAVE = CDFV 03211099
WRITE(6,*) 'END FLOW CALCULATIONS'
C_____ 03220099
C LIQUID EQUATION OPTION 03230099
C_____ 03240099
C *** THE CONSTANT 0.525019 IS A UNIT CONVERSION FACTOR BASED ON: 03250099
C *** WL IN LB/S, DELTA P IN PSID, RHO IS LB/FT3, AND D2 IN INCHES *** 03260099
C *** K = 3.14159/4*SQRT(2*GC/144) = 0.5250204 *** 03270099
IF (IOPI.EQ. 1) THEN 03280099

```

```

WRITE(6,*) 'BEGIN LIQ EQUATION OPTION'
ENERGY = CONST*RHO*DP                                03290099
WL = MACHCOR * TE * CW * AREAC * SQRT(ENERGY)        03300099
C ***** CURVE FIT FOR ID = 247 *****            03320099
C IB32 = 1                                           03340099
C GO TO 301                                         03341099
C300 CONTINUE                                       03350099
CW = D2**2.*CDFV / (SQRT(1. - B4))                  03350199
ENERGY = CONST*RHO*DP                                03350299
WL = MACHCOR * TE * CW * AREAC * SQRT(ENERGY)        03350399
C301 CONTINUE                                       03381099
C RE = 48.0 * WL / (3.14159 * D2 * VU)              03390099
C IF (ID.NE. 247) THEN                              03392099
C CDFVT = AO - ABS(BO*(REDT/RE)**AA)                03391099
C ELSE
C CDFVT = .97253 + 3.3476E-08 * RE - 2.862E-14 * RE**2 + 03400099
C X 8.6492E-21 * RE**3 - 7.048E-28 * RE**4          03410099
C ENDIF                                             03411099
C CALL PSLP5 (CDFV,CDFV,CDFVT,B31,B32,0.0001,IB31,IB32,20,300) 03420099
C IF (IB31.EQ. 1) GO TO 300                          03430099
WLG = WL                                             03441099
WRITE(6,*) 'END LIQ EQUATION OPTION'
C                                                    03450099
C                                                    03480099
C _____ 03490099
C GAS EQUATION OPTION -- IOPI = 2                    03500099
C _____ 03510099
ELSE 03520099
WRITE(6,*) 'BEGIN GAS EQUATION OPTION'
ENERGY = CONST*RHO*DP                                03521099
WG = MACHCOR * YA * TE * CW * AREAC * SQRT(ENERGY) 03740099
C IB42 = 1                                           03742099
C GO TO 601                                         03743099
C600 CONTINUE                                       03744099
CW = D2**2.*CDFV / (SQRT(1. - B4))                  03744199
ENERGY = CONST*RHO*DP                                03744299
WG = MACHCOR * YA * TE * CW * AREAC * SQRT(ENERGY) 03744399
C601 CONTINUE                                       03748099
C RE = 48.0 * WG / (3.14159 * D2 * VU)              03749099
C CDFVT = AO - ABS(BO*(REDT/RE)**AA)                03749199
C CALL PSLP5 (CDFV,CDFV,CDFVT,B41,B42,0.0001,IB41,IB42,20,600) 03749399
C IF (IB41.EQ. 1) GO TO 600                          03749499
WLG = WG                                             03749699
WRITE(6,*) 'END GAS EQUATION OPTION'
ENDIF 03750099
C *** VENTURI RESISTANCE CALCULATION ***            03751099
IF (ID.EQ. 296) THEN                                03751299
VDPT = DP * (0.436 - 0.86 * B + 0.59 * B**2.)      03751399
ELSE 03752199
VDPT = DP * (0.218 - 0.42 * B + 0.38 * B**2.)      03752299
ENDIF 03754099
C 03760099
IF (ID.EQ. 275) ID = 2741
IF (ID.EQ. 274) ID = 2742
IF (ID.EQ. 303) ID = 3021
IF (ID.EQ. 302) ID = 3022
WRITE (86,*) 'VENTURI ID NO:',ID                    03761099
IF (IOPI.EQ. 1) THEN                                03761199
WRITE (86,*) 'FLOW ORIFICE OUTPUT--LIQUID'          03761299
WRITE (86,*) 'ID, ID,P1',P1,'T1',T1,'DP',DP        03761399
WRITE (86,*) 'WL',WL,'RHO',RHO,'GAMMA',GAM,'VISCO',VU 03761499
WRITE (86,*) 'RE NO.',RE,'CDFV',CDFV,'CDFV THEO',CDFVT 03763099
WRITE (86,*) 'GAMMA',GAM,'VDPT',VDPT,'MACH COR',MACHCOR 03763199
WRITE (86,*) 'NVAR',NVAR,'H',H,'DH',DH
C WRITE (55,*) 'NVAR',NVAR,'H',H,'DH',DH
ELSE 03764099
WRITE (86,*) 'FLOW ORIFICE OUTPUT--GAS'            03770099
WRITE (86,*) 'ID, ID,P1',P1,'T1',T1,'DP',DP        03770199
WRITE (86,*) 'WG',WG,'RHO',RHO,'GAMMA',GAM,'VISCO',VU 03771099
WRITE (86,*) 'XP',XP,'YA',YA,'XK',XK,'CW',CW       03780099
WRITE (86,*) 'RE NO.',RE,'CDFV',CDFV,'CDFV THEO',CDFVT 03780199

```

```
WRITE (86,*) 'VDPT,VDPT,MACH COR',MACHCOR          03780299
WRITE (86,*) 'NVAR',NVAR,'H',H,'DH',DH
C WRITE (55,*) 'NVAR',NVAR,'H',H,'DH',DH
ENDIF                                               03781099
C                                               03790099
C WRITE (55,*) 'LEAVING SUBROUTINE FLOWOR'          03802099
999 RETURN                                         03810099
END                                               03820099
```

**{THE THERMOPHYSICAL PROPERTY SUBROUTINE FOLLOWS
AT THIS POINT IN THE PROGRAM, HOWEVER .
IT IS NOT INCLUDED IN THIS PRINTOUT}**